Active Cellular Nematics

Collective behaviors

Population scale

Fish

D. Hall

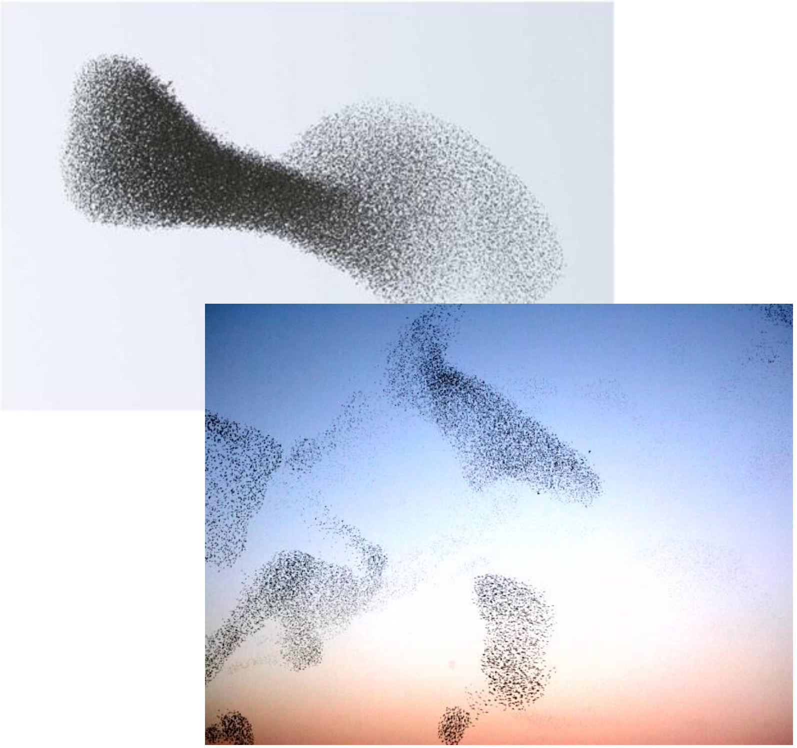

Starlings

M. Presti

Similar framework / concepts to multi-cellular systems

Review on collective cell migration: Hakim V., Silberzan P.: *Collective cell migration: a physics perspective.* Rep. Prog. Phys. **80**, (2017), 076601

HBE cells (Human Bronchial Epithelial)

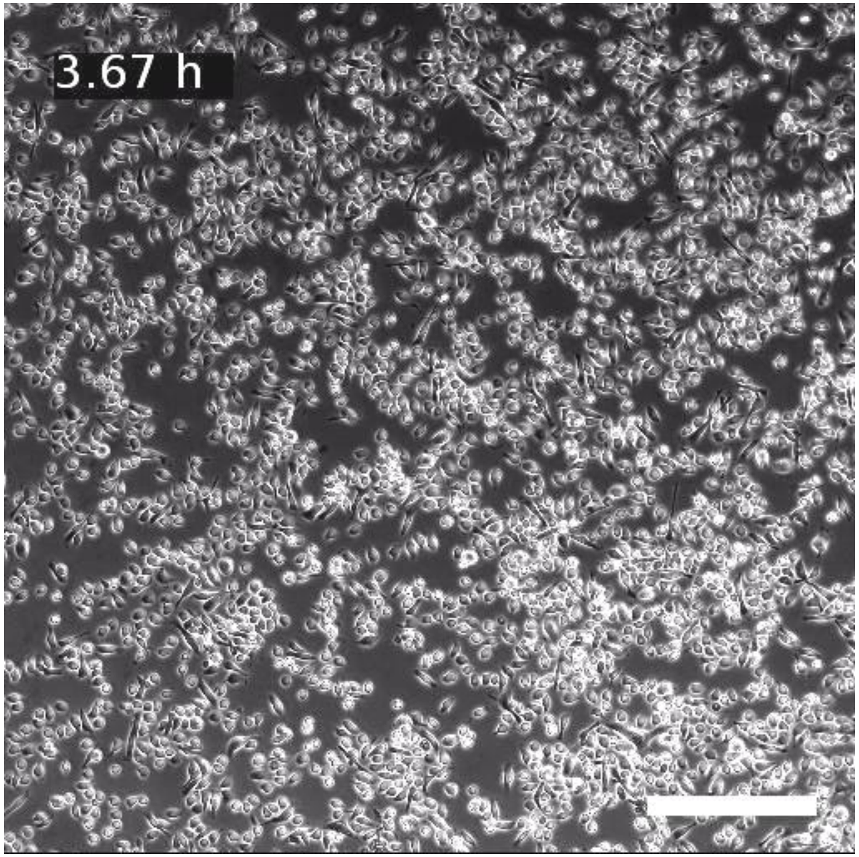

300 µm

Slowing down as a consequence of cell-cell interactions and cell crowding:

Contact inhibition of locomotion

Contact inhibition of locomotion: a single cell concept

« *Contact inhibition consists of the abolition or reduction of the power of the leading membrane to direct the general cell movement, and hence the assumption of dominance by another membrane, which then redirects the cell.* »

M. Abercrombie (1958)

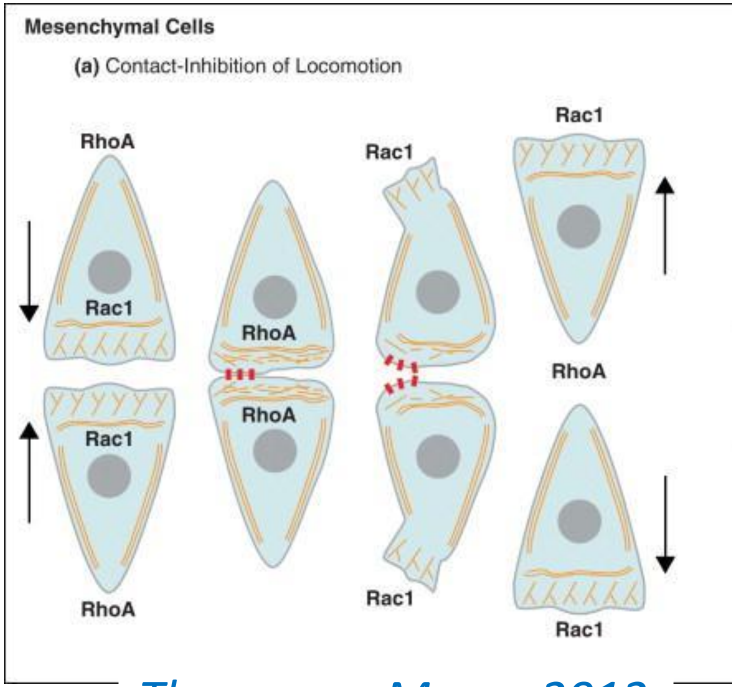

Theveneau Mayor 2012

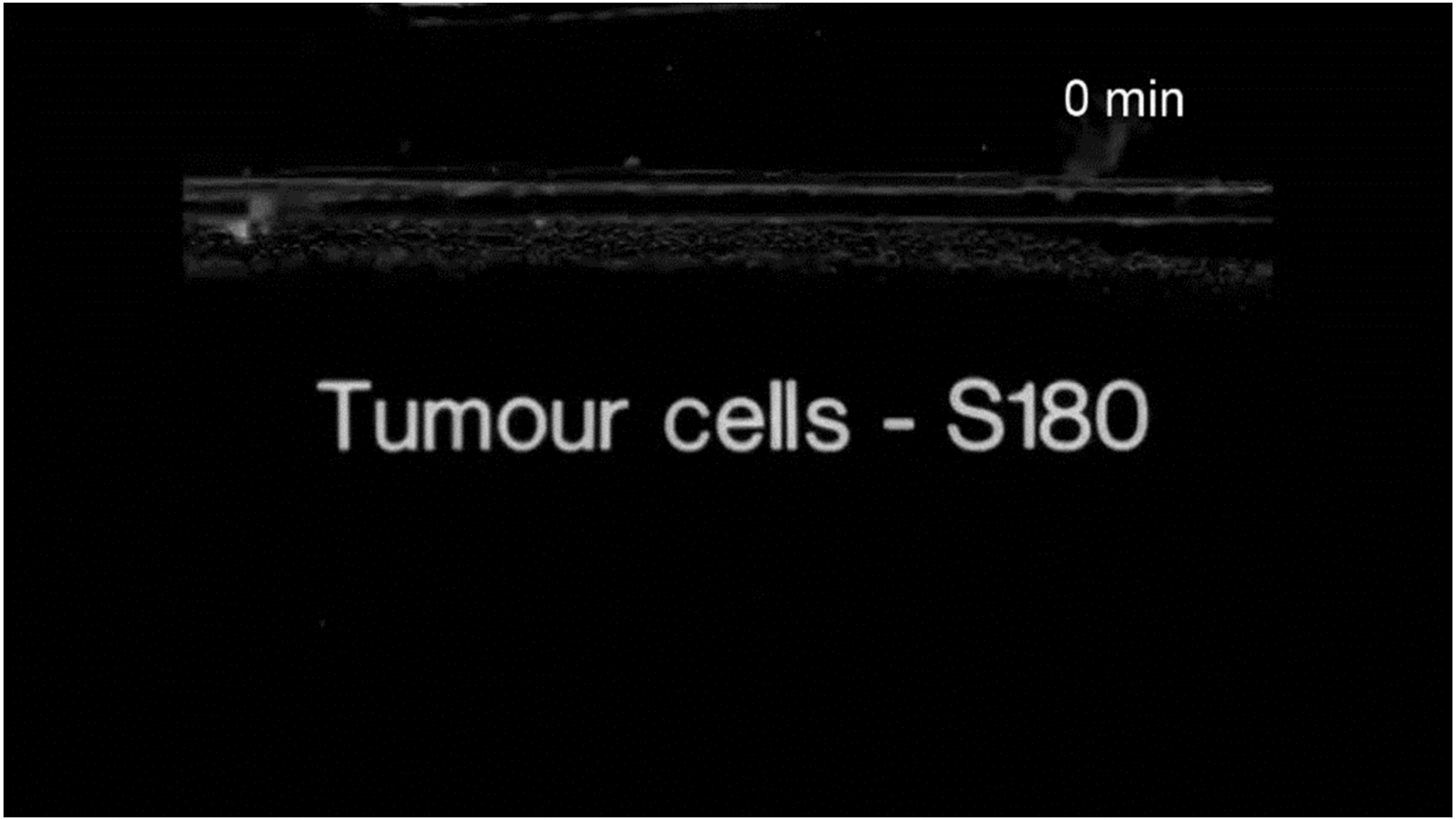

Michaël Abercrombie (UCL, 50's)

HBECs

(*Human bronchial epithelial cells*)

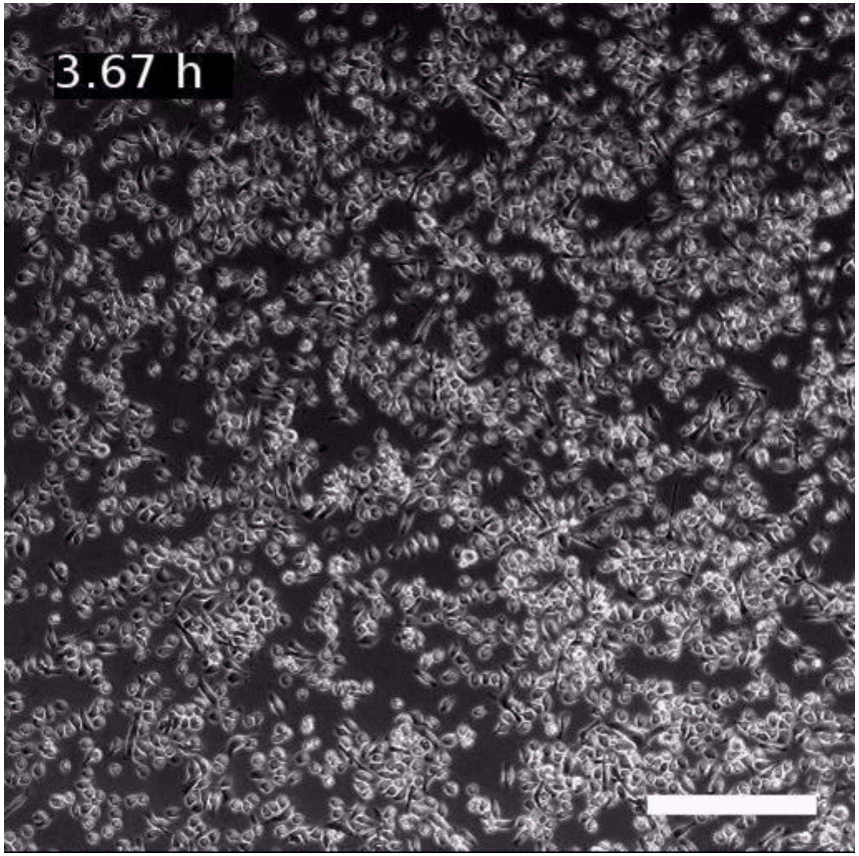

300 µm

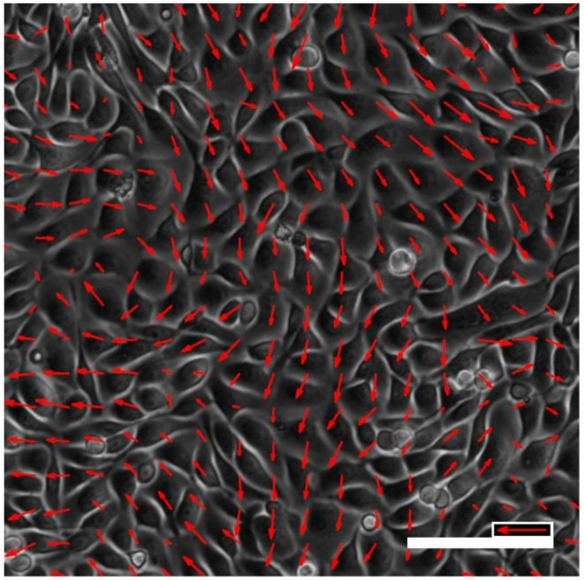

100 µm/h

100 µm

Garcia PNAS 2015

HBECs

(*Human bronchial epithelial cells*)

Cell jamming ?

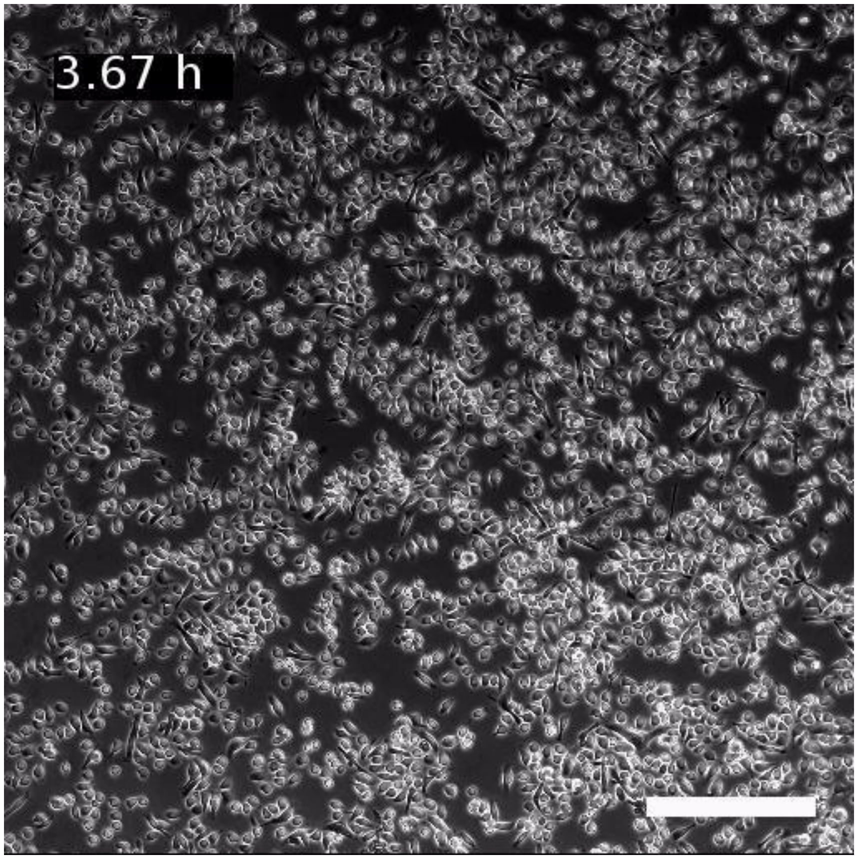

300 µm

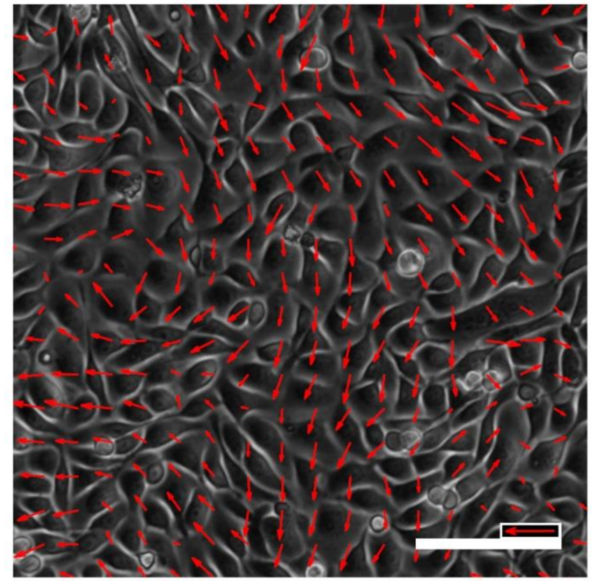

100 µm/h ←

100 µm

Garcia PNAS 2015

Slow down of displacements with time

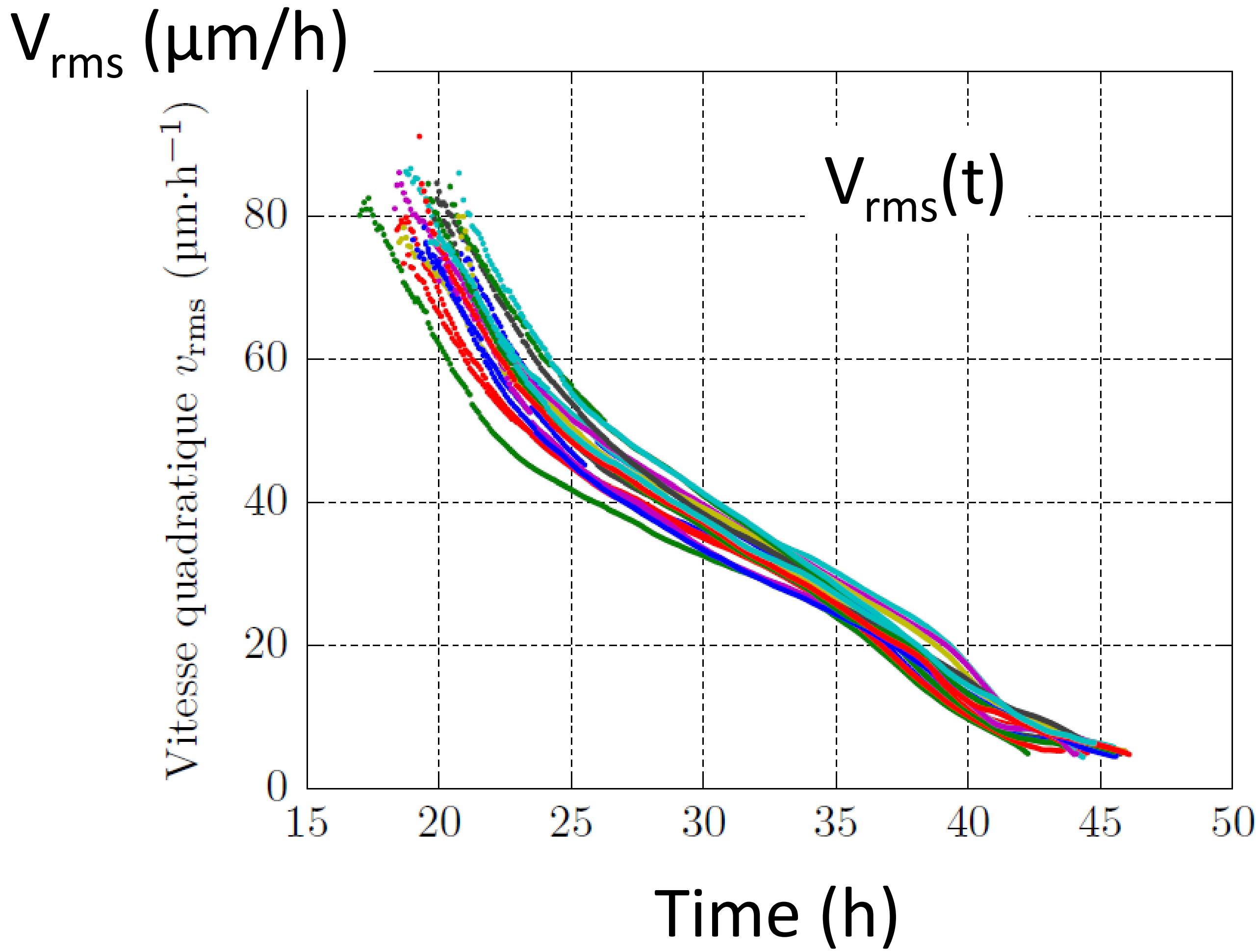

$$v_{\mathrm{rms}}(t) = \sqrt{\left\langle \vec{v}(\vec{r},t)^2 \right\rangle_{\vec{r}}}$$

Jamming of a HBEC monolayer

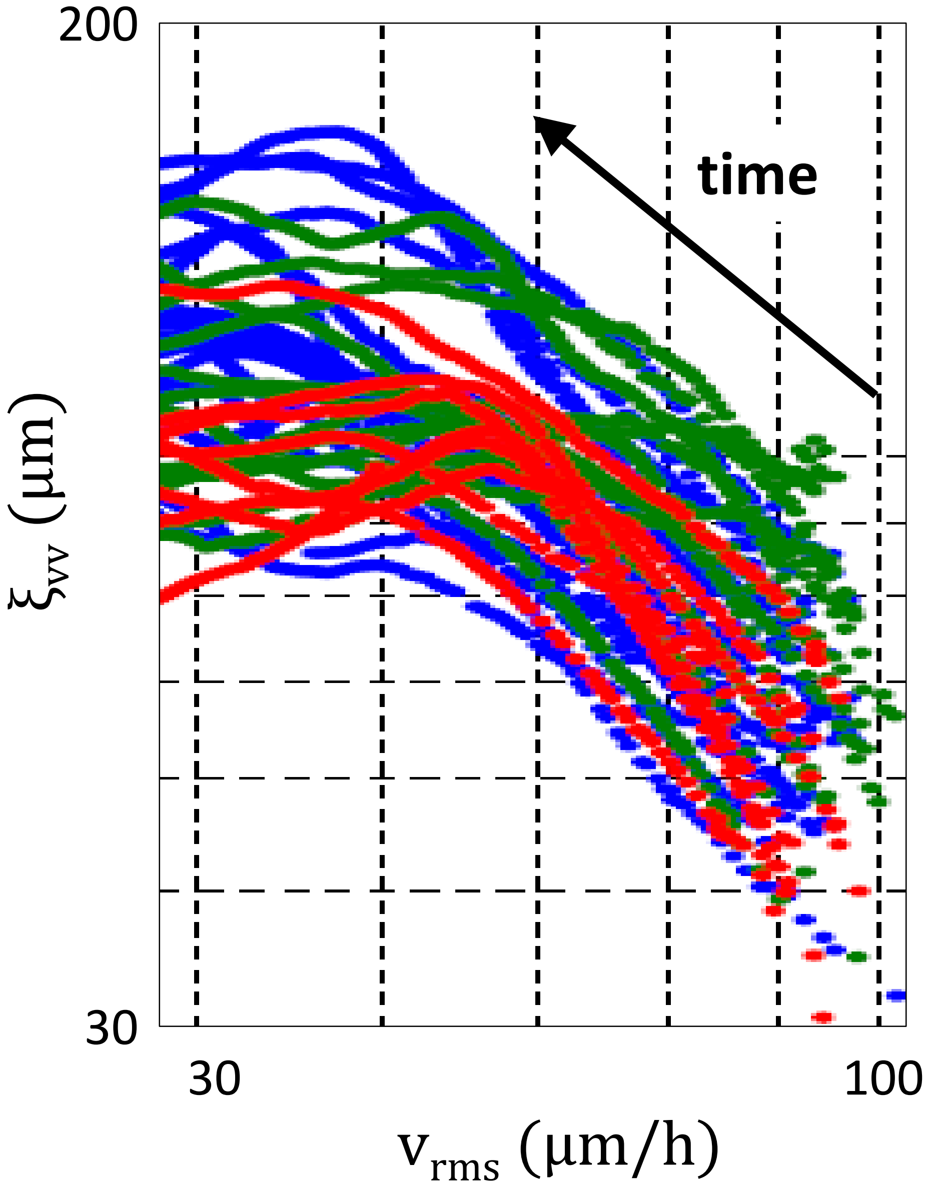

$$\xi_{vv} \propto \frac{1}{v_{rms}}$$

Garcia PNAS 2015

Jamming of a HBEC monolayer

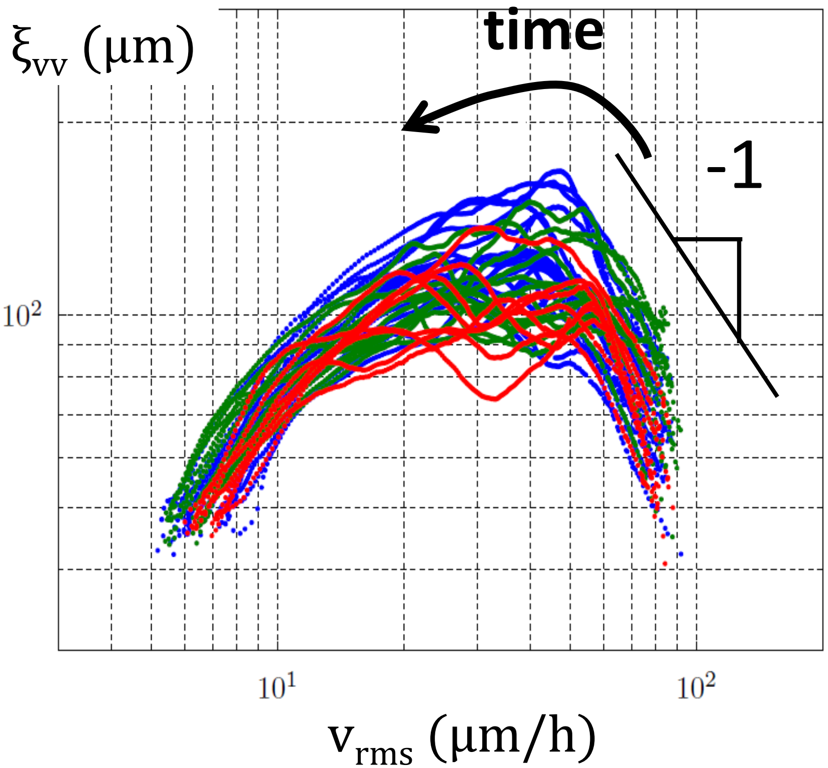

Garcia PNAS 2015

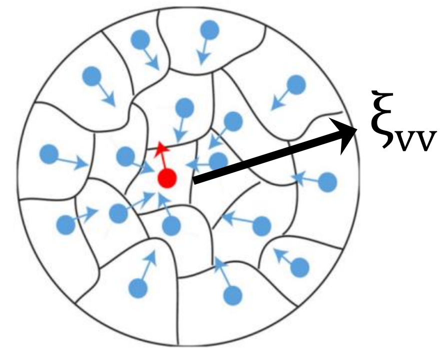

Cluster model (Nir Gov)

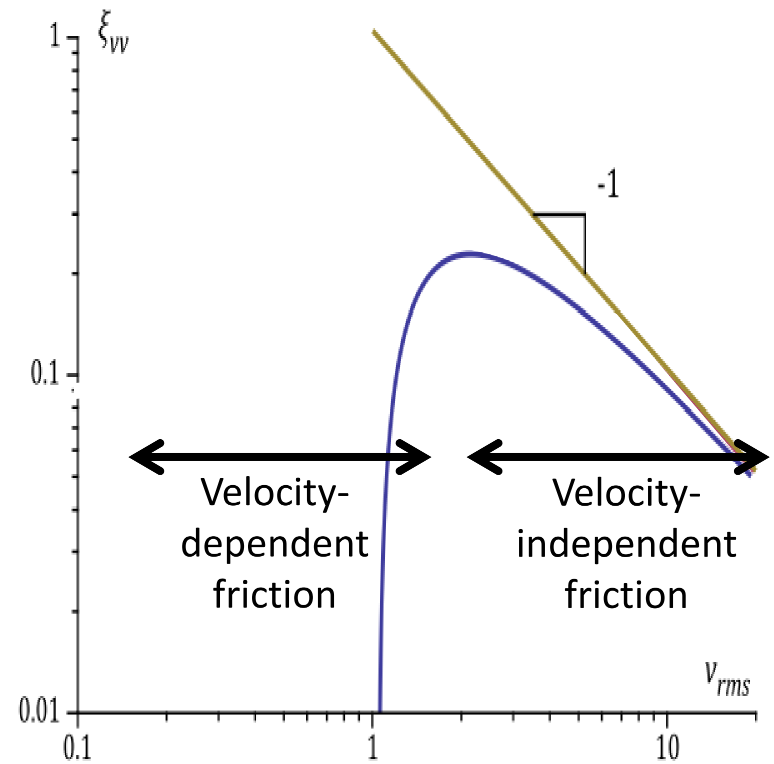

Cell Jamming

Contact Inhibition of Locomotion
(M. Abercrombie (1958))
Single cell concept

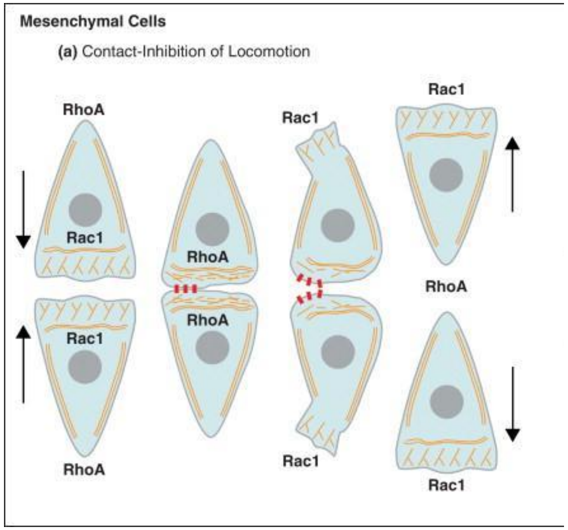

Theveneau Mayor 2012

Cell Jamming
(D. Weitz, J. Fredberg (2010's))
Collective

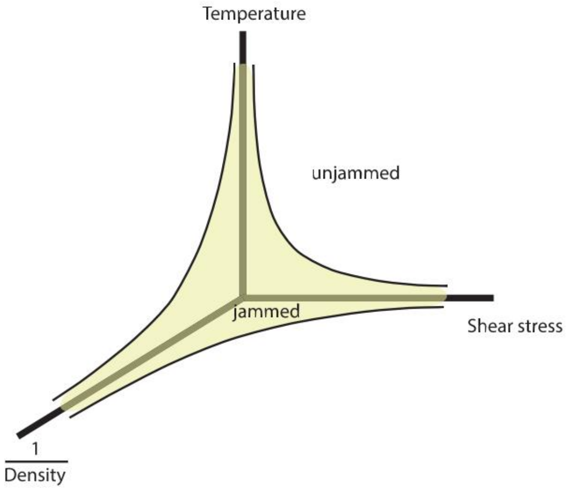

Dynamics and architecture of cells in their route to jamming

3T3 fibroblasts

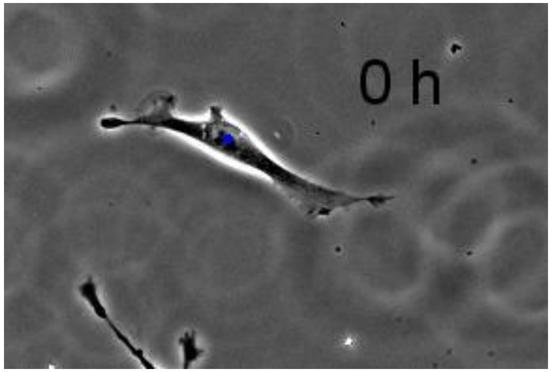

50 µm

Spindle-shaped cells
Apolar

Cell division :

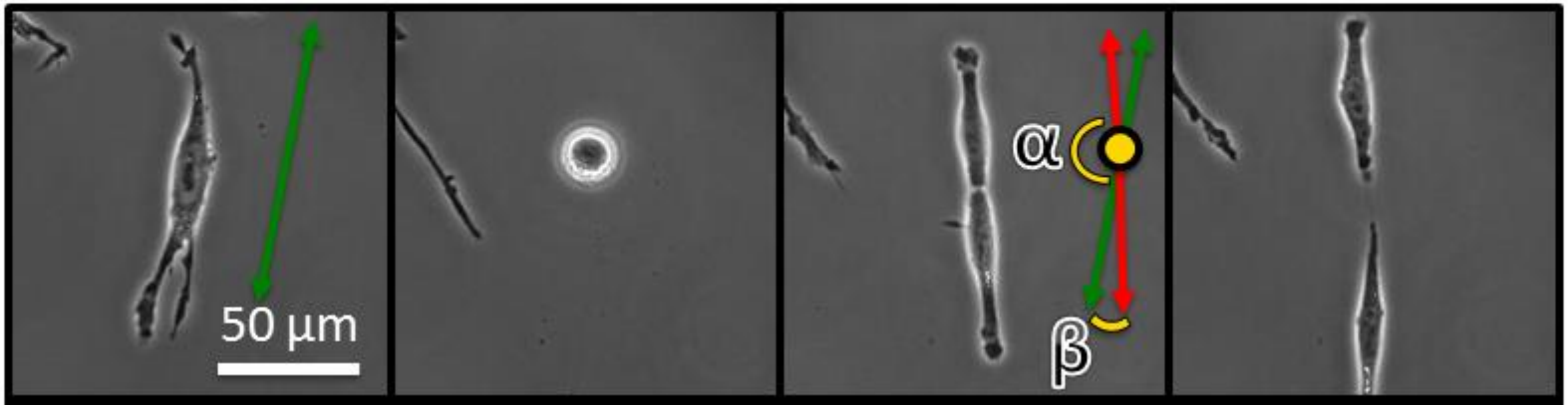

No cadherin-mediated cell-cell adhesion

Fibroblasts
NIH-3T3

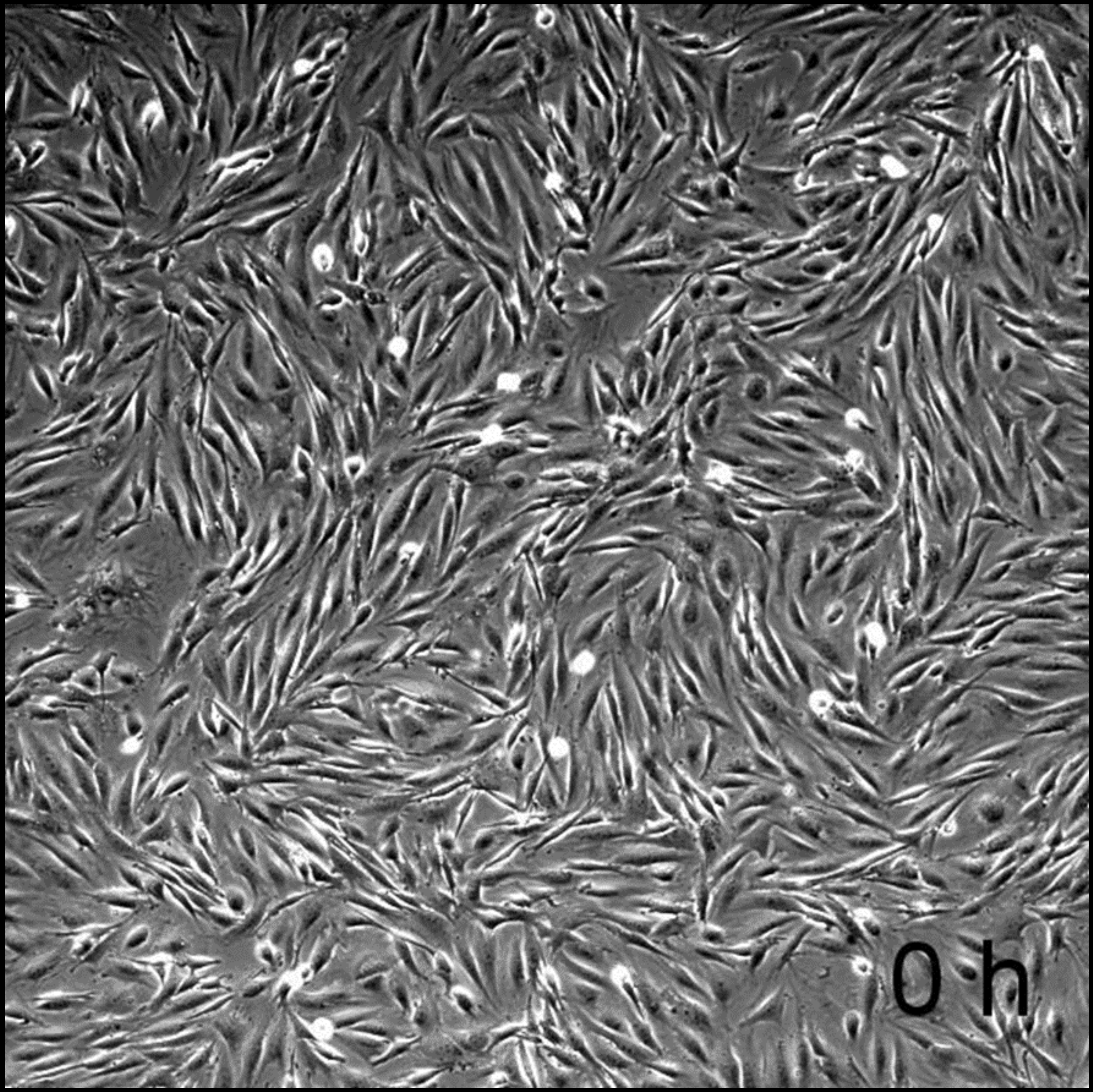

400 μm

Duclos Soft Matter 2014

Fibroblasts
NIH-3T3

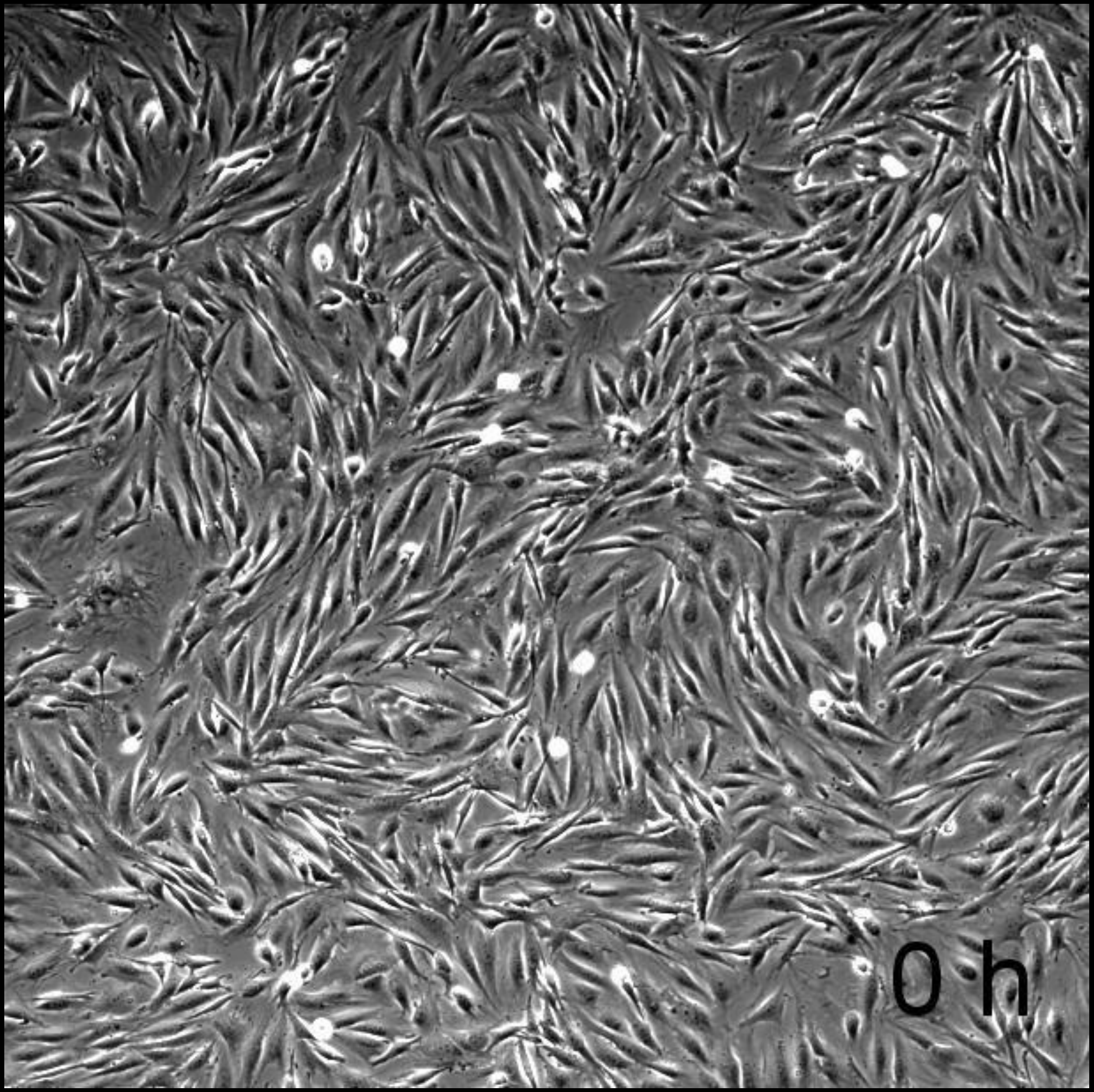

400 μm

Duclos Soft Matter 2014

Fibroblasts
NIH-3T3

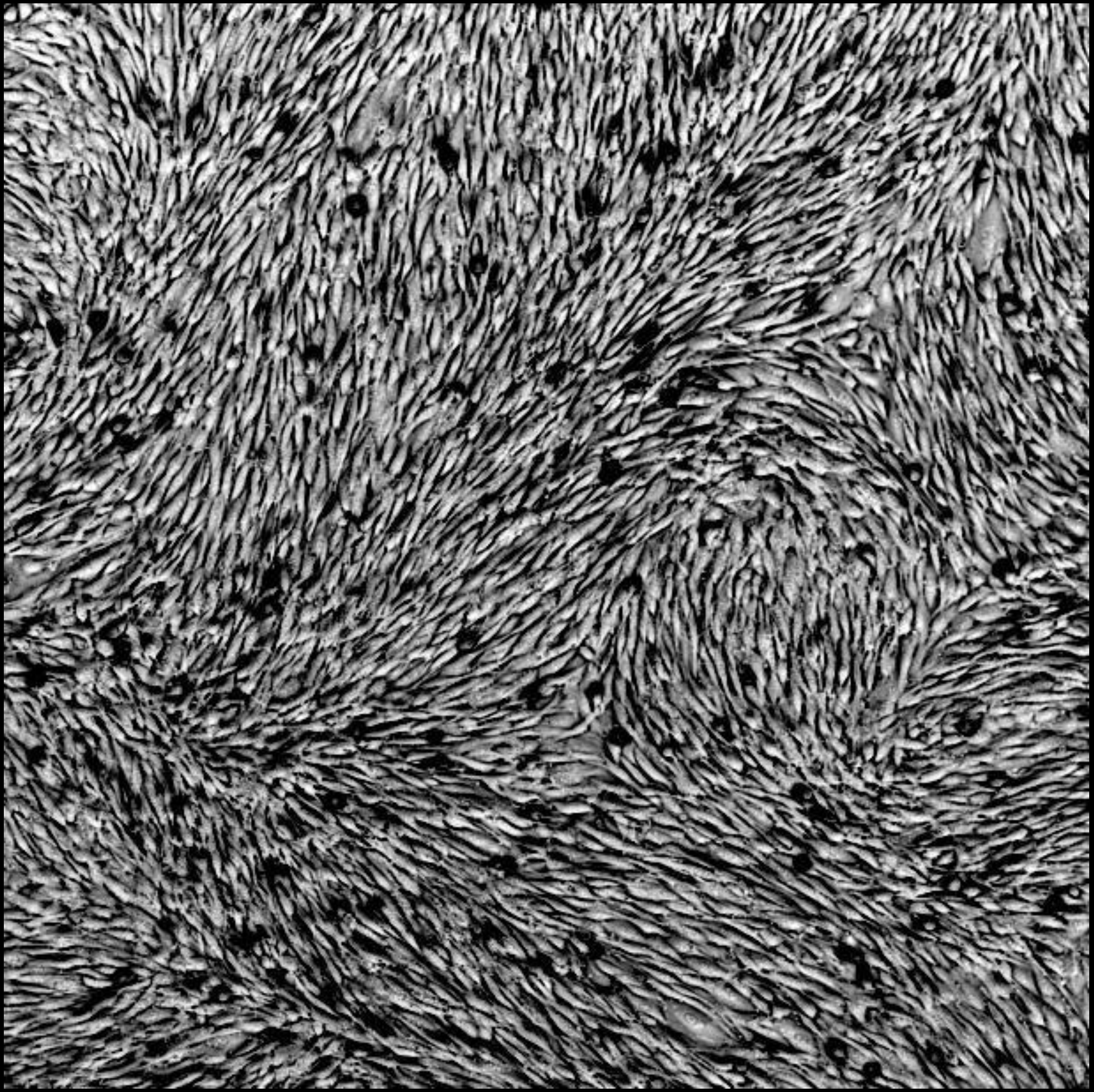

400 μm

Duclos Soft Matter 2014

A nematic-like ordering also observed in vivo

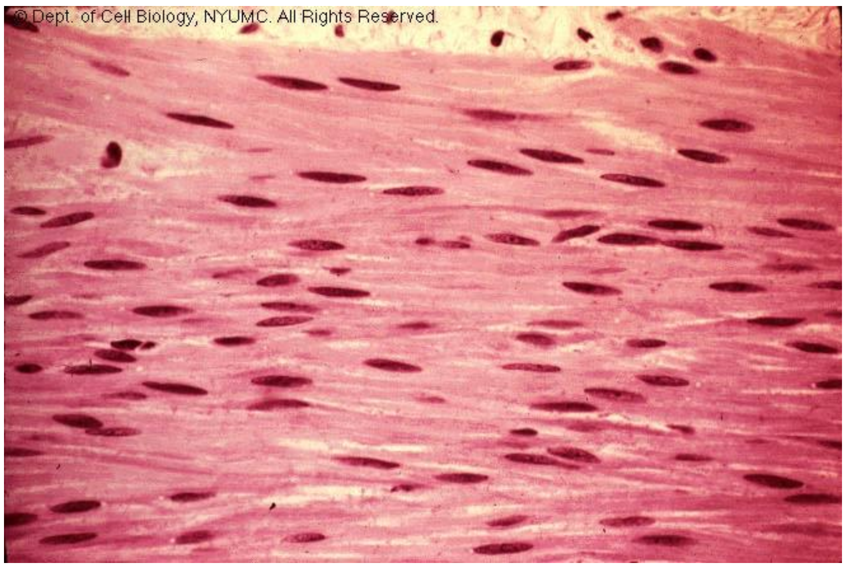

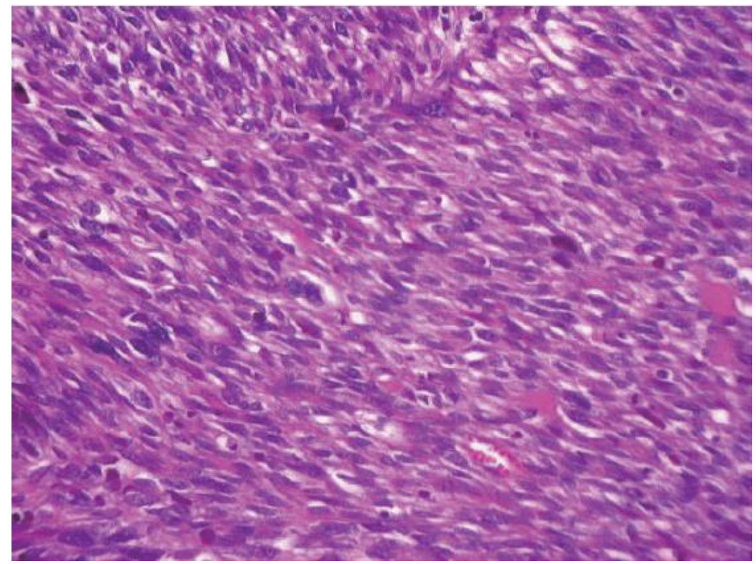

Smooth muscle

Sarcoma

Dpt of Cell Biology NYUMC

Braham Ann Trans Med 2013

Order in a fibroblasts monolayer

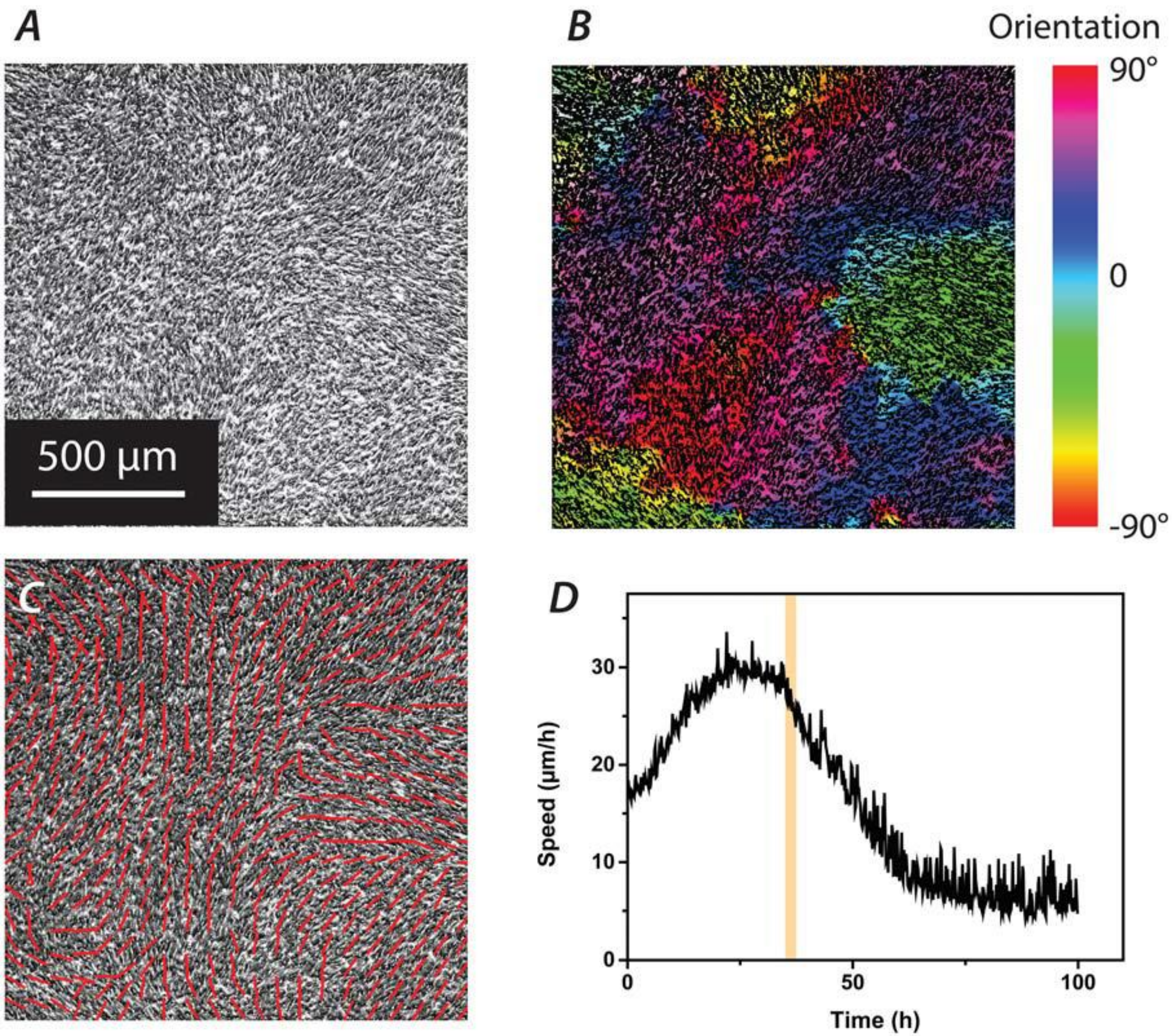

Nematic ordering of spindle-shaped cells

Fibroblasts
NIH-3T3

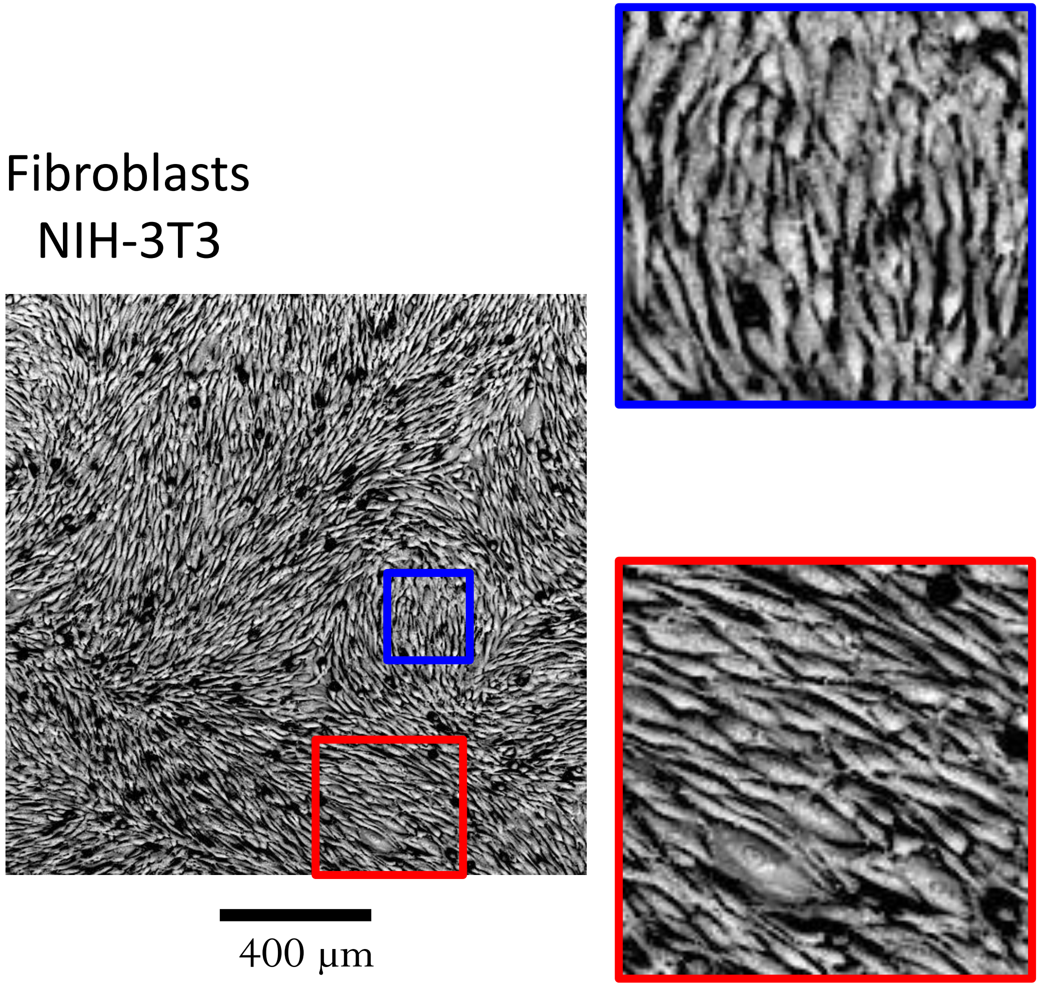

Duclos Soft Matter 2014
Duclos Nat Phys 2017
Duclos Nat Phys 2018

Orientation clusters

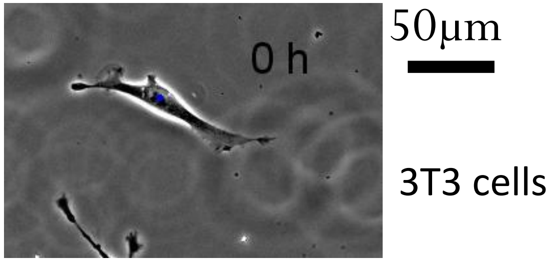

Activity

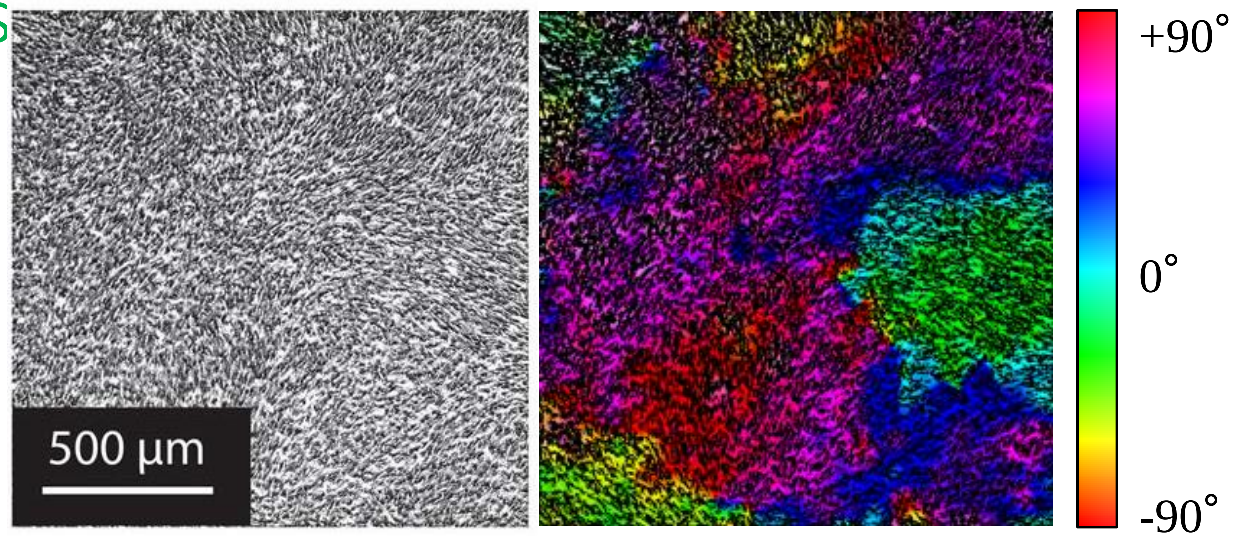

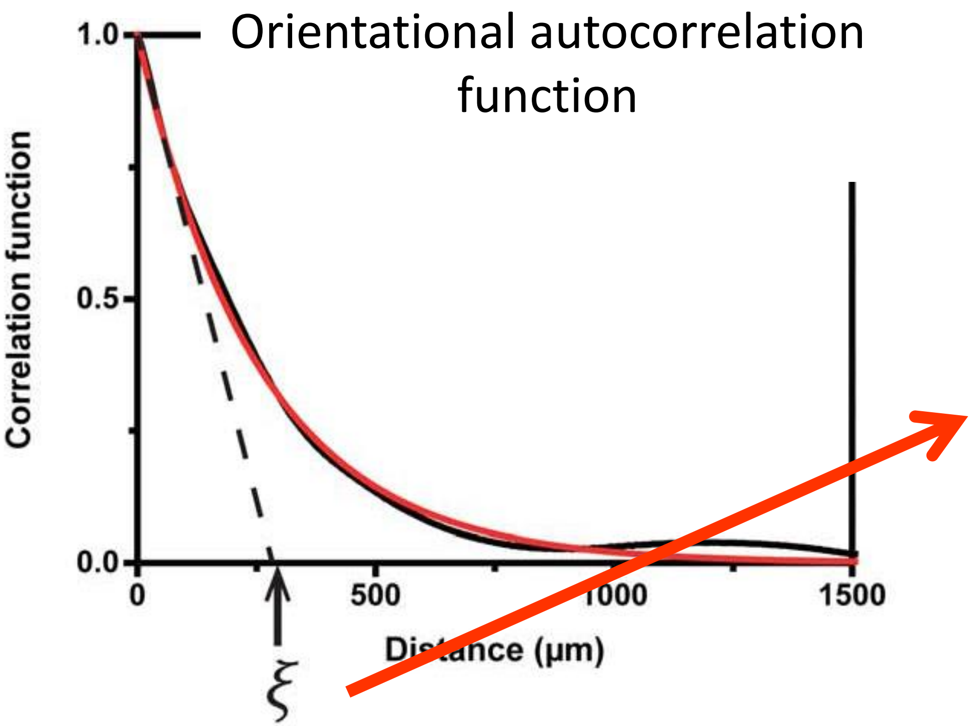

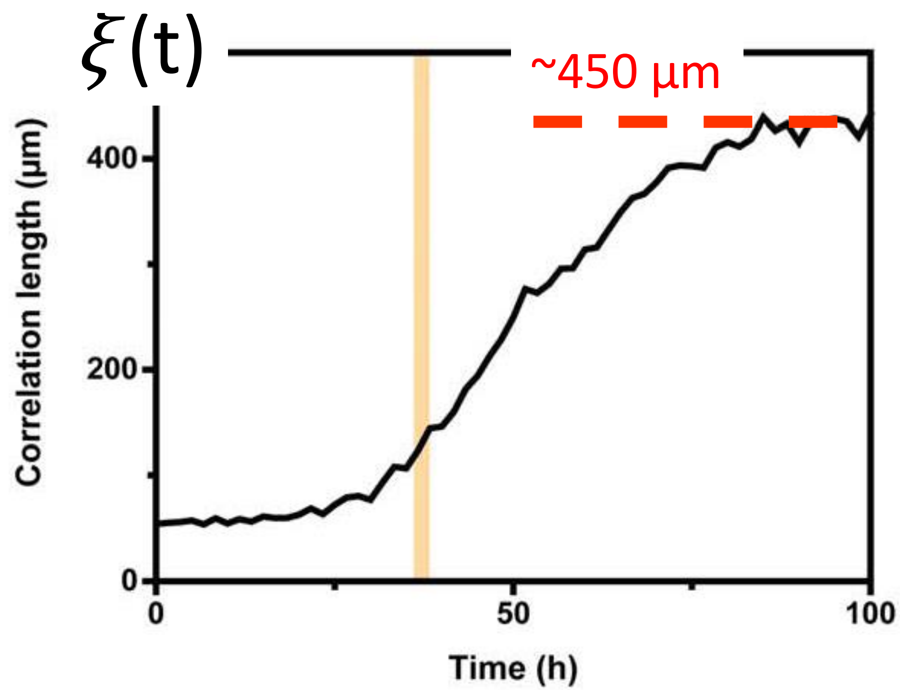

As time goes on

Better orientation

Steric interactions

Less movement

Jamming

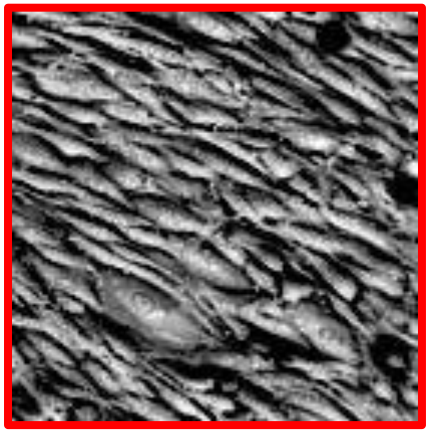

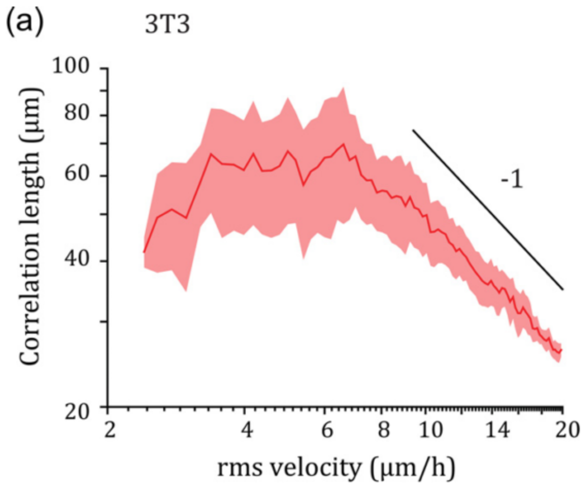

Garcia, PNAS 2015

A true nematic ? The proof is in the defects

+1/2

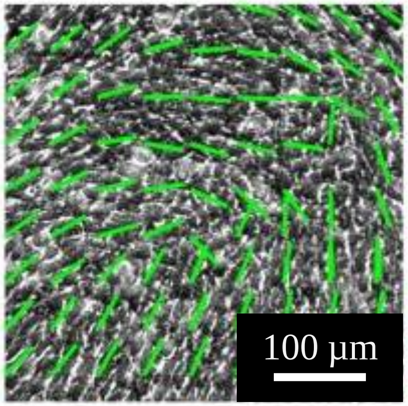

-1/2

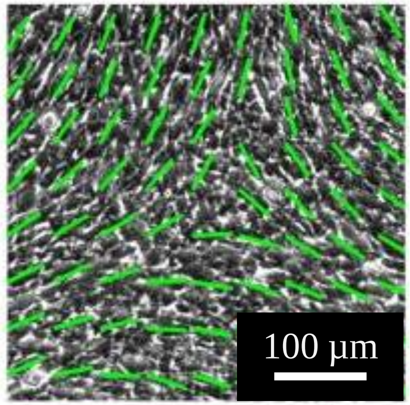

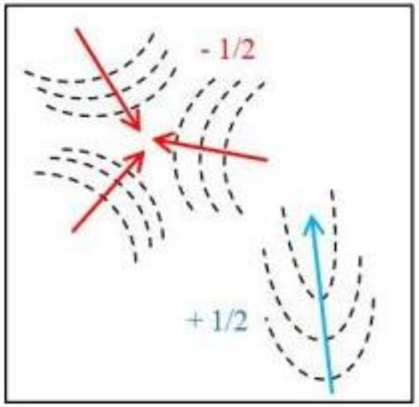

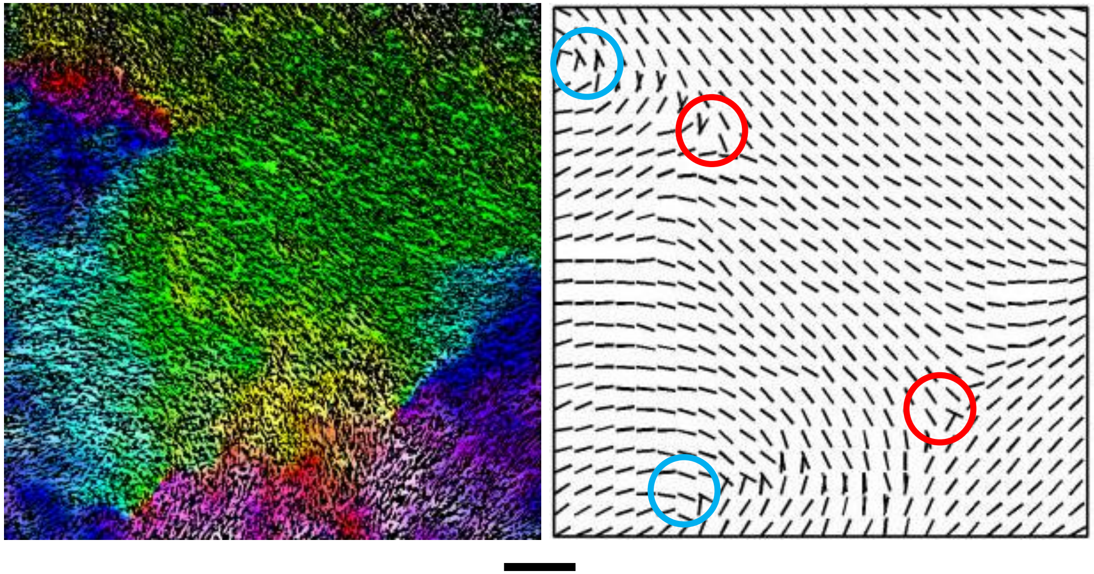

200 µm

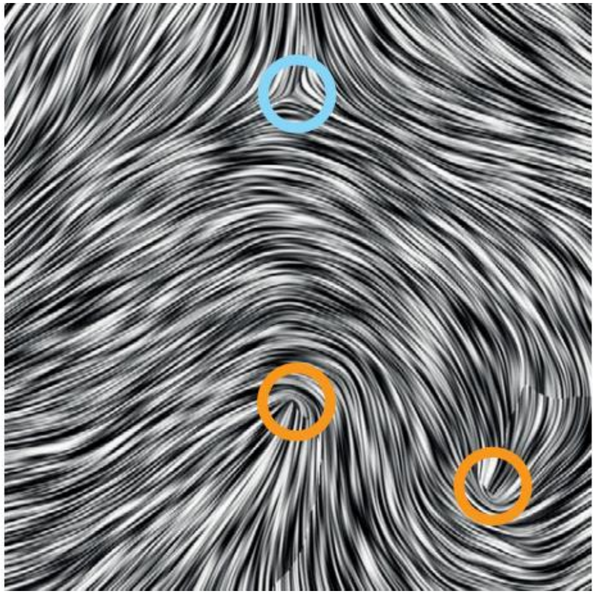

An active nematic

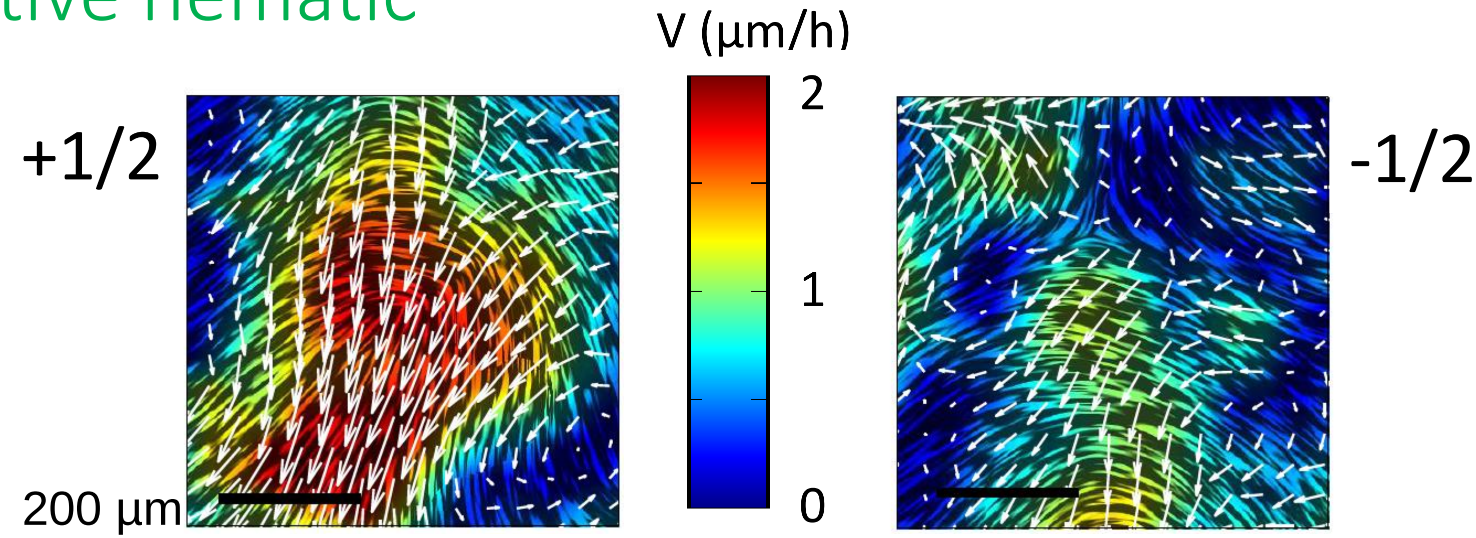

- Self-propulsion of +1/2 defects
- Active nematic backflow via the monolayer itself

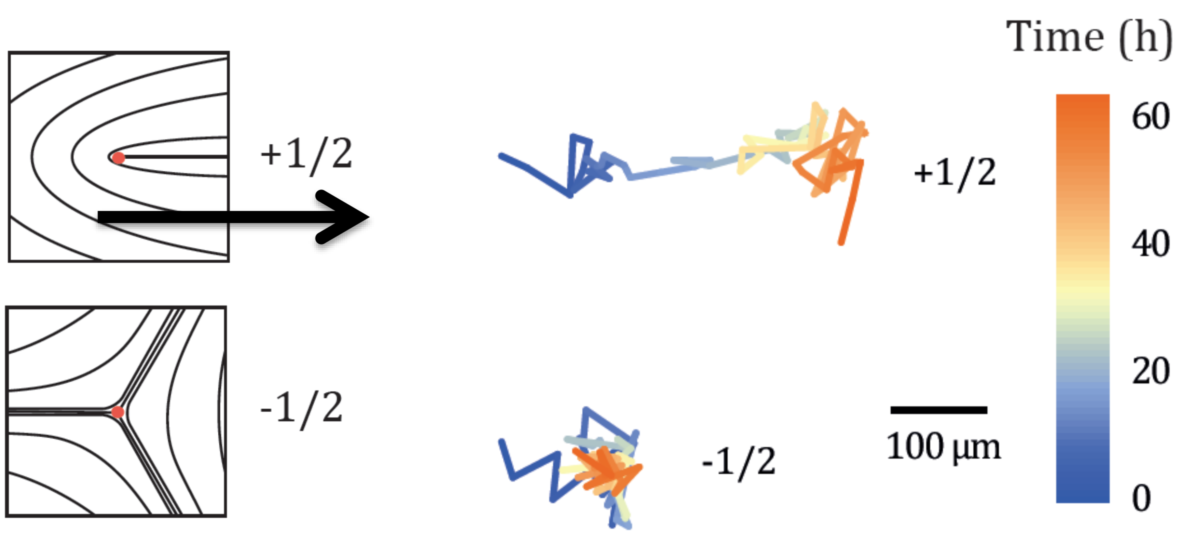

Contractile behavior of the defects

How to reach perfect alignment ?

Liquid Crystal strategy :
Use **boundaries**

non adhesive

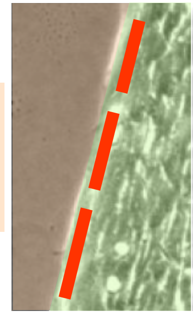

adhesive

Cells align along boundaries

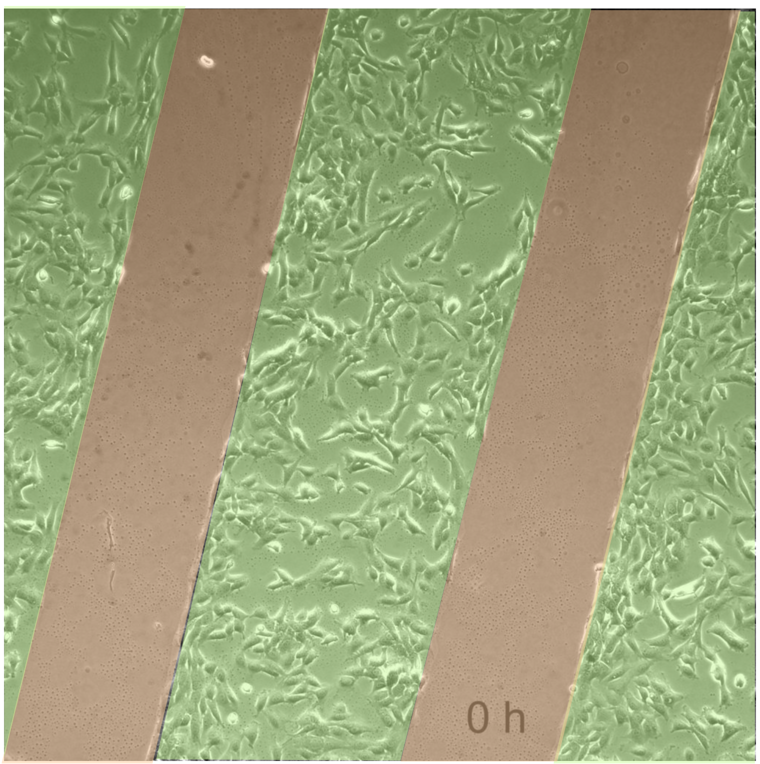

200 µm

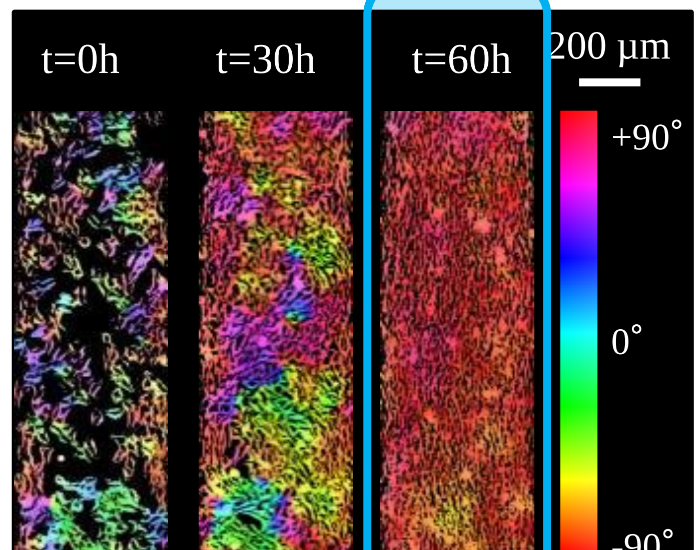

Q≈0.98

Duclos et al. Soft Matter 2014

- Cells align at borders
- After confluence, this order propagates from the edges toward the center.

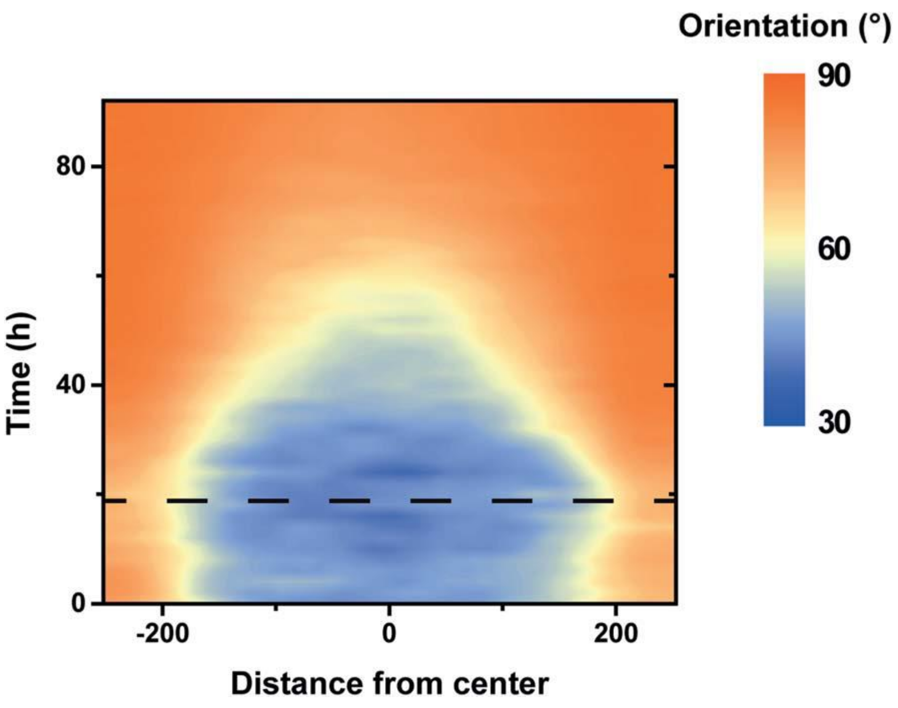

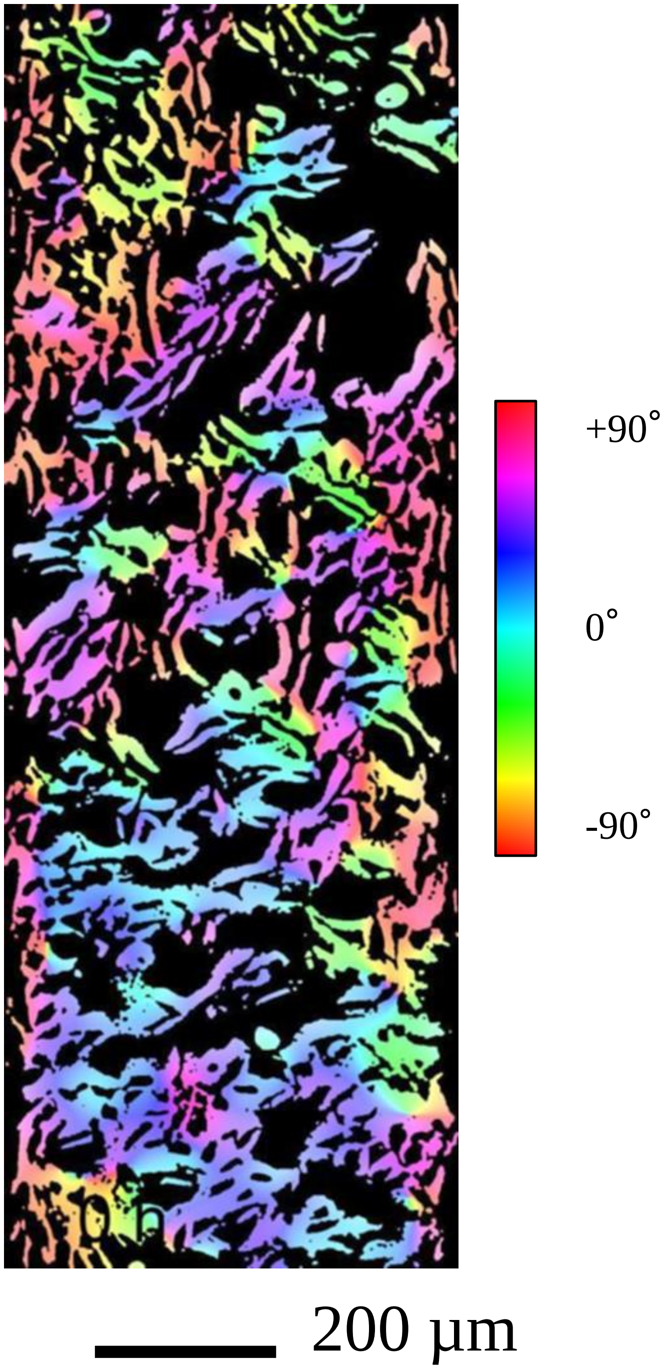

- Cells align at borders
- After confluence, this order propagates from the edges toward the center.

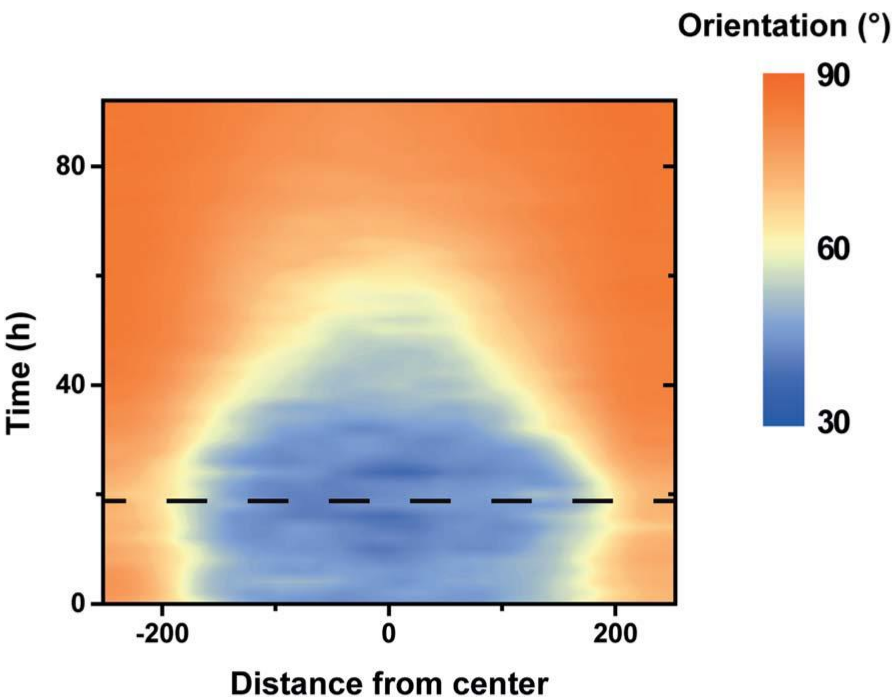

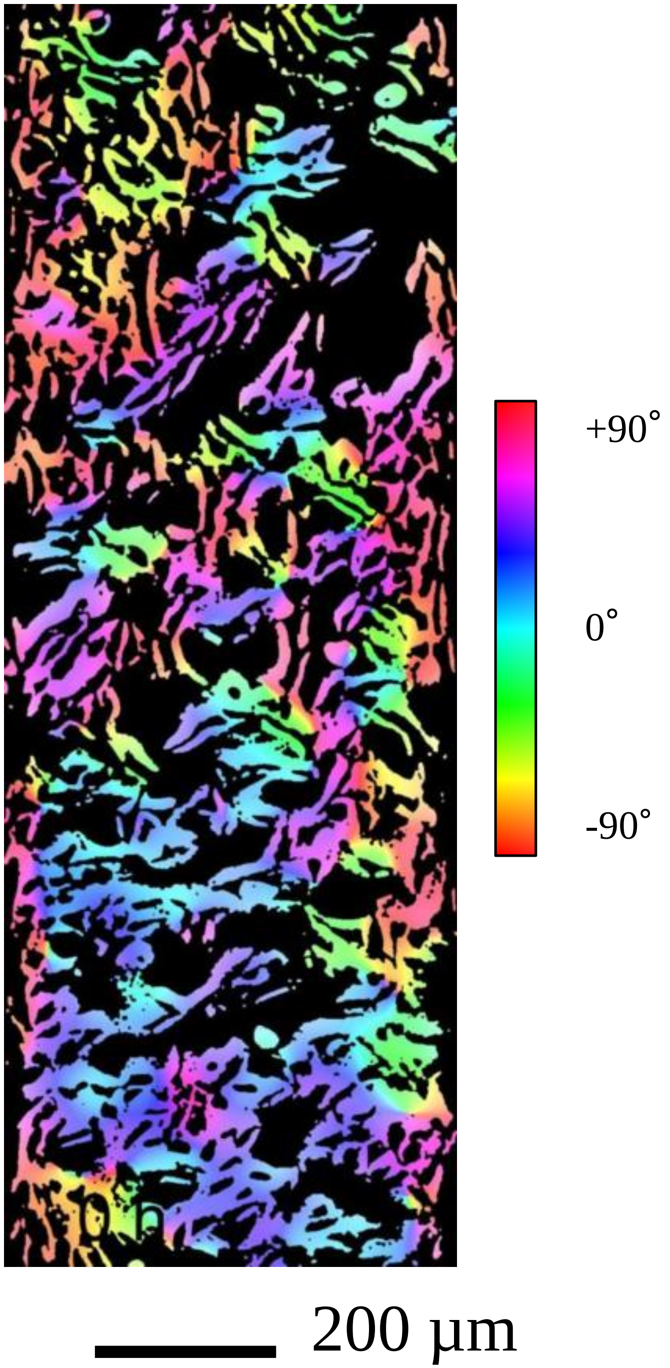

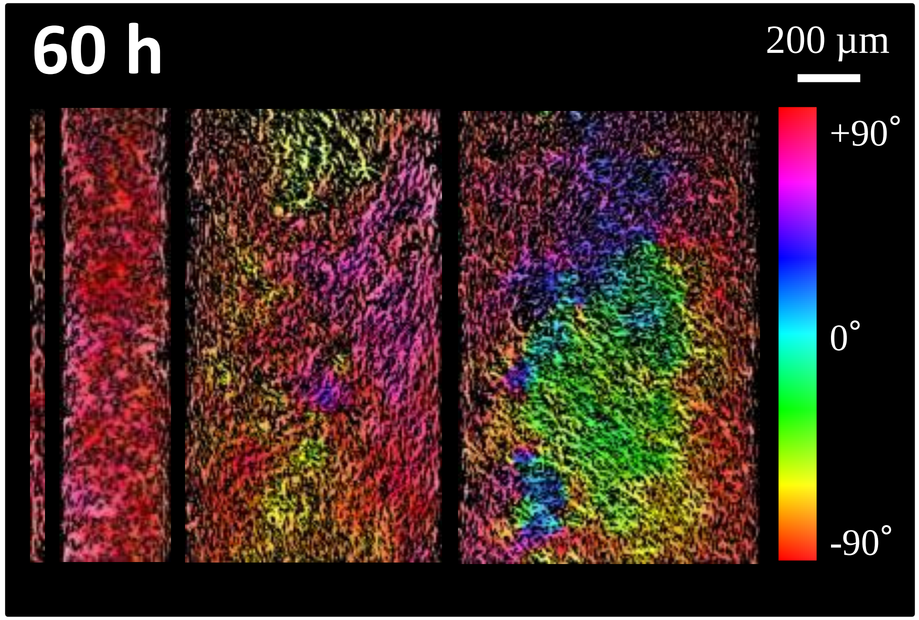

60 h
200 μm
+90°
0°
-90°

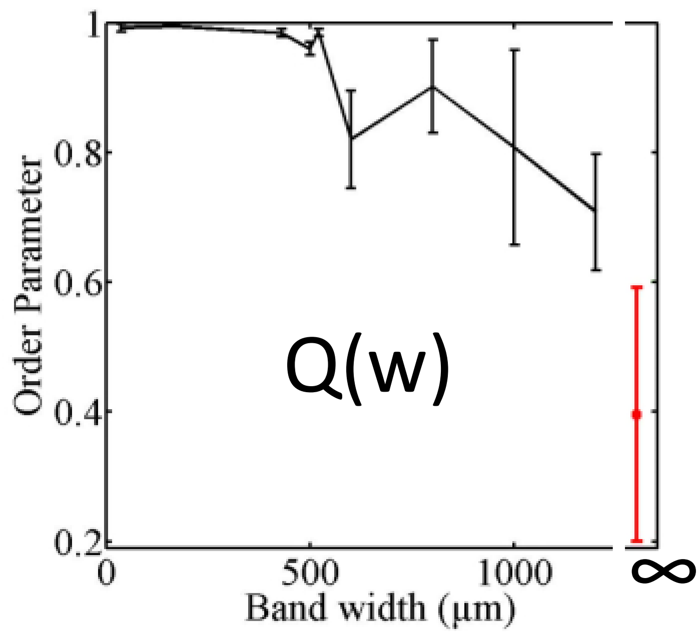

Order Parameter
Band width (μm)
Q(w)
∞

Population-scale vs. individual-scale template

Nanoscale cues regulate the structure and function of macroscopic cardiac tissue constructs

PNAS | January 12, 2010 | vol. 107 | no. 2 | 565–570

Deok-Ho Kim[a,b,1], Elizabeth A. Lipke[a,1], Pilnam Kim[c], Raymond Cheong[a,b], Susan Thompson[a], Michael Delannoy[d], Kahp-Yang Suh[c,2], Leslie Tung[a,2], and Andre Levchenko[a,b,2]

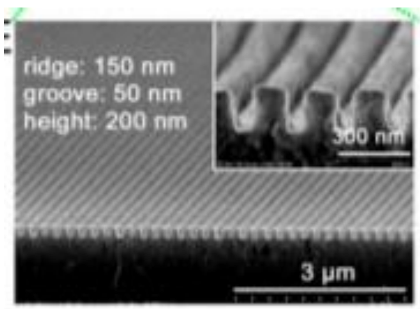

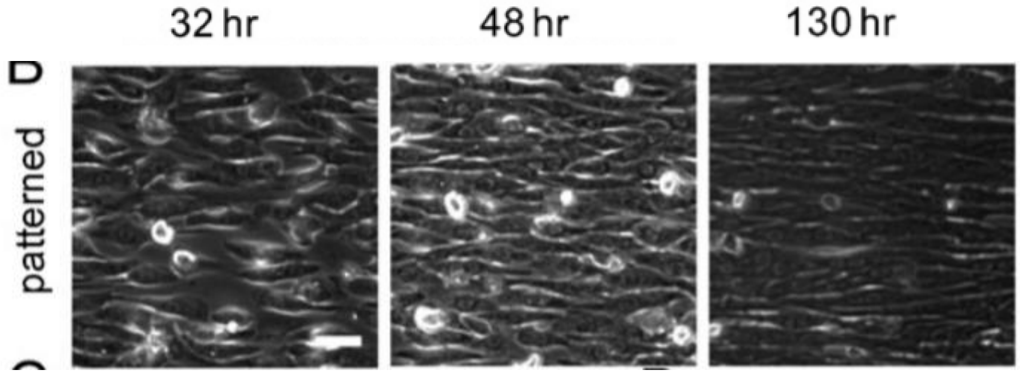

Micro-nano tracks

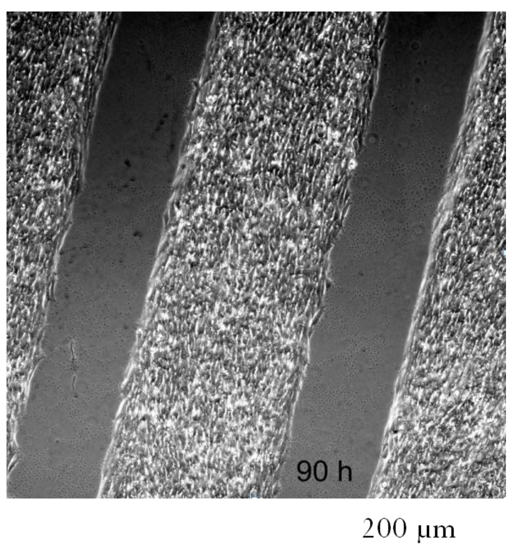

Mesoscopic pattern

Mesoscale contact guidance

Topological defects

Duclos et al. Nat Phys 2017

Defect density decreases with time

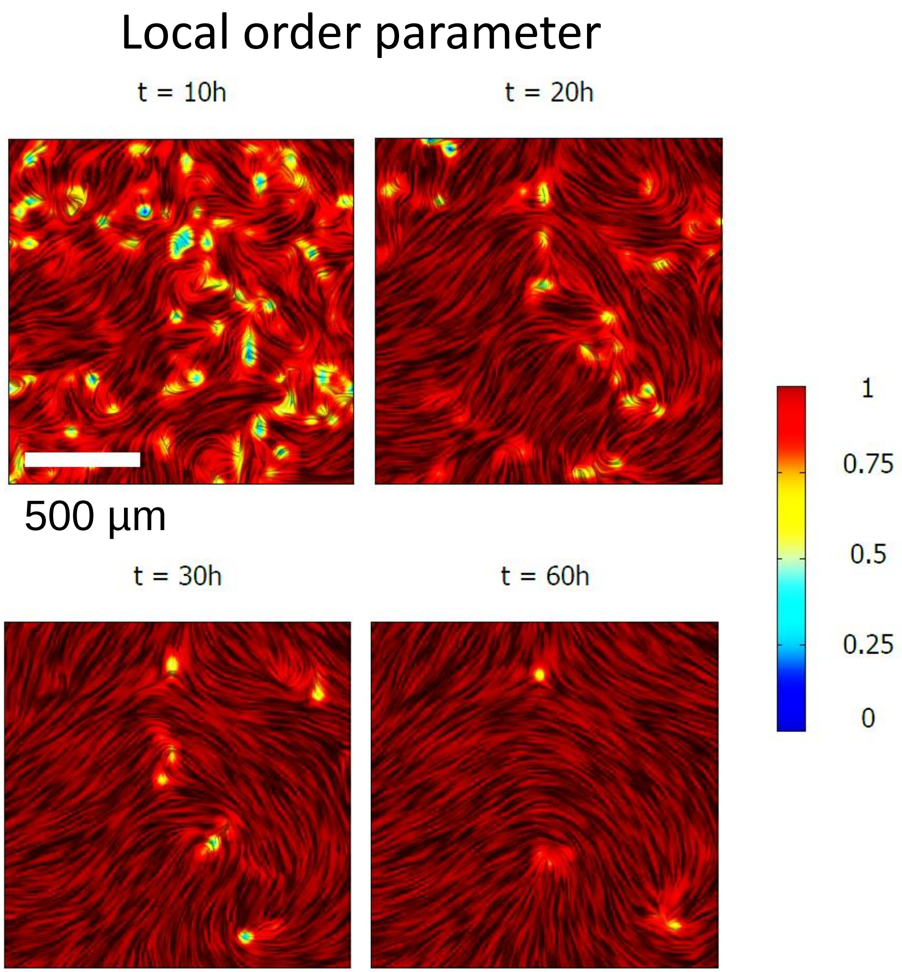

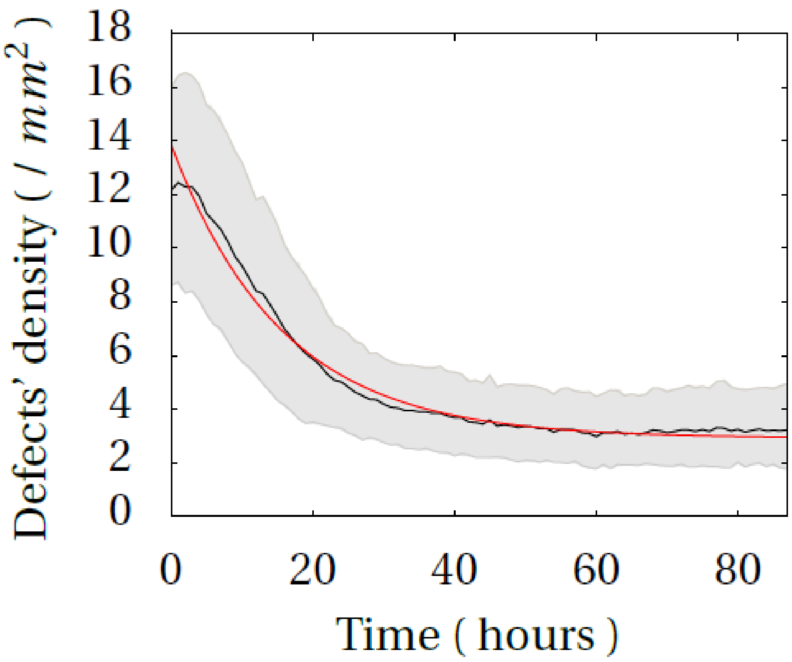

No defect creation
(consistent with contractile system)

Pairwise defects annihilation

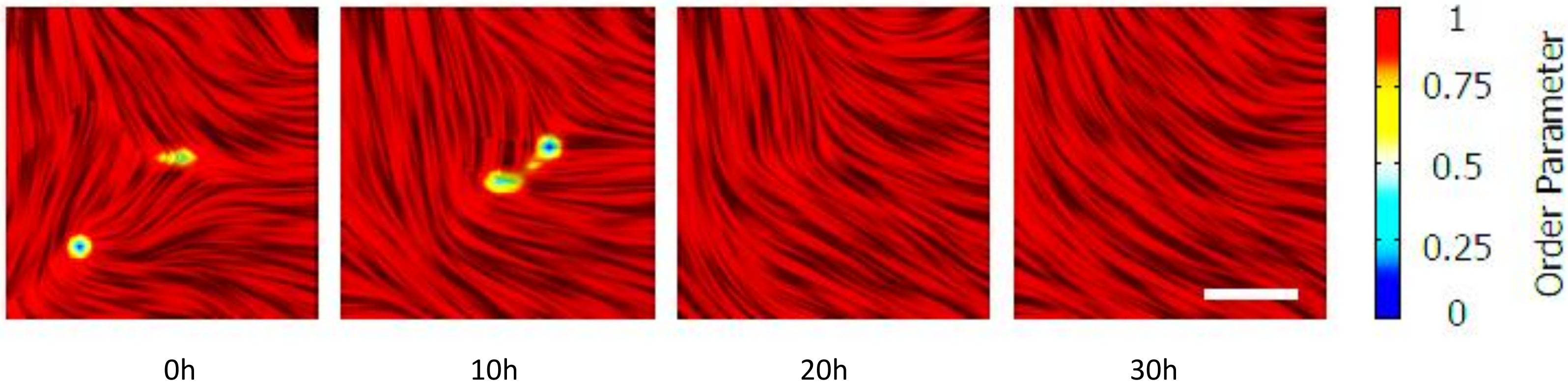

100 μm

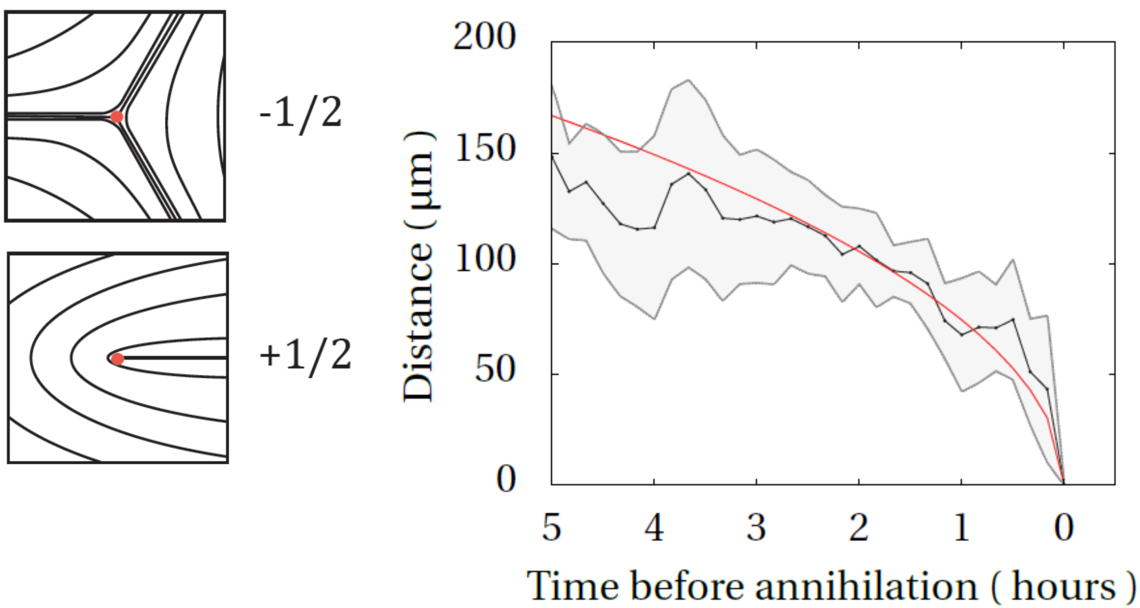

$$d \propto \sqrt{t}$$

(like passive LC)

Confinement in micropatterned circular domains

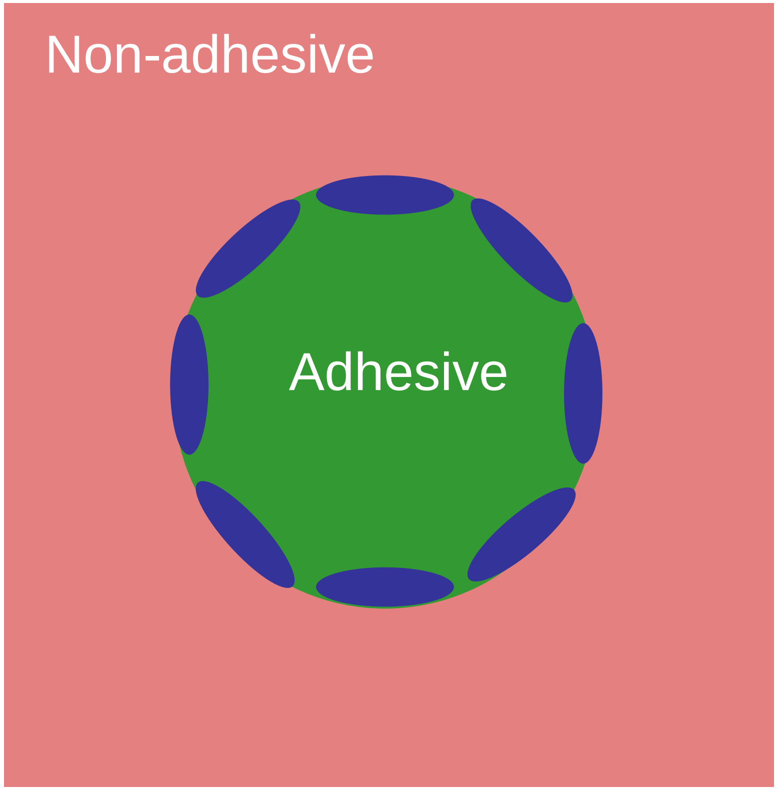

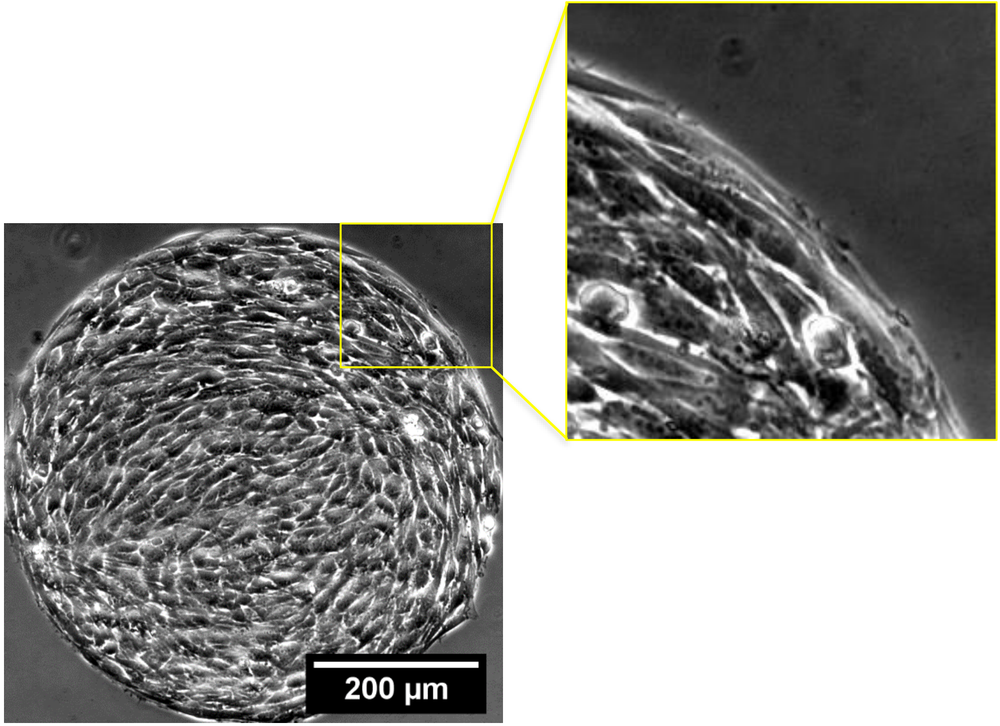

R = 250 µm – 400 µm

➡ Total charge = +1

A central defect ...

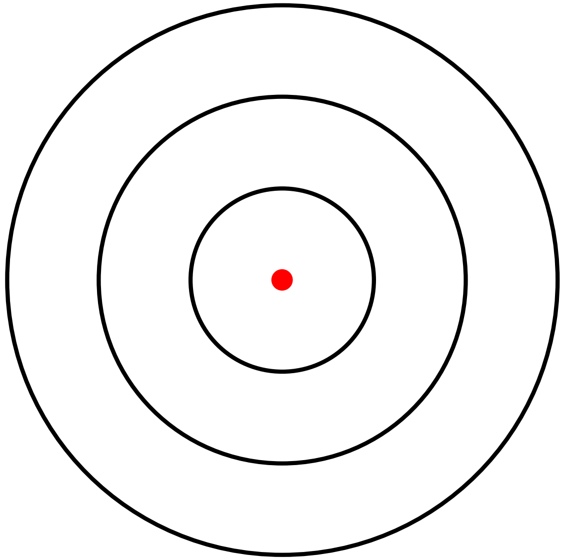

+1

... or two ?

+1/2

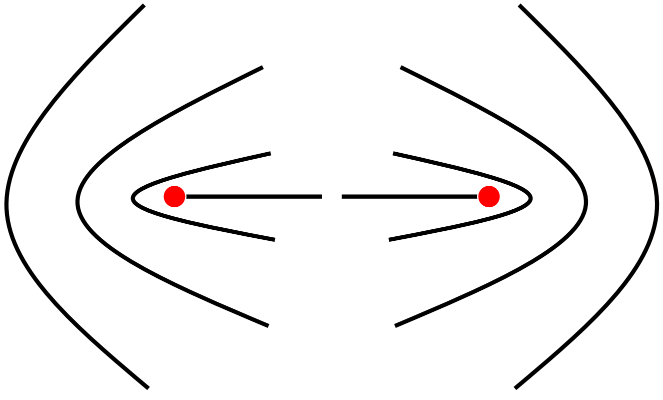

In 2D, +1 defects are not stable and give rise to two +1/2 defects

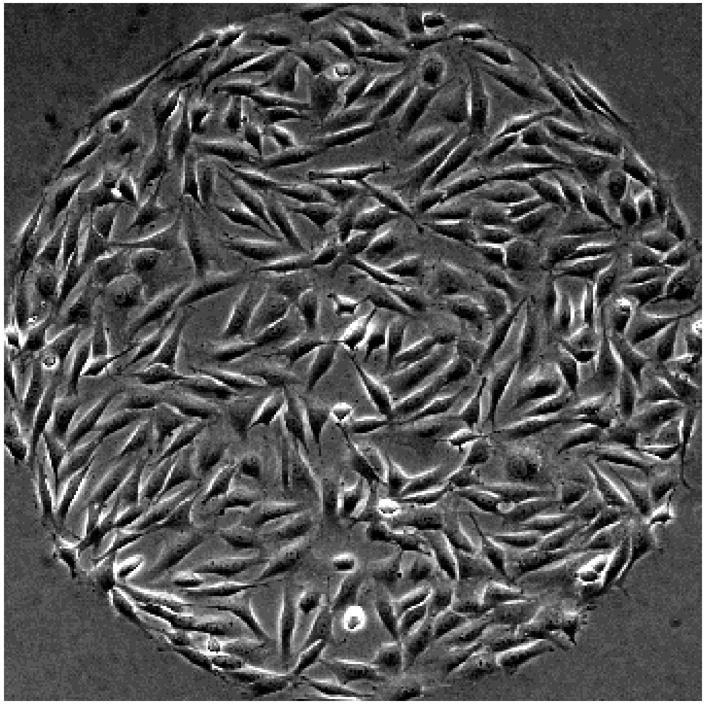

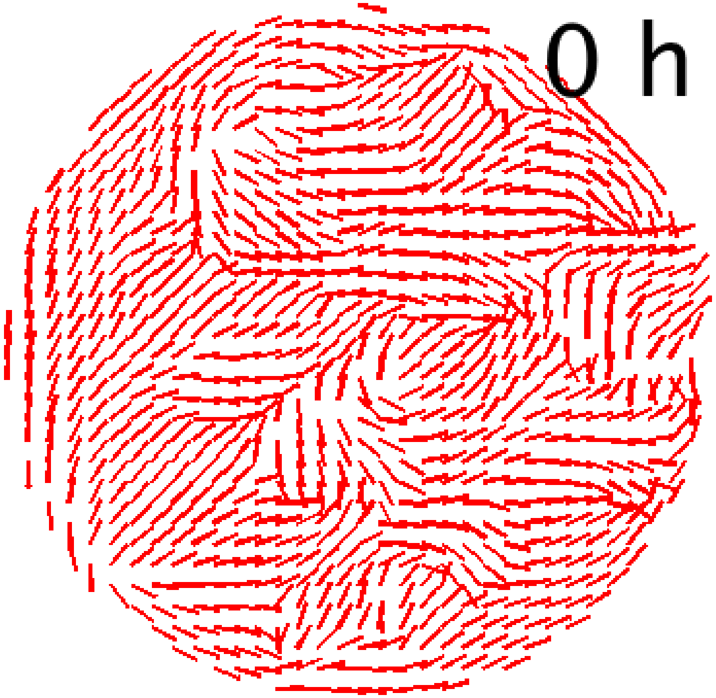

200 µm

Stationary state, 60h after confluence: two +1/2 defects

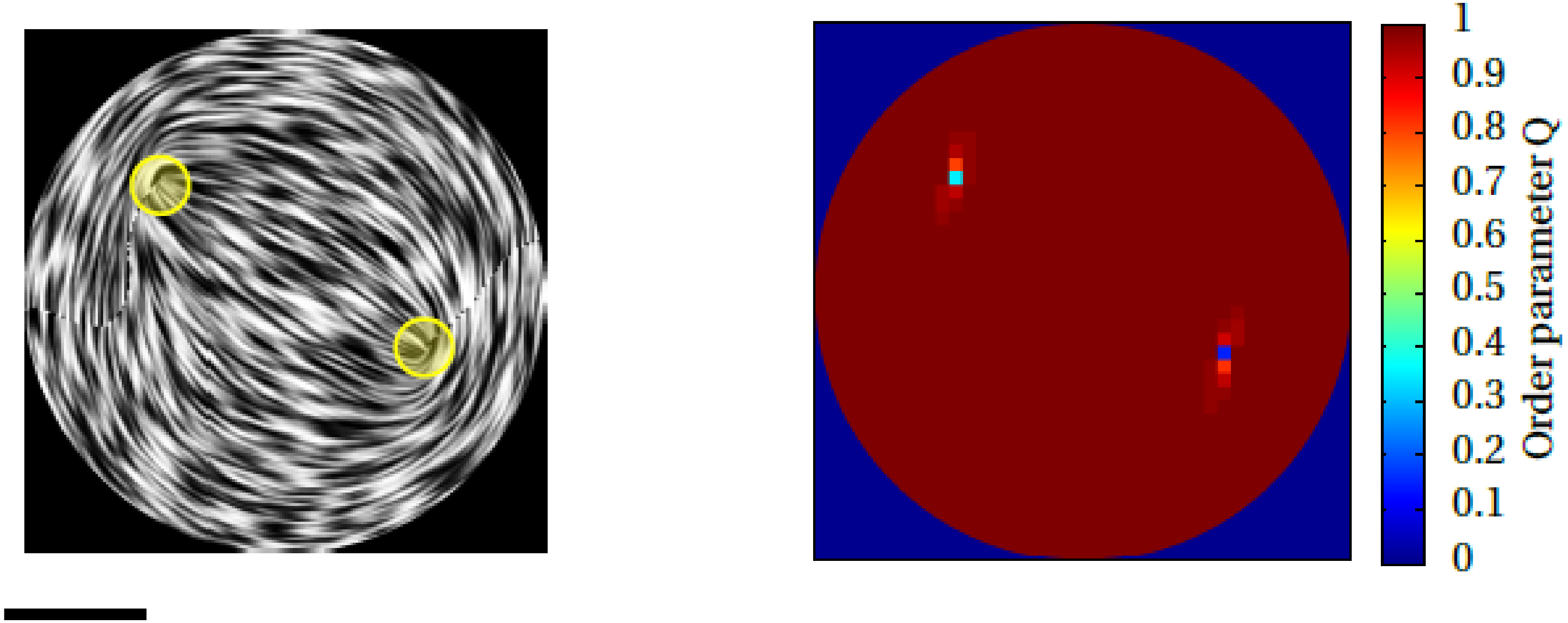

200 µm

Defects' positioning

Steady state - R = 350 μm

$R_1, R_2 > 0$
$\Phi \in [0, \pi]$

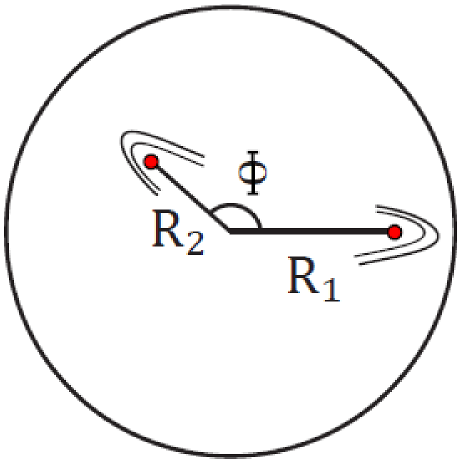

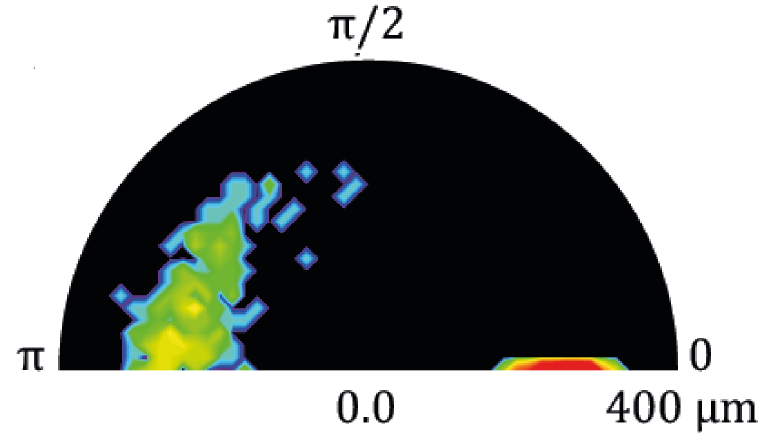

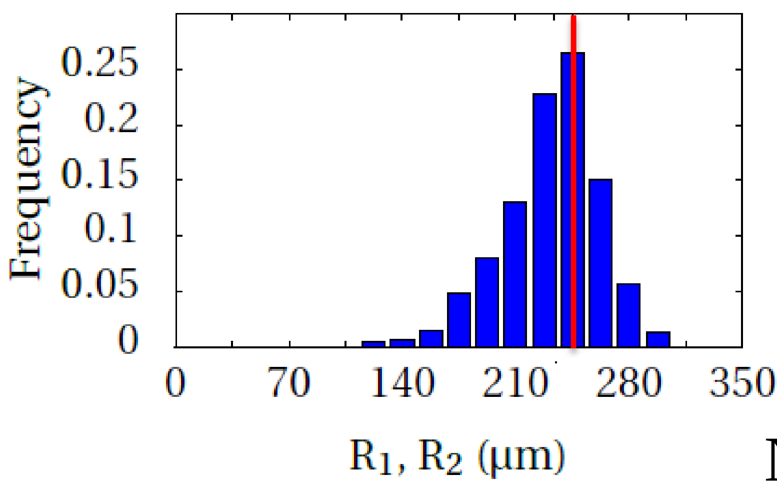

N=357

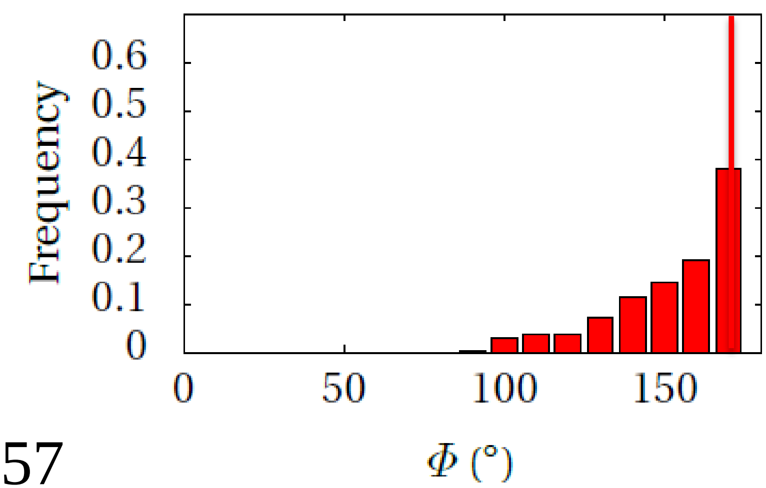

$R_0^* = 245\mu m \pm 30\mu m$ / $\Phi^* = \pi$

The defects' radial position scales with the domain radius

$r_0^* = \alpha \cdot R$ with α = 0.67 $\pm$ 0.02

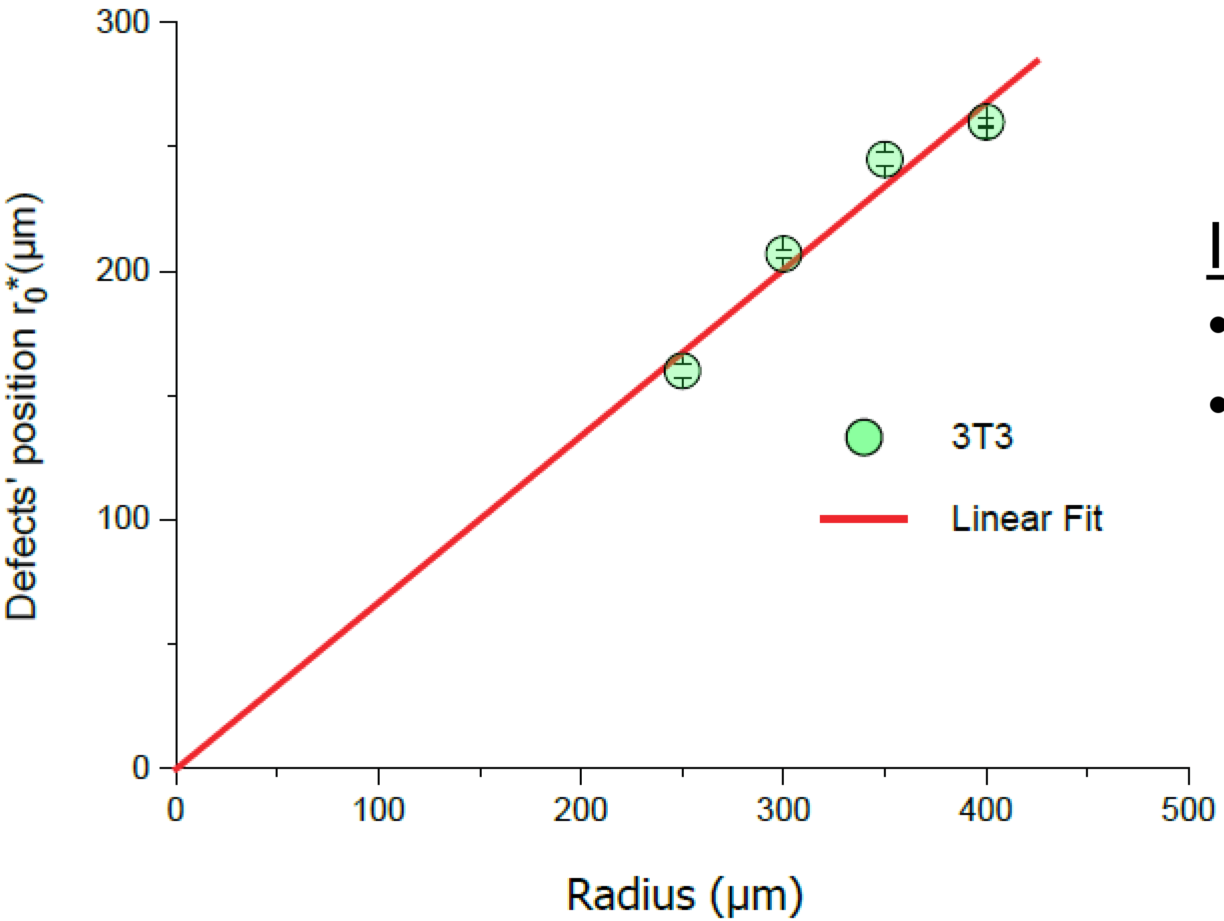

Independent of:

- Cell contractility
- Cell type

The nematic disk model

(Christoph Erlenkaemper, Jean-François Joanny)

Hypotheses:

- Parallel alignment at the edges
- $K_1=K_3=K$
- No active stress

2 degrees of freedom

R and Φ

(Defects' positions uncorrelated)

Experimental data

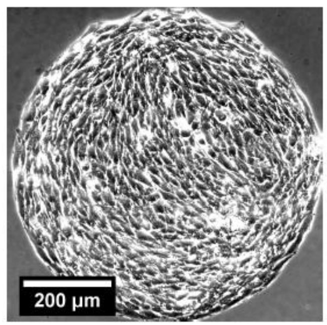

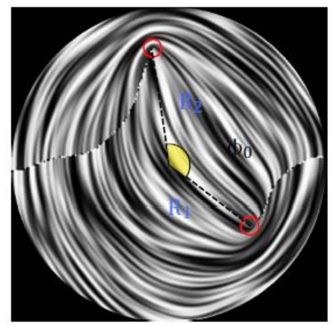

Model

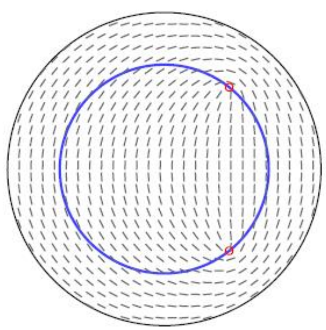

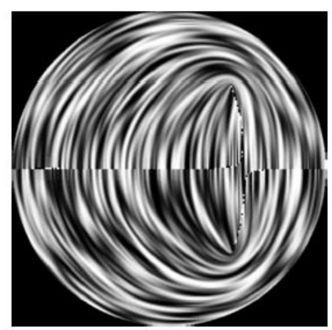

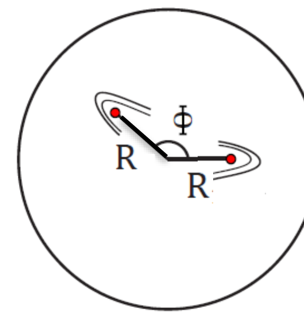

Frank-Oseen free energy

$$F(r_0,\phi_0) = \frac{K}{2}\int_{\Omega}(\nabla \vec{n})^2 dS$$

2D Energy map (polar)

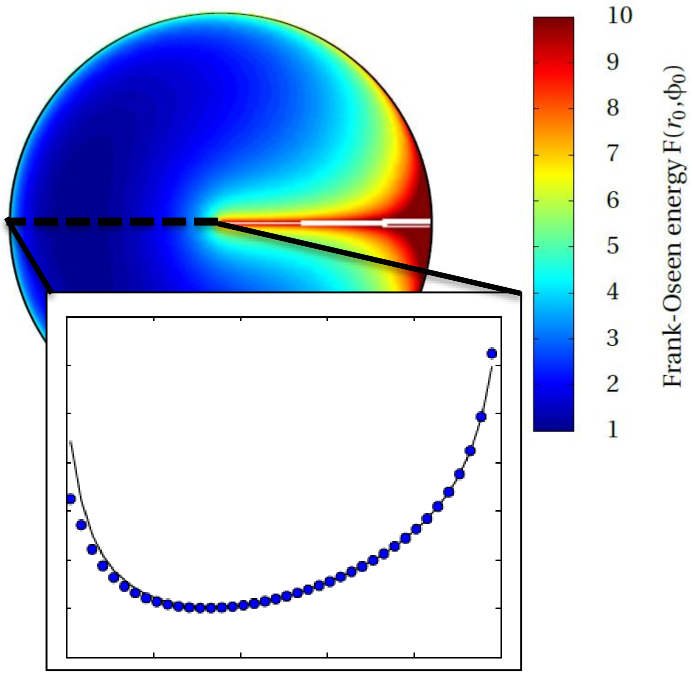

1D Energy map (Φ=π)

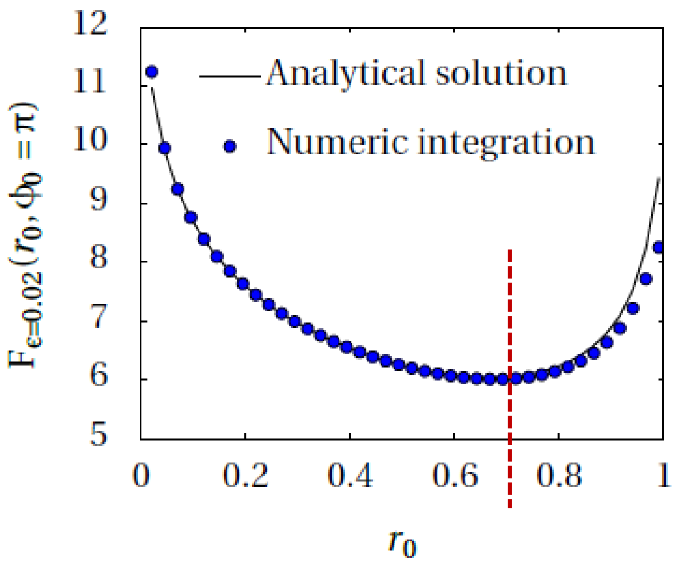

$r_0^* = 5^{-1/4}\cdot R \approx 0.67\cdot R$

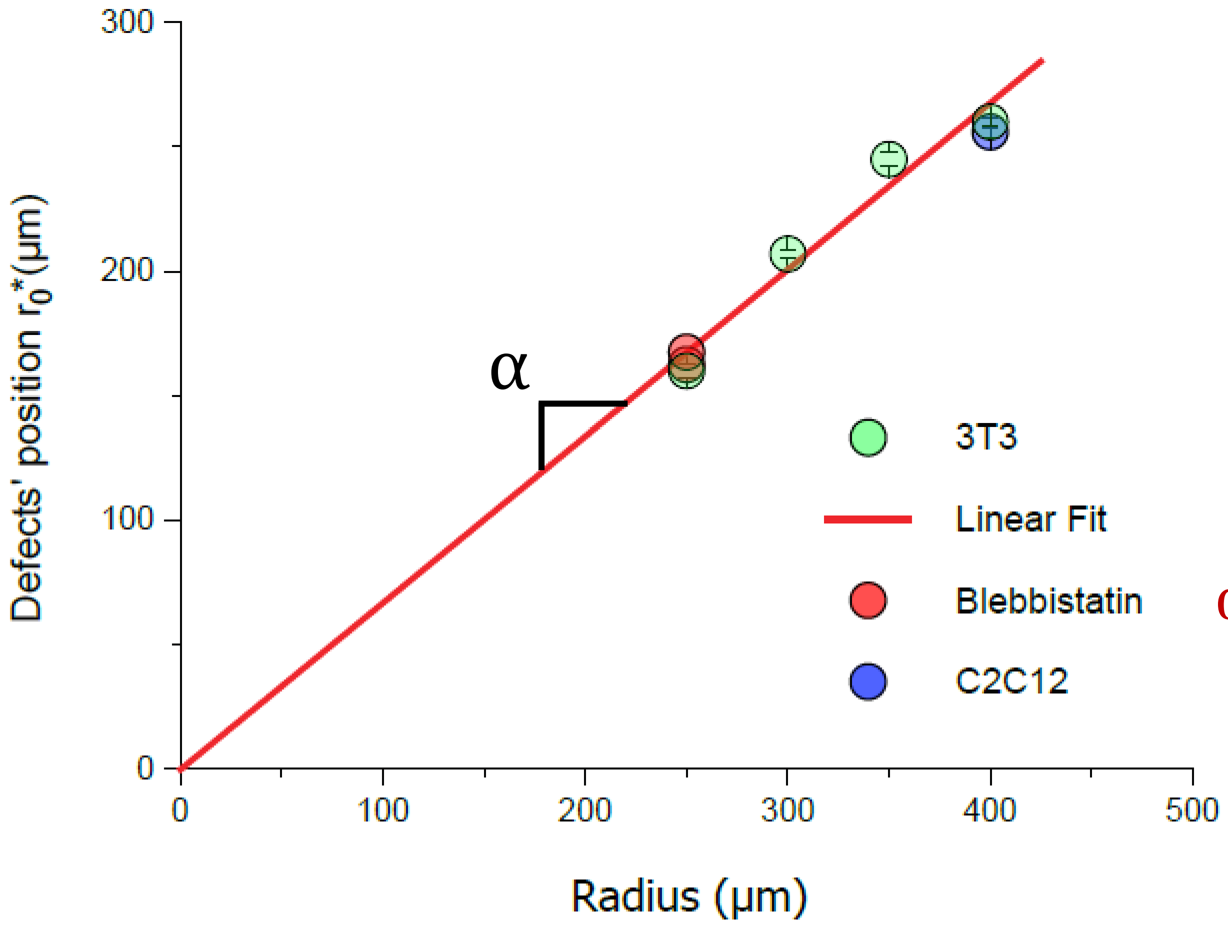

$\alpha_{exp} = 0.67 \pm 0.02$

$\alpha_{theory} = 5^{-1/4} \approx 0.668$

<u>α independant of:</u>

- Activity
- Nematic elasticity K

Epithelial branching (lung) (C. Nelson)

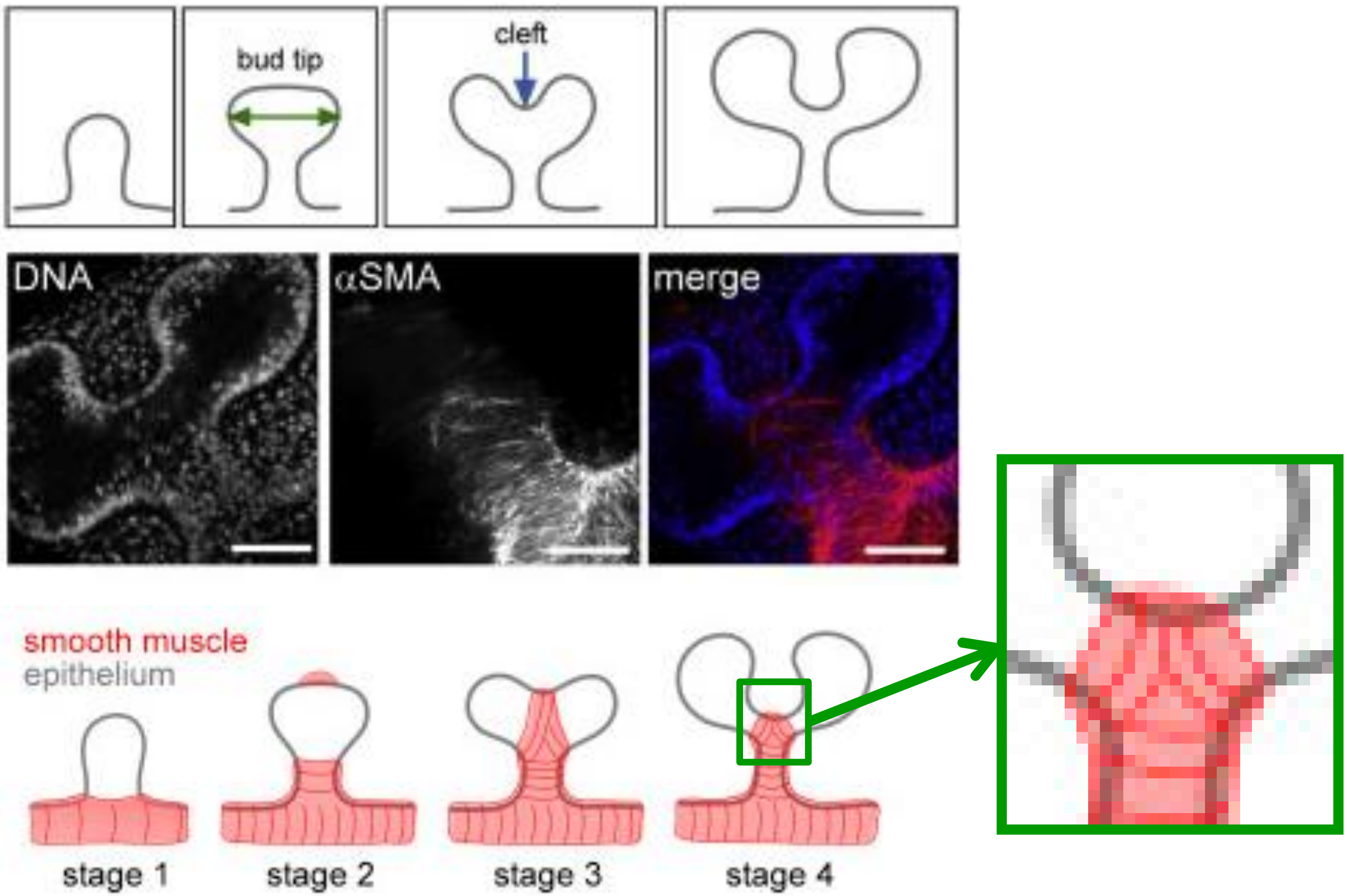

Kim et al. Dev. Cell 2015

Spontaneous shear flows

Duclos et al. Nat Phys 2018

Spontaneous tilt

RPE1
C2C12

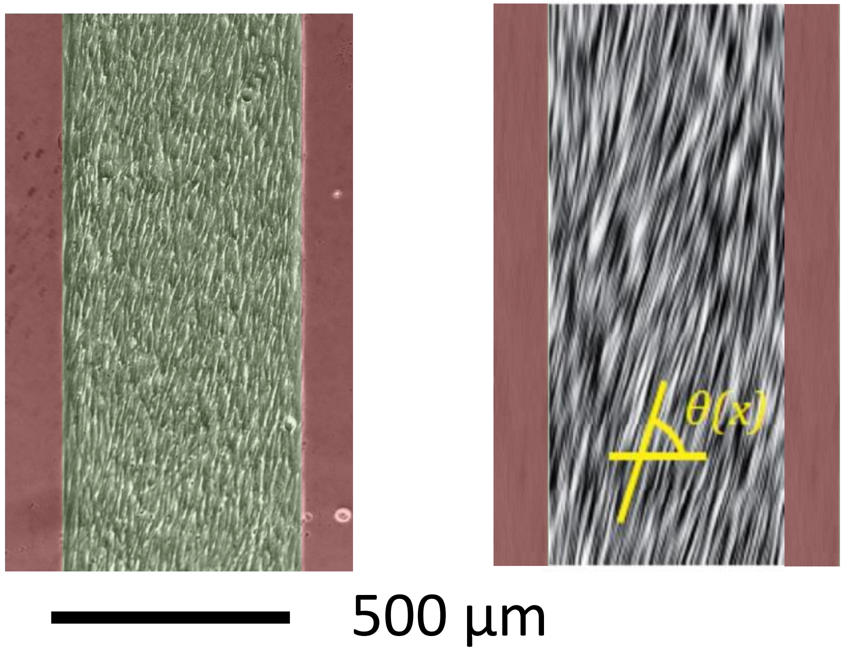

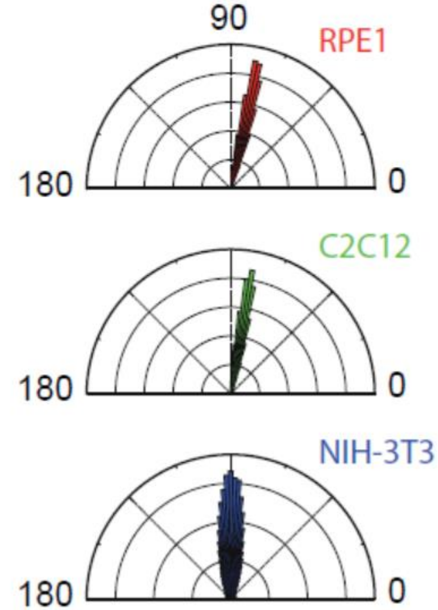

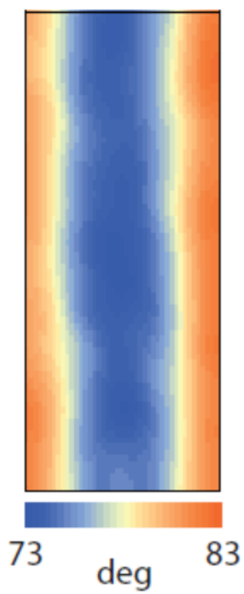

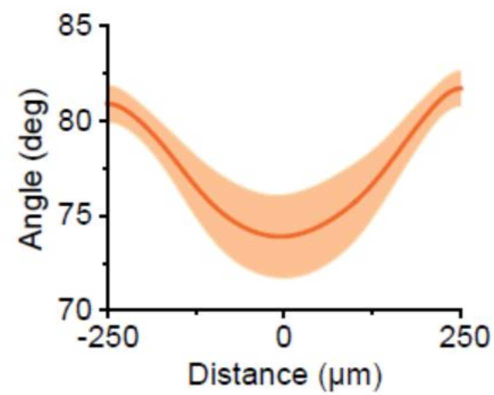

3T3

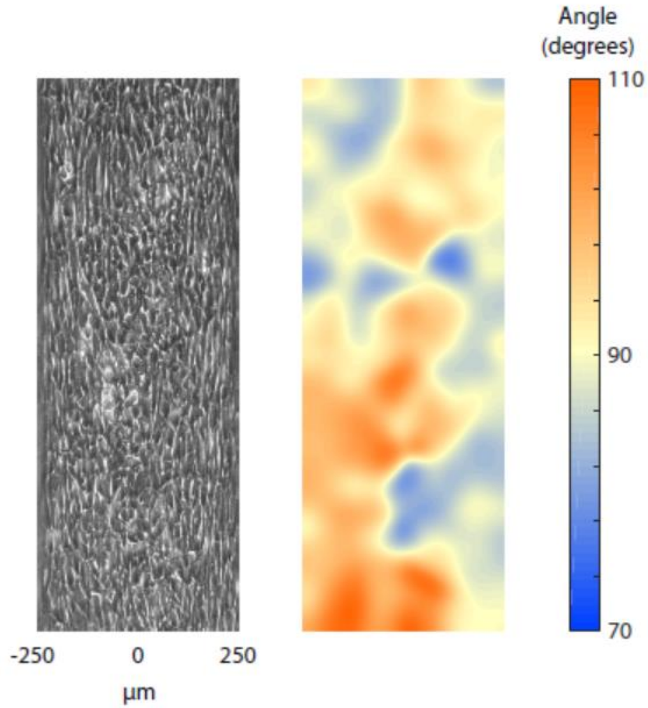

The dynamics: Spontaneous Flows

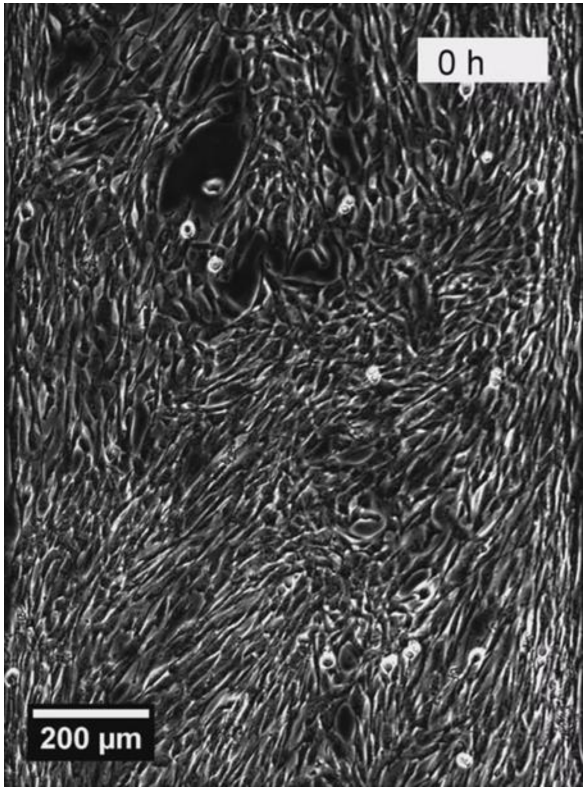

Spontaneous Flows

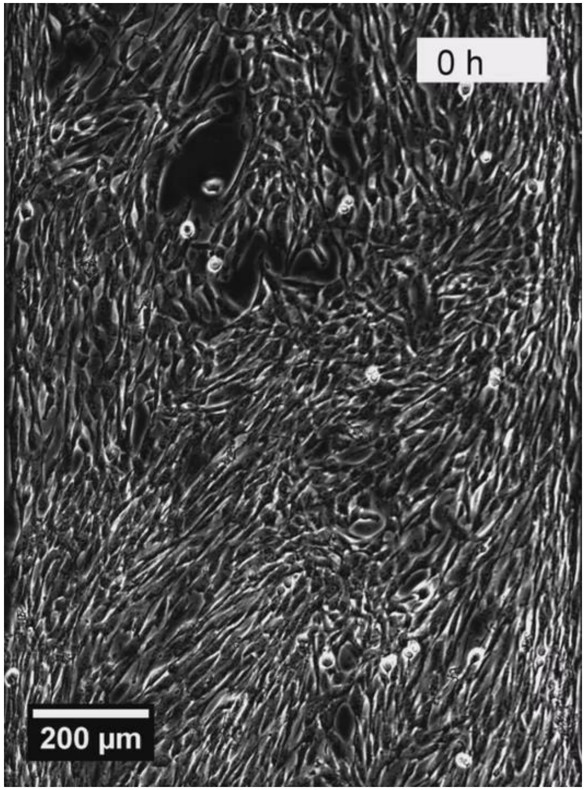

Supplementary Movie 4

Intra-strand dynamics of file-like collective invasion

Excitation: 850nm (25mW) and 910nm (30mW)
Frame rate: 1 frame / 10min
Total time: 70min

SHG (red): Collagen fibers, striated muscles
Histone-2B/eGFP (blue): Tumor cell nuclei
TM-Rhodamine (green): 70kDa-dextran labeling blood vessels, phagocytes

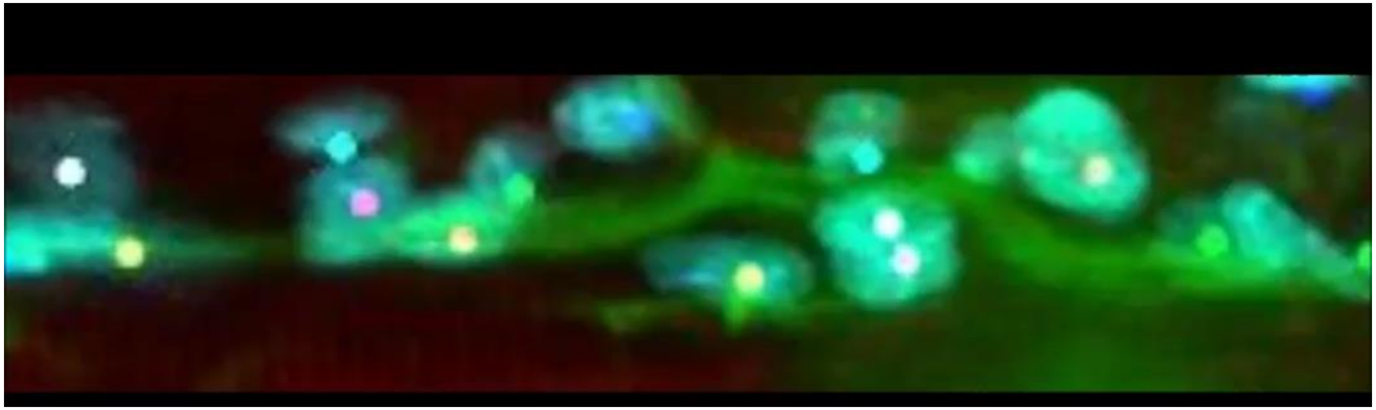

P Friedl 2012

Supplementary Movie 4

Intra-strand dynamics of file-like collective invasion

Excitation: 850nm (25mW) and 910nm (30mW)
Frame rate: 1 frame / 10min
Total time: 70min

SHG (red): Collagen fibers, striated muscles
Histone-2B/eGFP (blue): Tumor cell nuclei
TM-Rhodamine (green): 70kDa-dextran labeling blood vessels, phagocytes

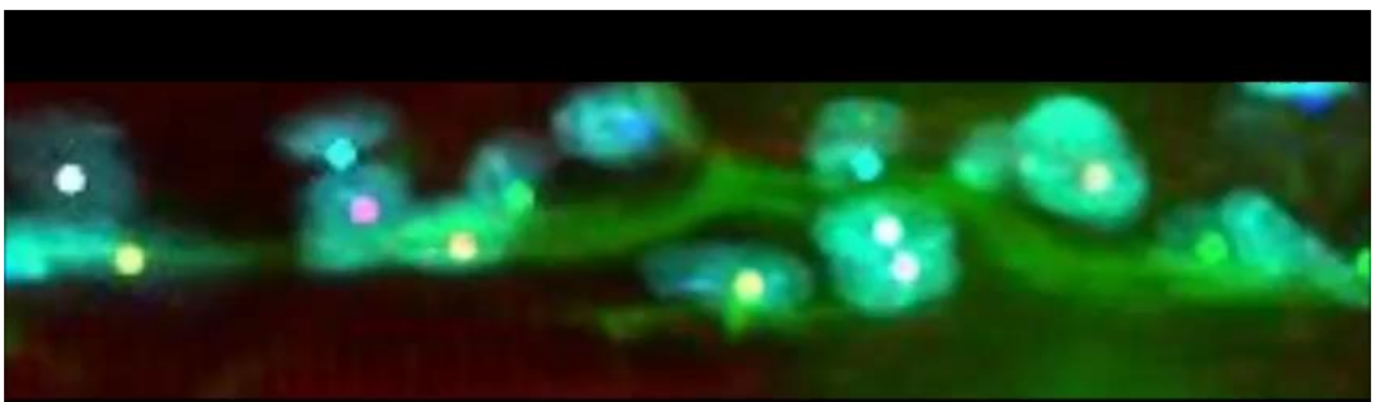

P Friedl 2012

Spontaneous Flows

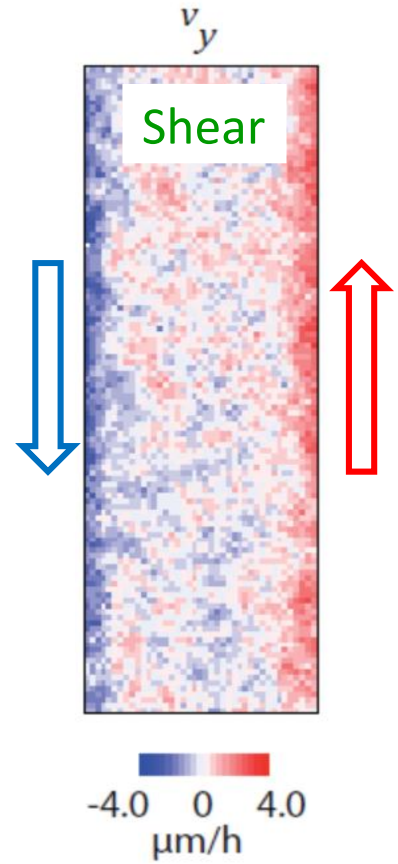

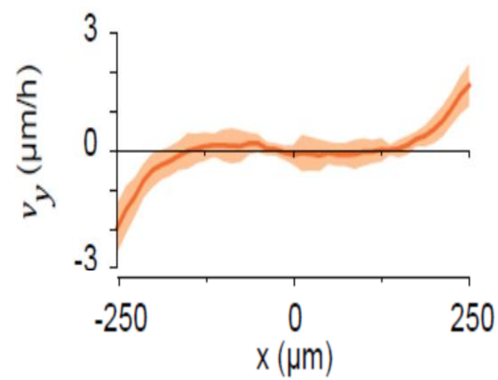

Inhibiting cell activity (blebbistatin)

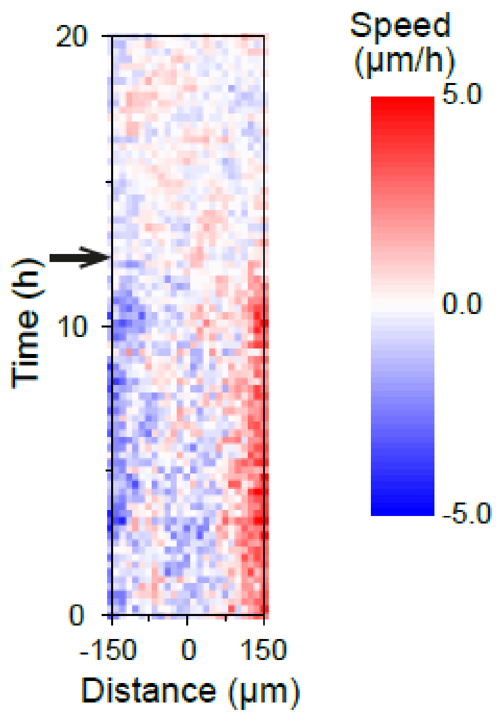

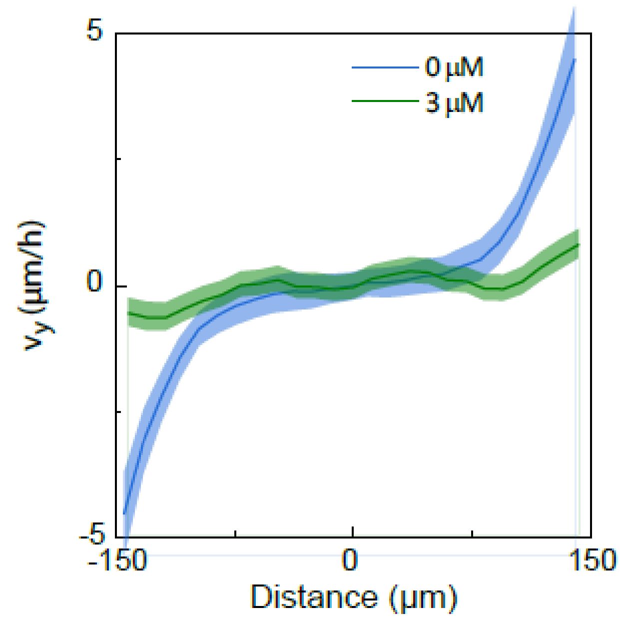

- Shear flow results from cell activity

Width dependence

NIH 3T3
C2C12
RPE1

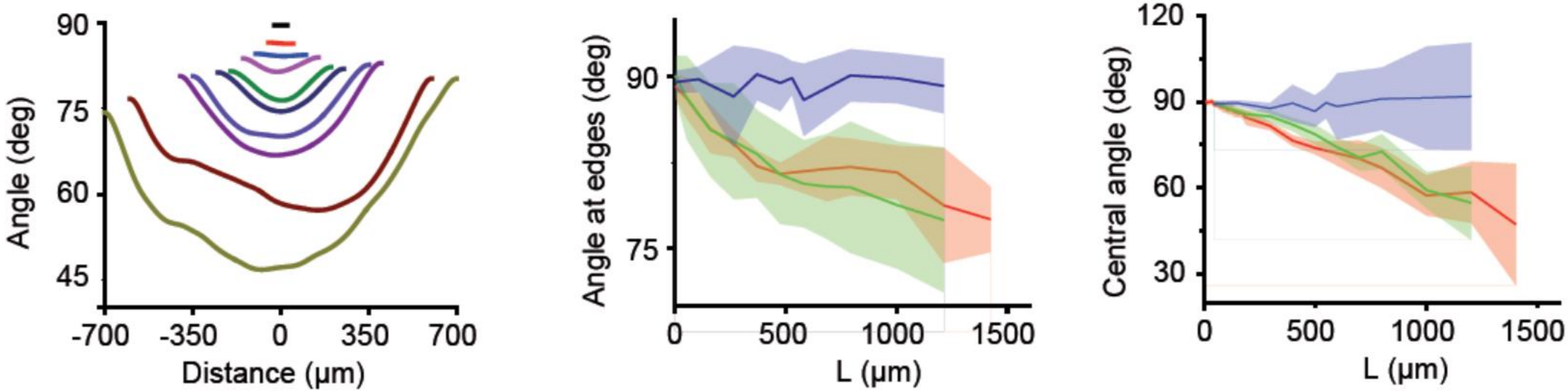

Active gel theory

Spontaneous flows in actomyosin systems

(R. Voituriez, J.-F. Joanny, J. Prost EPL 2005)

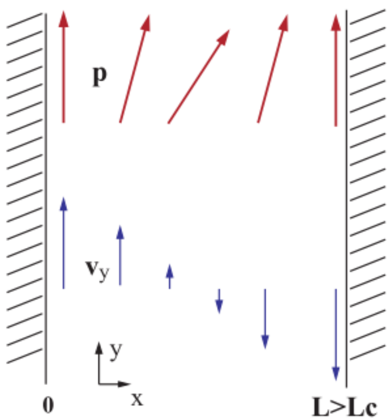

+

New boundary conditions to account for finite edge angle:

$$\pm K\partial_x\theta + W_s(\theta - \frac{\pi}{2}) = 0|_{x=\pm L/2}$$

$$\partial_t\theta = \frac{h_\perp}{\gamma}\frac{(4\eta + \gamma(\nu^2 - 2\nu\cos 2\theta + 1))}{(4\eta + \gamma\nu^2\sin 2\theta^2)} - \frac{\zeta\Delta\mu\sin 2\theta(\nu\cos 2\theta - 1)}{(4\eta + \gamma\nu^2\sin 2\theta^2)}$$ with $$h_\perp = K\partial_x^2\theta$$

Abstract. – We study theoretically the effects of confinement on active polar gels such as the actin network of eukaryotic cells. Using generalized hydrodynamics equations derived for active gels, we predict, in the case of quasi–one-dimensional geometry, a spontaneous flow transition from a homogeneously polarized immobile state for small thicknesses, to a perturbed flowing state for larger thicknesses. The transition is not driven by an external field but by the activity of the system. We suggest several possible experimental realizations.

Active gel theory

Spontaneous flows in actomyosin systems

(R. Voituriez, J.-F. Joanny, J. Prost EPL 2005)

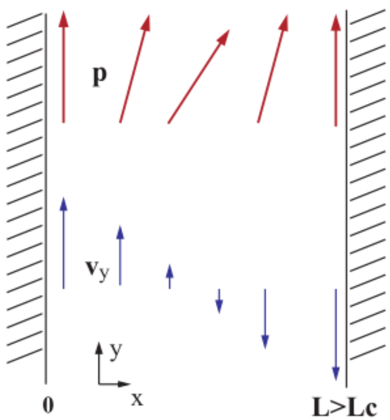

+

New boundary conditions to account for finite edge angle:

$$\pm K\partial_x\theta + W_s(\theta - \frac{\pi}{2}) = 0|_{x=\pm L/2}$$

$$\partial_t\theta = \frac{h_\perp}{\gamma}\frac{(4\eta+\gamma(\nu^2-2\nu\cos 2\theta+1))}{(4\eta+\gamma\nu^2\sin 2\theta^2)} - \frac{\zeta\Delta\mu\sin 2\theta(\nu\cos 2\theta-1)}{(4\eta+\gamma\nu^2\sin 2\theta^2)}$$ with $$h_\perp = K\partial_x^2\theta$$

Abstract. – We study theoretically the effects of confinement on active polar gels such as the actin network of eukaryotic cells. Using generalized hydrodynamics equations derived for active gels, we predict, in the case of quasi–one-dimensional geometry, a spontaneous flow transition from a homogeneously polarized immobile state for small thicknesses, to a perturbed flowing state for larger thicknesses. The transition is not driven by an external field but by the activity of the system. We suggest several possible experimental realizations.

Active gel theory

$$L \gtrsim L_c \longrightarrow \theta \sim \sqrt{L - L_c}$$

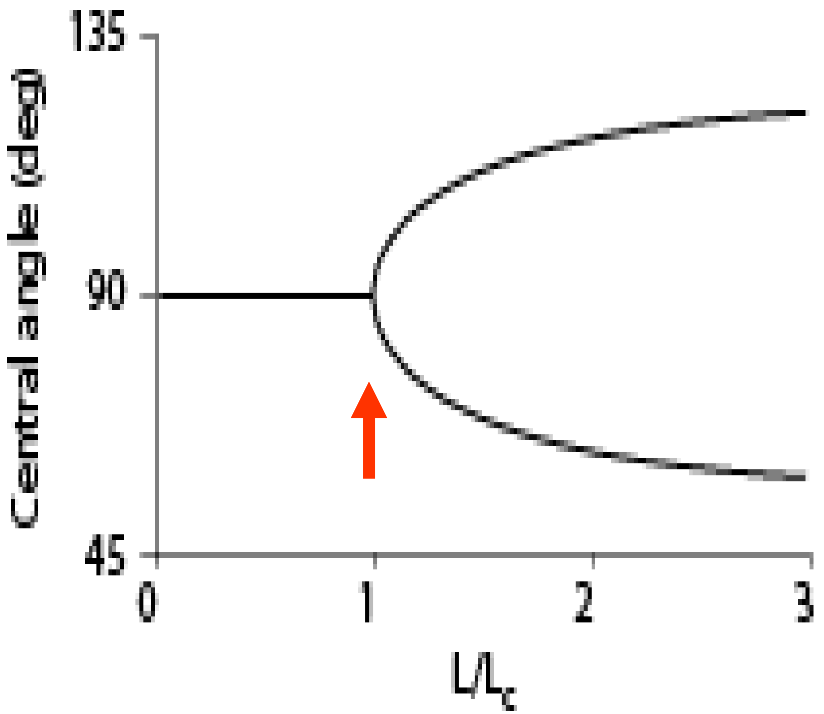

A *Fréedericksz transition* controlled by the activity of the cells

Width dependence

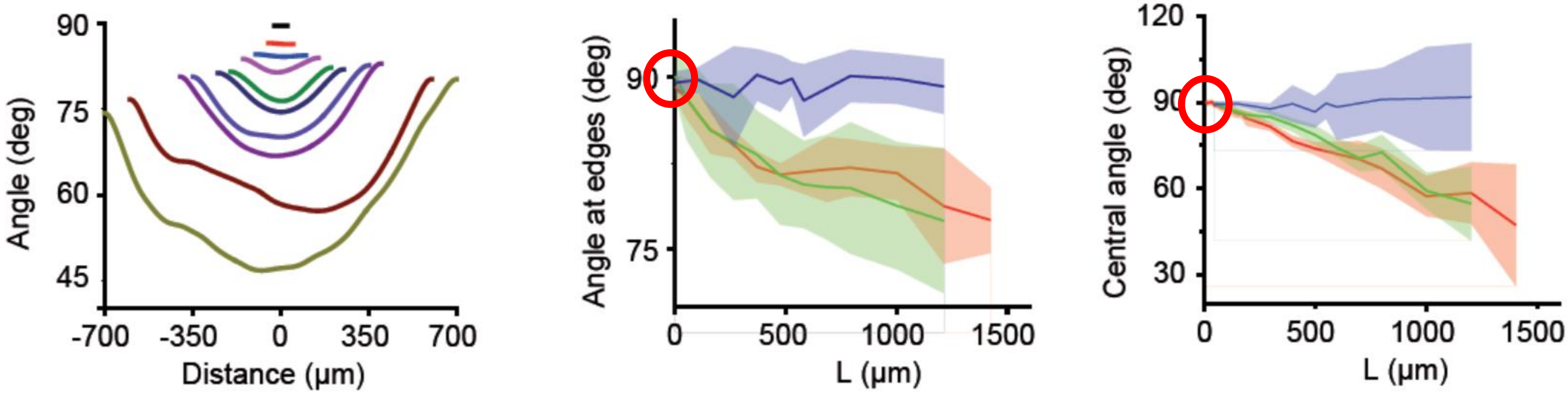

Narrow stripes

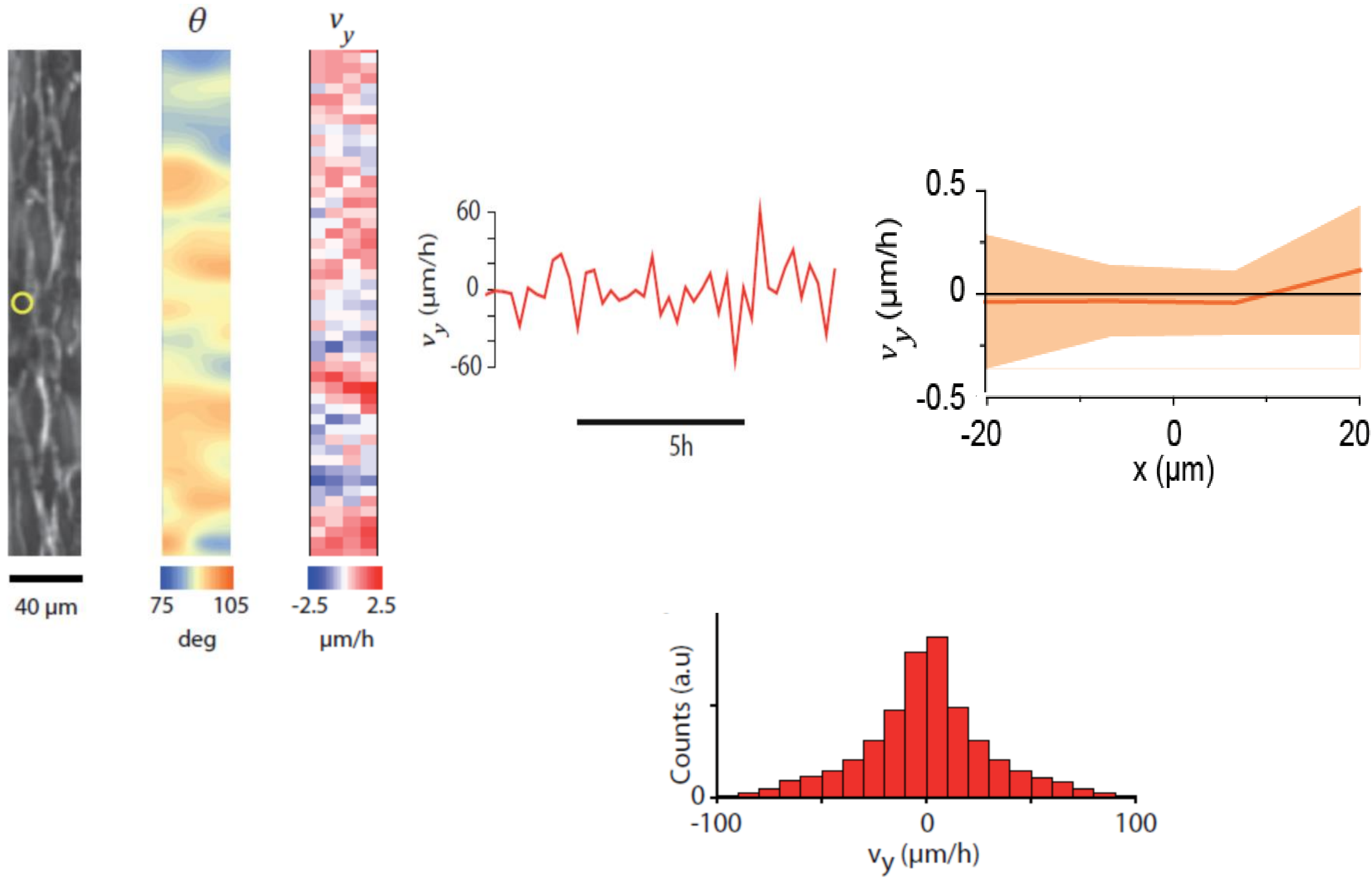

A transition at small widths

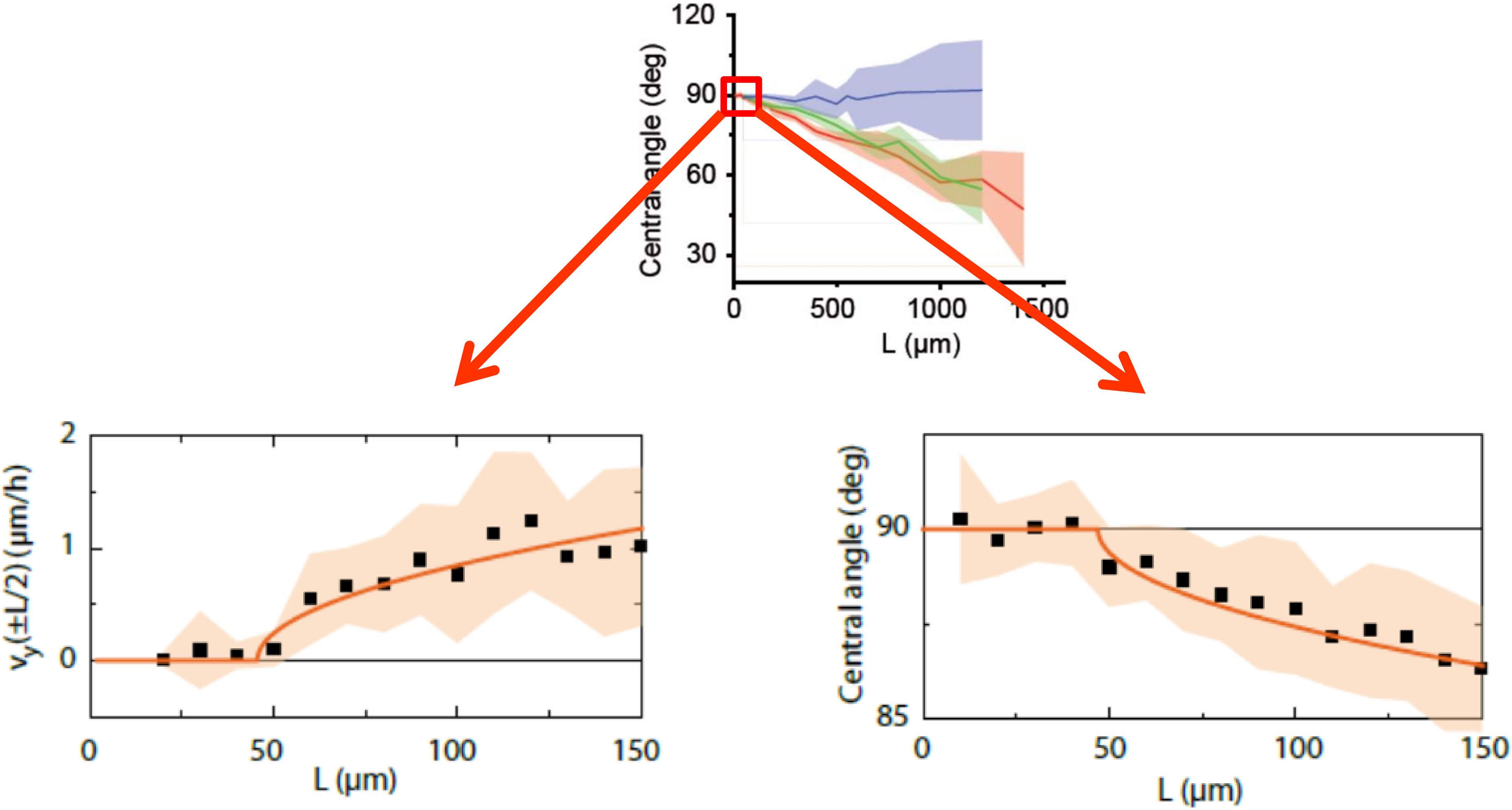

$$L \gtrsim L_c \longrightarrow \theta \sim v_y \sim \sqrt{L - L_c}$$

A *Fréedericksz transition* controlled by the activity of the cells

Cell proliferation → Convergent flows

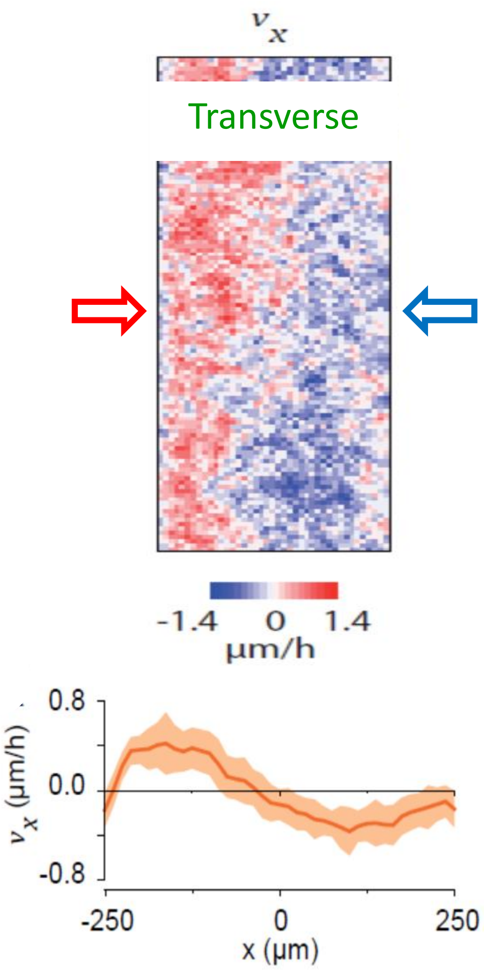

The return of friction

Friction-less profile
(expected from theory)

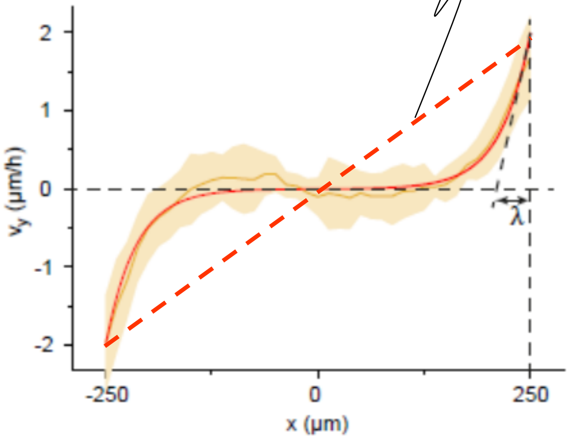

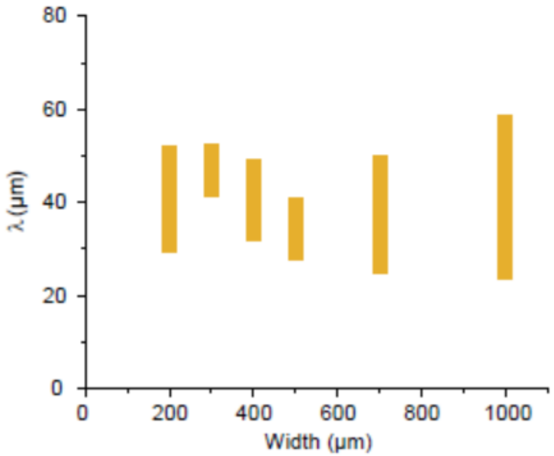

Friction is independent of geometry

A chiral arrangement

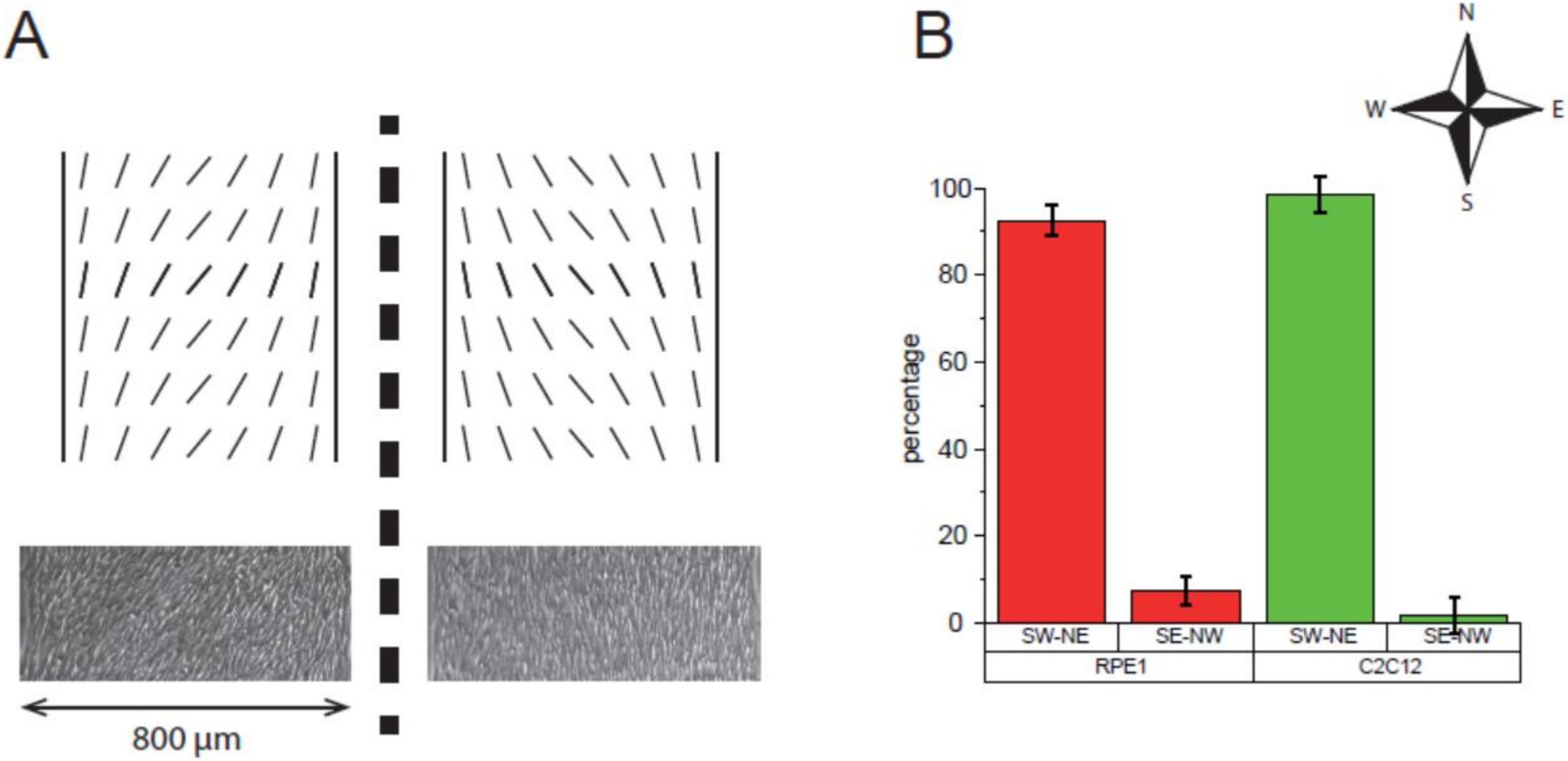

Single cell vs. population-scale chirality: origin ? Amplification ?

Cancer cells HT1080

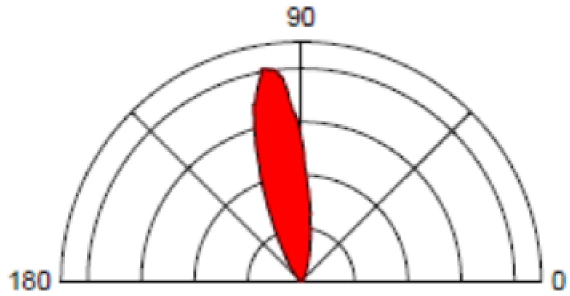

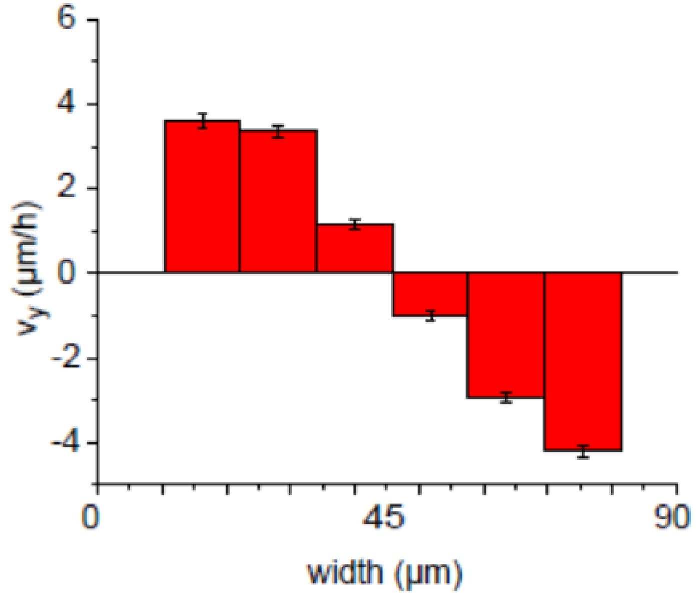

Opposite sign of the chirality !

friction

transverse flow

chirality

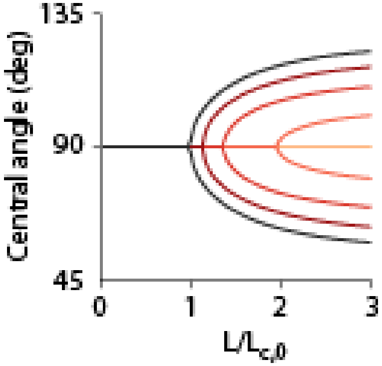

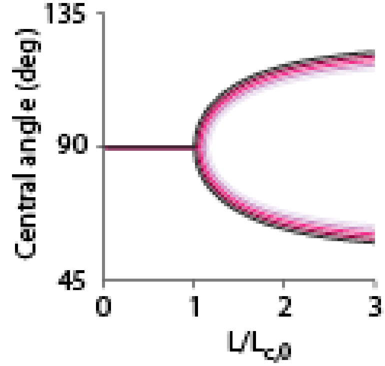

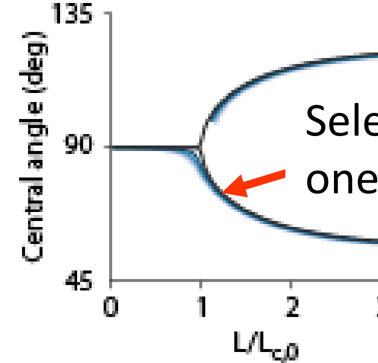

Selection of one branch

3T3 (?)

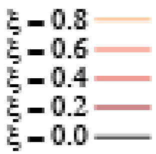

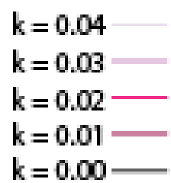

- Controls the dynamics of the director’s orientation

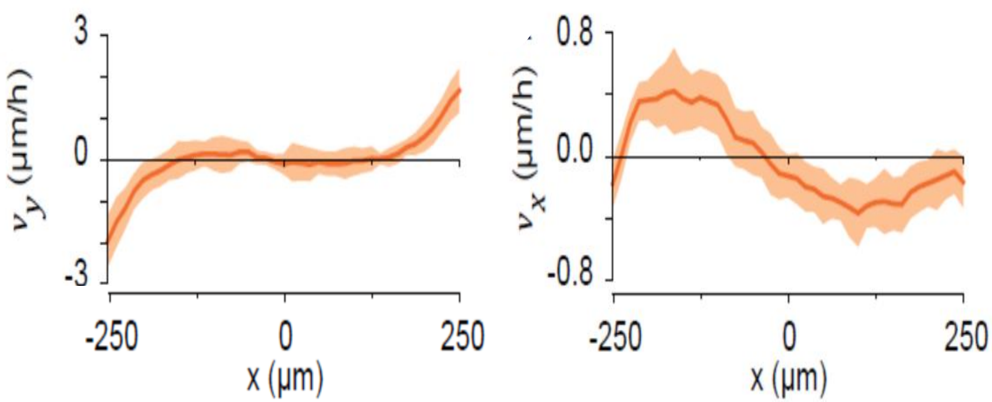

Cranking up the activity: Cellular turbulence

Blanch-Mercader, Yashunsky et al. PRL 2019

HBE cells (Human Bronchial Epithelial)

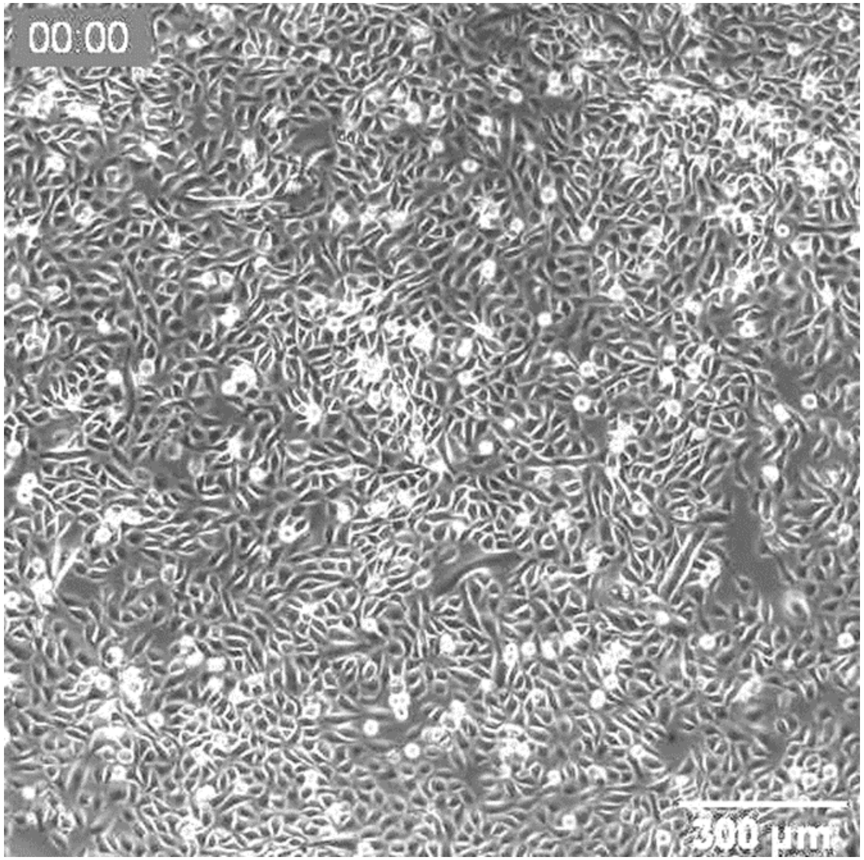

HBE cells (Human Bronchial Epithelial)

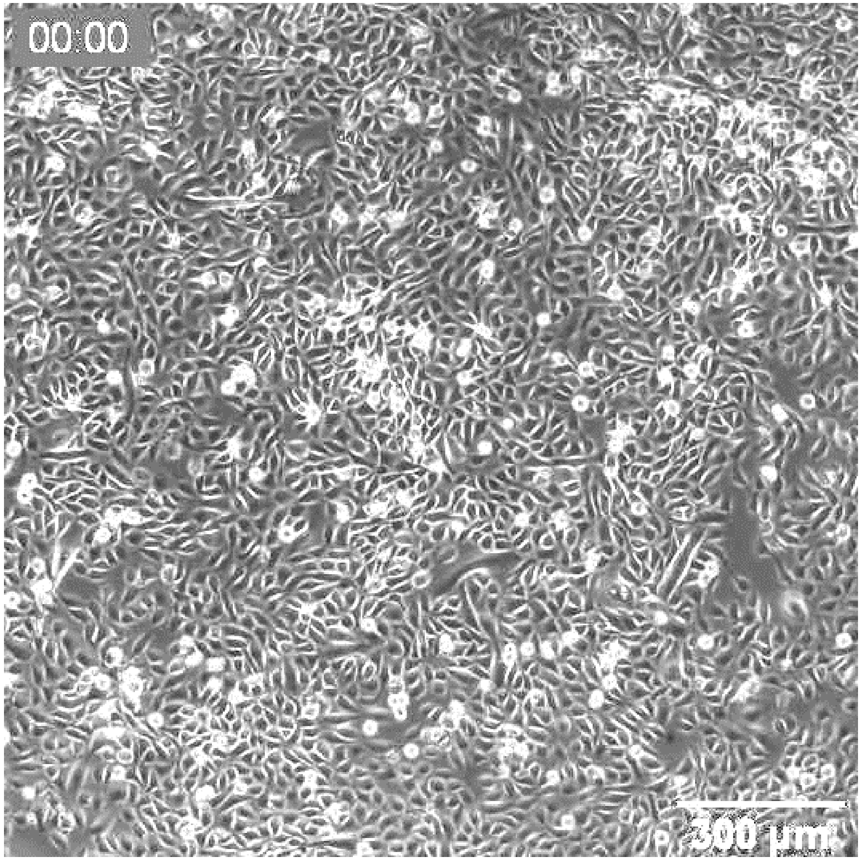

Vorticity field

$$\omega = \partial_x v_y - \partial_y v_x$$

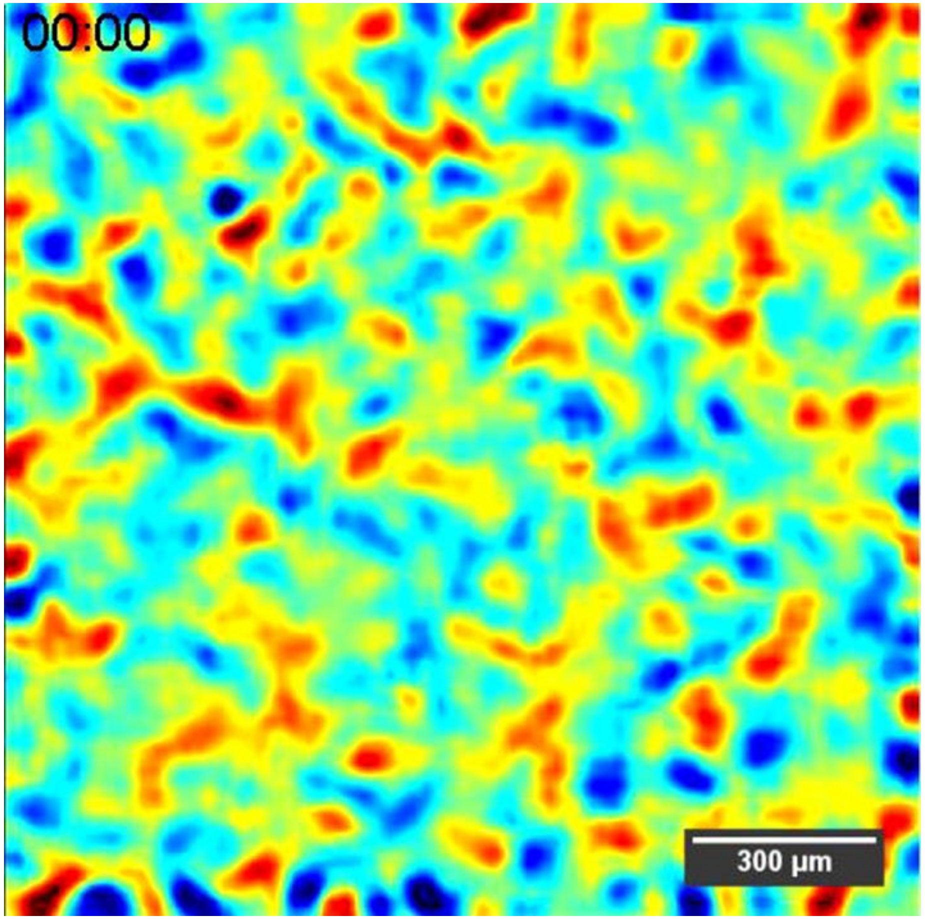

Vorticity field

$$\omega = \partial_x v_y - \partial_y v_x$$

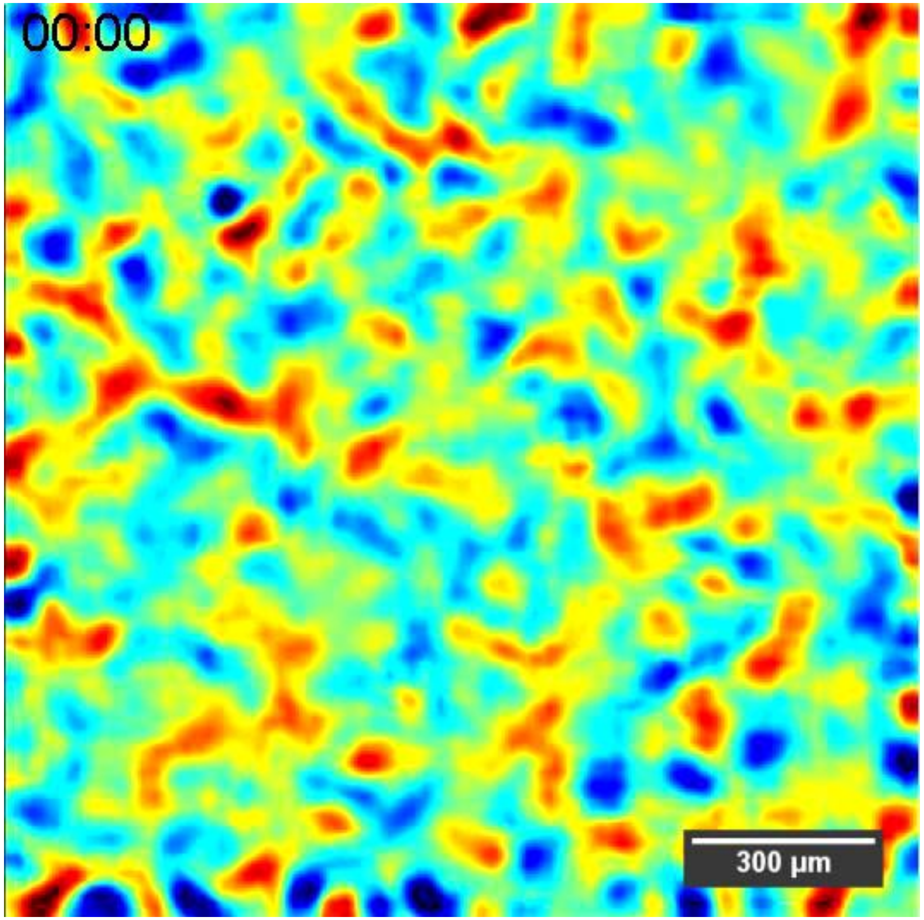

Examples of low-Reynolds number turbulence

Bacterial turbulence

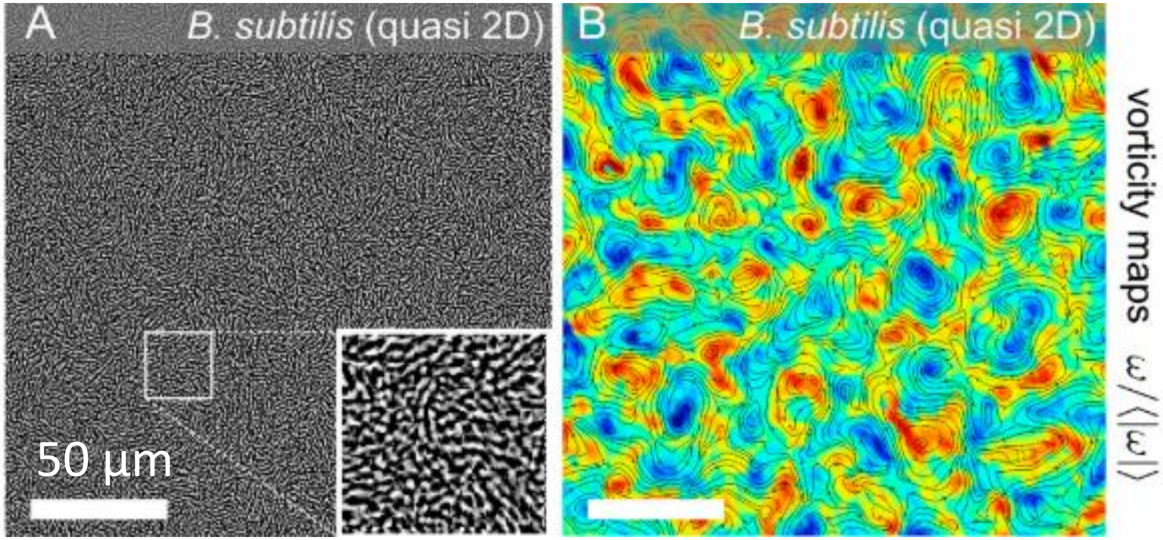

Wensink PNAS 2012

Microtubules + kinesin

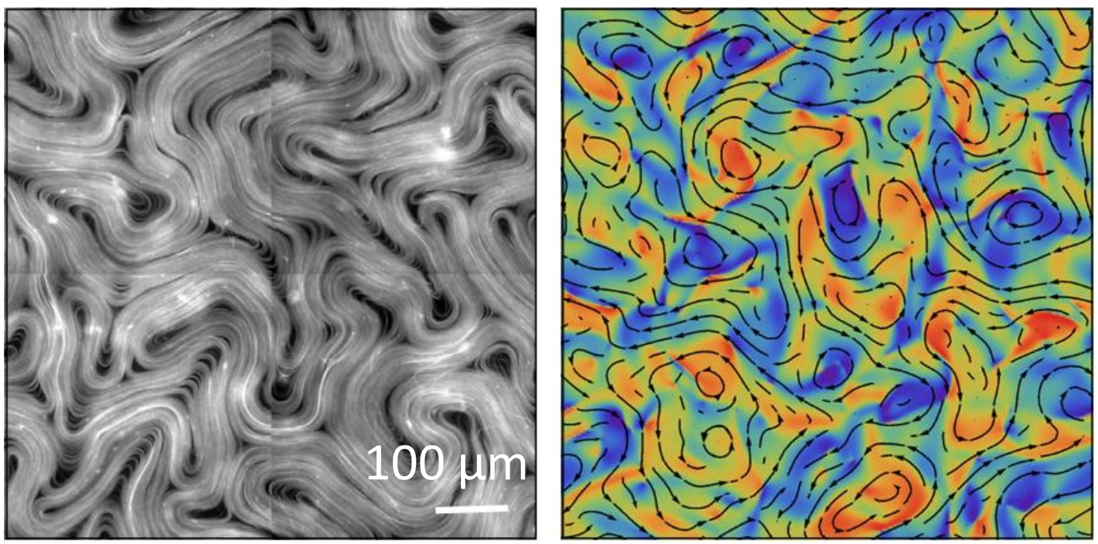

Z. Dogic lab

Low Reynolds number turbulence - Theory

L. Giomi PRX 2015:

$$\begin{cases} \rho \dfrac{Dv_i}{Dt} = \eta \nabla^2 v_i - \partial_i p + \partial_j \sigma_{ij}, \\ \dfrac{DQ_{ij}}{Dt} = \lambda S u_{ij} + Q_{ik}\omega_{kj} - \omega_{ik} Q_{kj} + \gamma^{-1} H_{ij}. \end{cases}$$

Q_{ij} alignment tensor
S nematic order parameter
p pressure
ν shear viscosity
λ flow alignment
γ rotational viscosity
u_{ij} strain rate tensor
ω_{ij} vorticity tensor
H_{ij} molecular tensor = $-\delta F/\delta Q_{ij}$ where $F_{\mathrm{LdG}} = \frac{1}{2}\int d^2 r [K|\nabla \boldsymbol{Q}|^2 + C \mathrm{tr} \boldsymbol{Q}^2 (\mathrm{tr} \boldsymbol{Q}^2 - 1)],$
stress tensor $\sigma_{ij} = \sigma_{ij}^e + \sigma_{ij}^a = \underbrace{-\lambda H_{ij} + Q_{ik}H_{kj} - H_{ik}Q_{kj}}_{\text{Elastic stress}} + \underbrace{|\zeta \Delta \mu| Q_{ij}}_{\text{Active stress}}$

Numerical simulation :

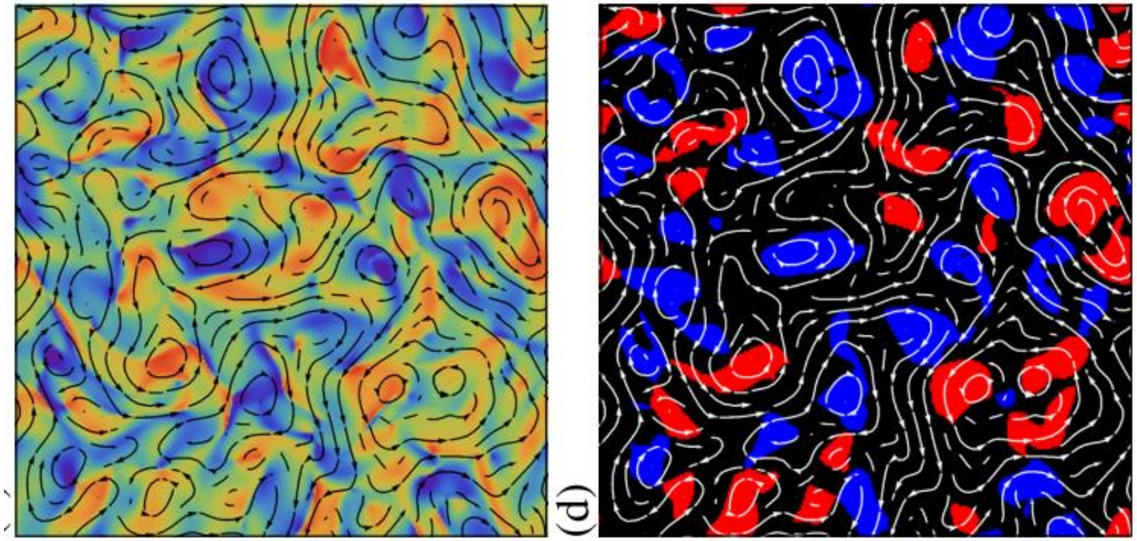

vorticity

$$\omega = \partial_x v_y - \partial_y v_x$$

Okubo-Weiss field

Measurements:

- Number of vertices, size, mean vorticity per vortex
- «Kinetic» energy $\mathcal{E} = \langle (v_x^2 + v_y^2)/2 \rangle$
- Enstrophy $\Omega = \langle \omega^2/2 \rangle$

Characteristic active length $l \sim \sqrt{\frac{K}{|\zeta \Delta \mu|}}$ Chaotic if $l \ll L$

Simulations: Vertices area and vorticity

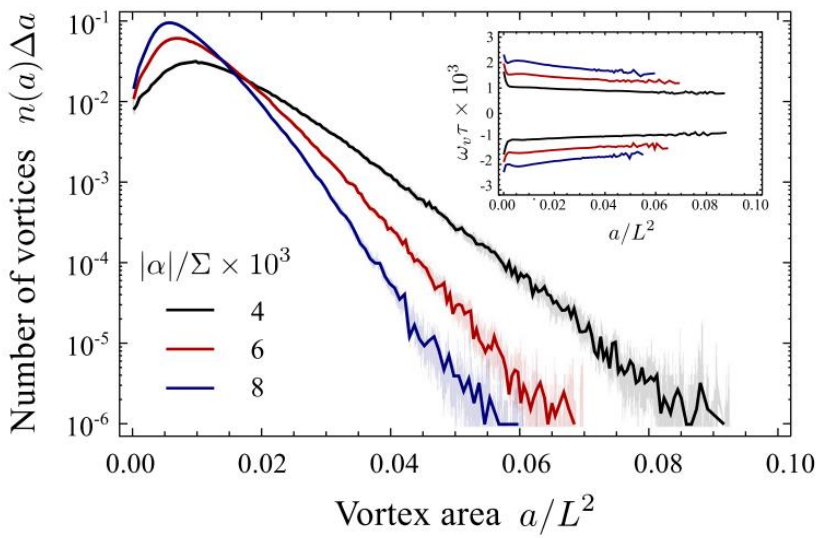

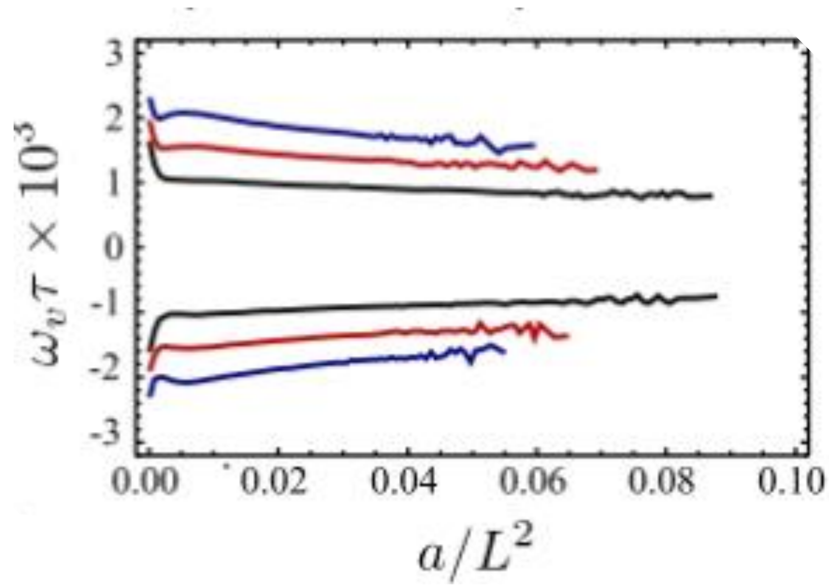

- Exponential distribution of the vertex areas (multiscale)
- Near-constant mean vorticity

Larger activity means smaller and faster vertices

Giomi PRX 2015

Impact of activity

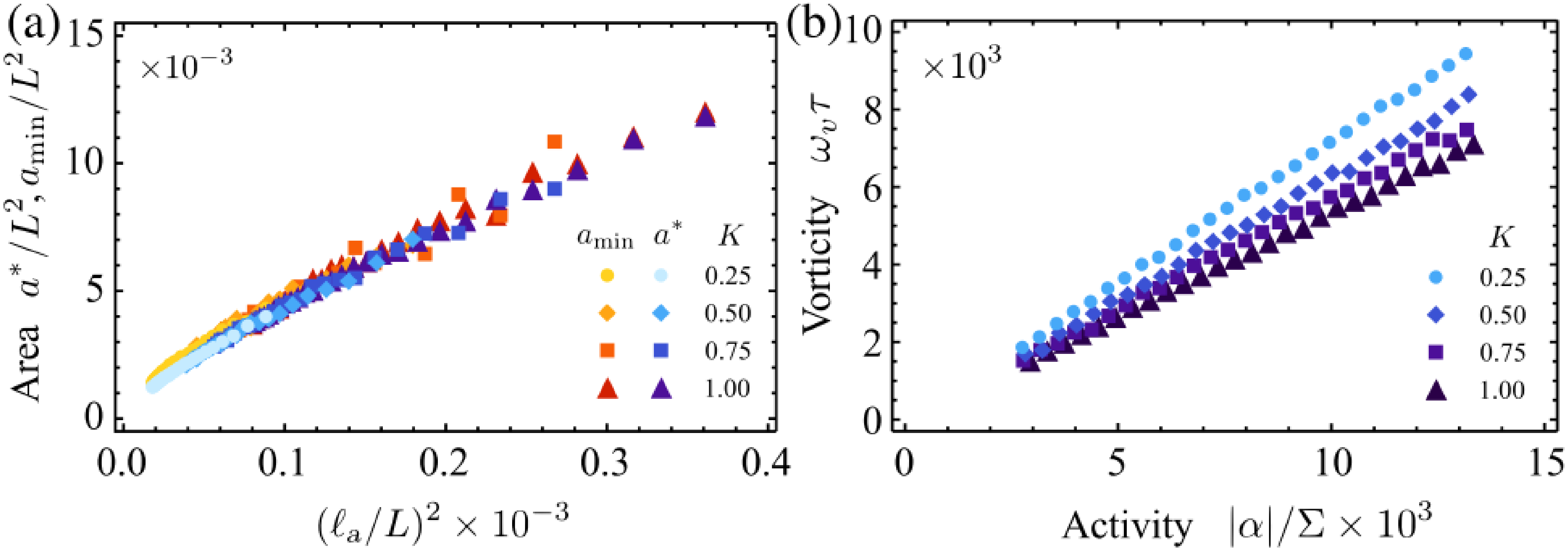

$$P(a) \propto \exp(-\frac{a}{l^2})$$

$$\omega_v \propto |\zeta \Delta \mu|$$

$$\rightarrow \omega_v = |\zeta \Delta \mu|/\eta$$

Experiments (HBECs)

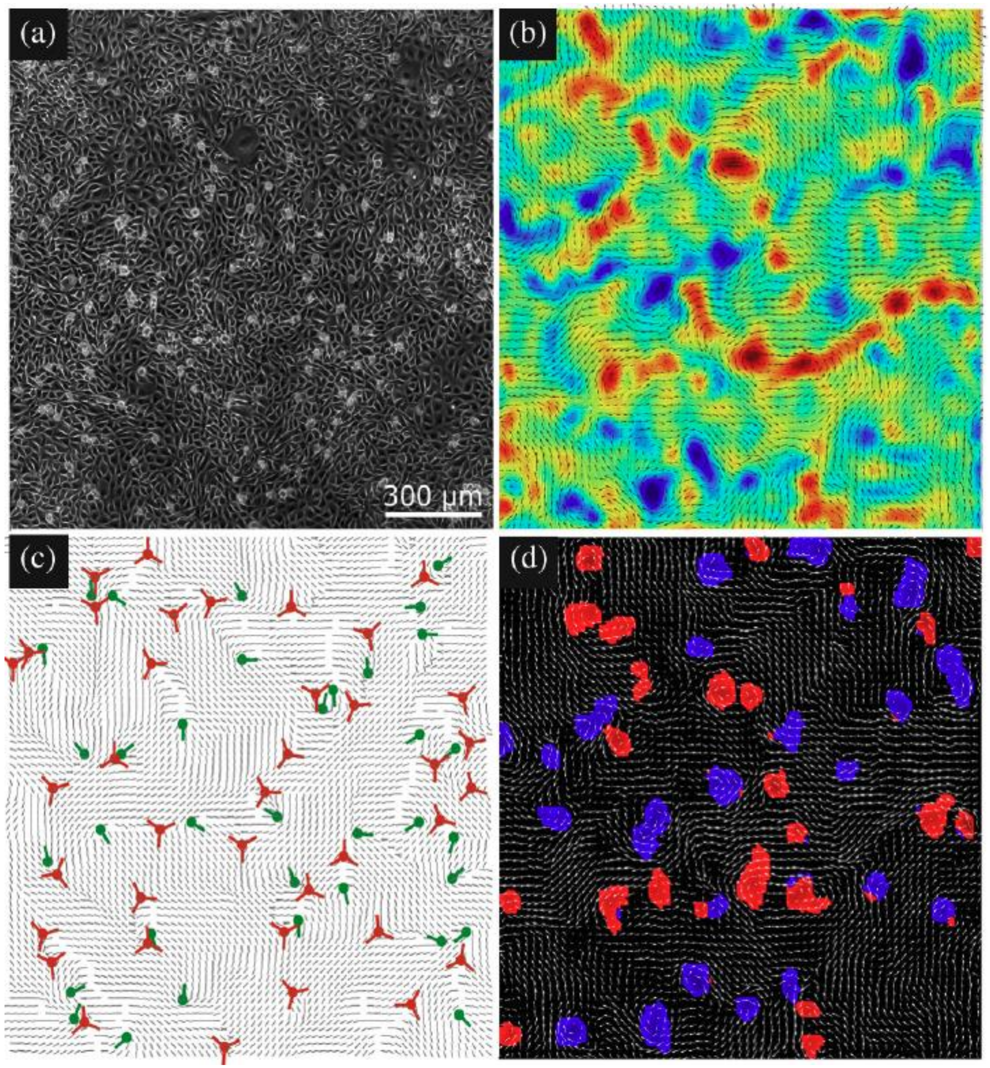

Okubo-Weiss field

Experiments

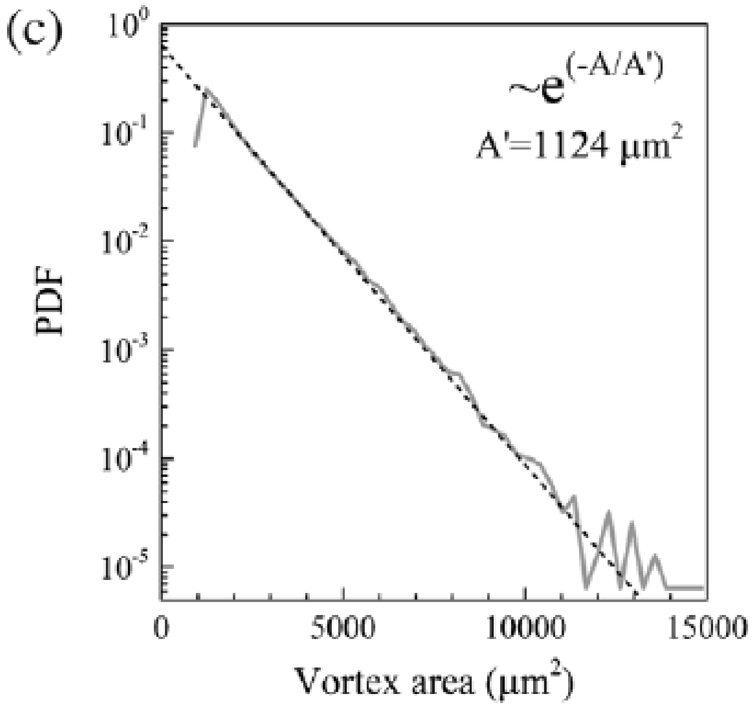

Exponential distribution

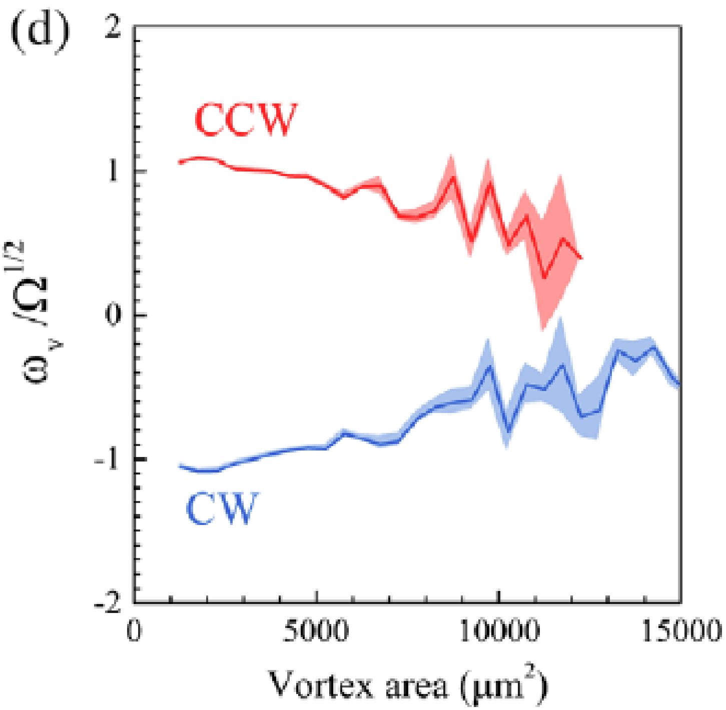

Low dependence of mean vorticity on vortex size

Signature of turbulence in the system

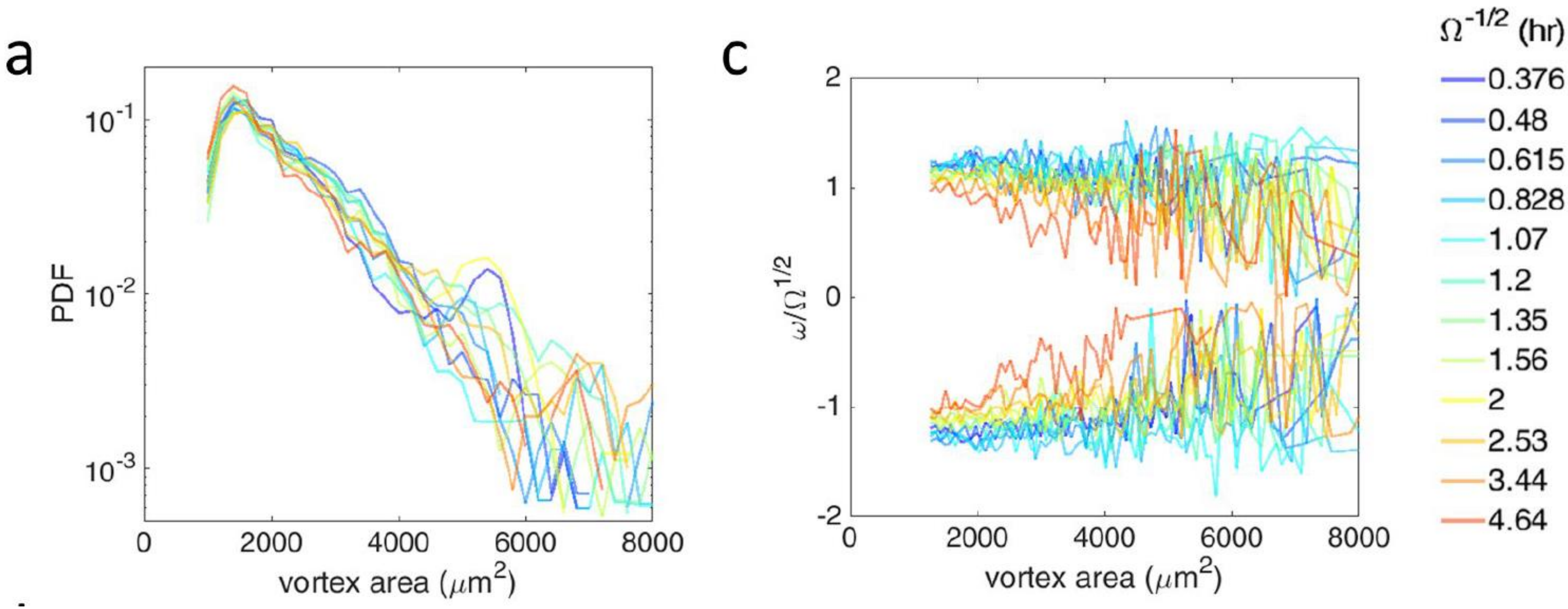

Activity and elastic constants don't vary with time

$$\sqrt{A'} \sim \ l \sim 50\mu m$$

$$\Longrightarrow \omega_v \sim |\zeta\Delta\mu|/\eta$$

Simulations: enstrophy and energy

$\Omega = \langle \omega^2/2 \rangle$

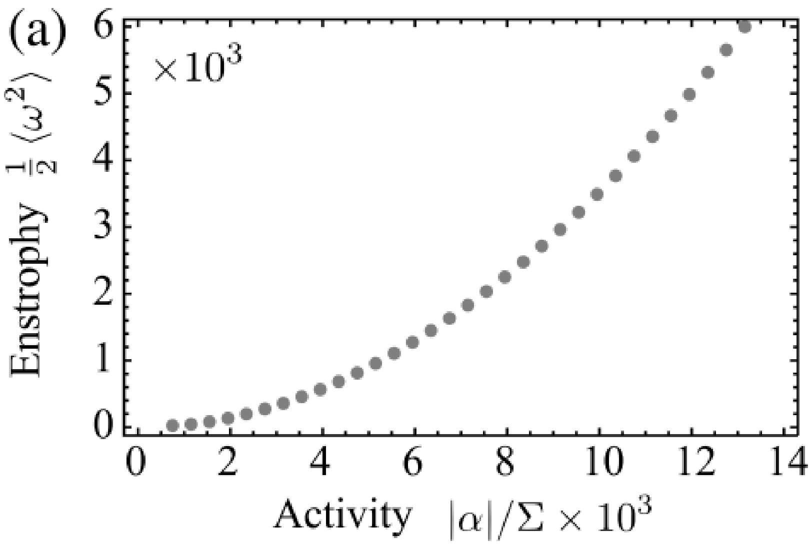

$\mathcal{E} = \langle (v_x^2 + v_y^2)/2 \rangle$

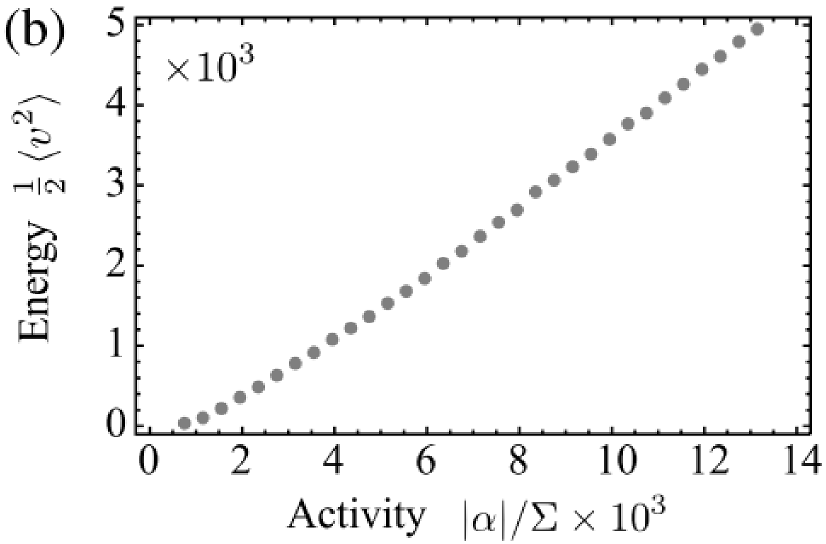

$\Omega \propto |\zeta\Delta\mu|^2$

$\varepsilon \propto |\zeta\Delta\mu|$

so: $\boxed{\varepsilon/\Omega \sim l^2}$

Experiments: Energy, Enstrophy

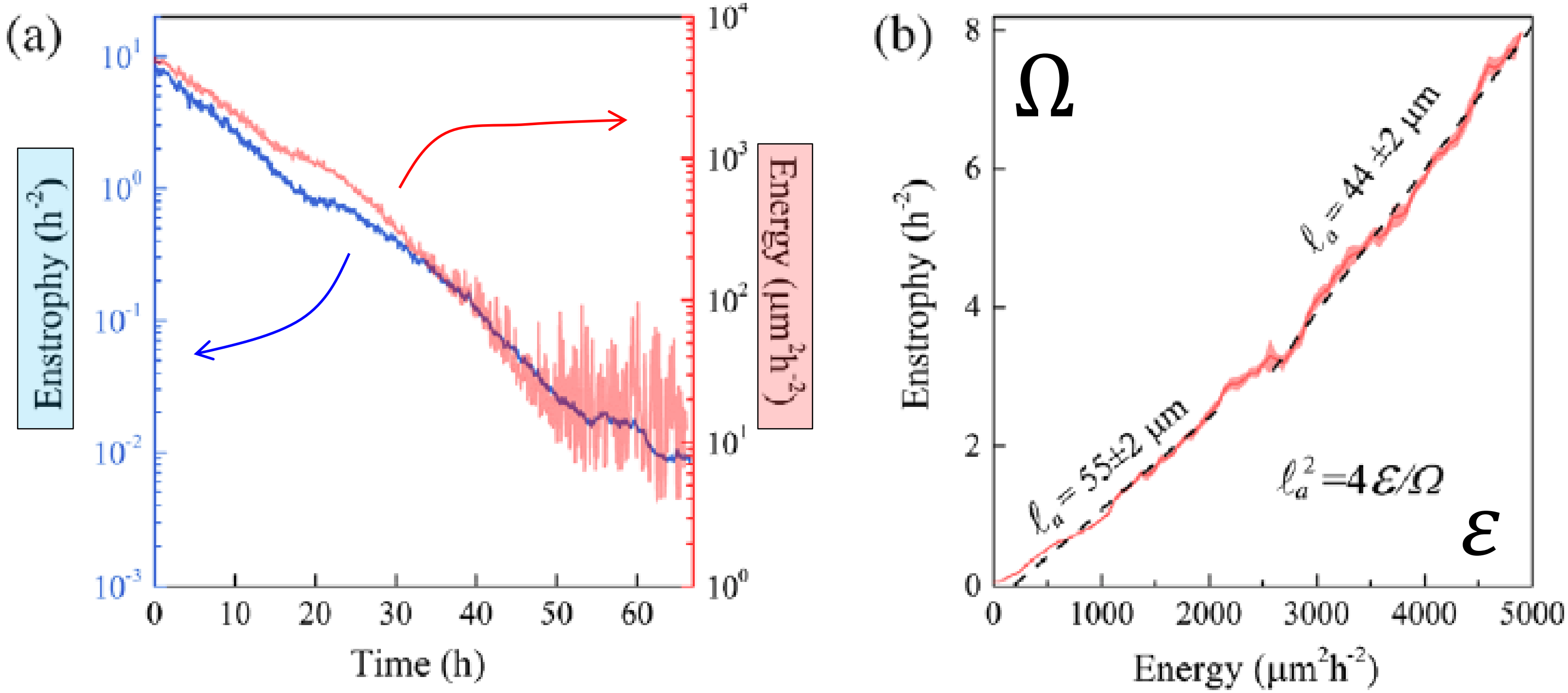

$$\Omega \sim \omega_v^2 \sim (|\zeta \Delta\mu|/\eta\ )^2$$

$$\varepsilon/\Omega \sim l^2$$

Increase of viscosity (x10) as the system enters jamming

Defects

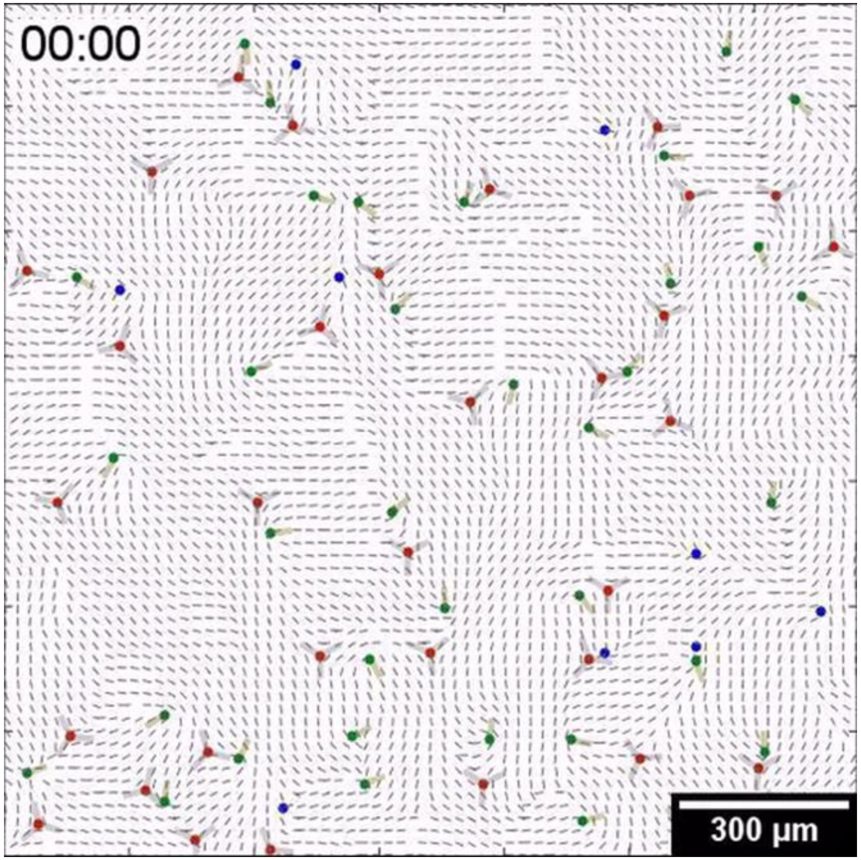

+1/2
-1/2

Defects

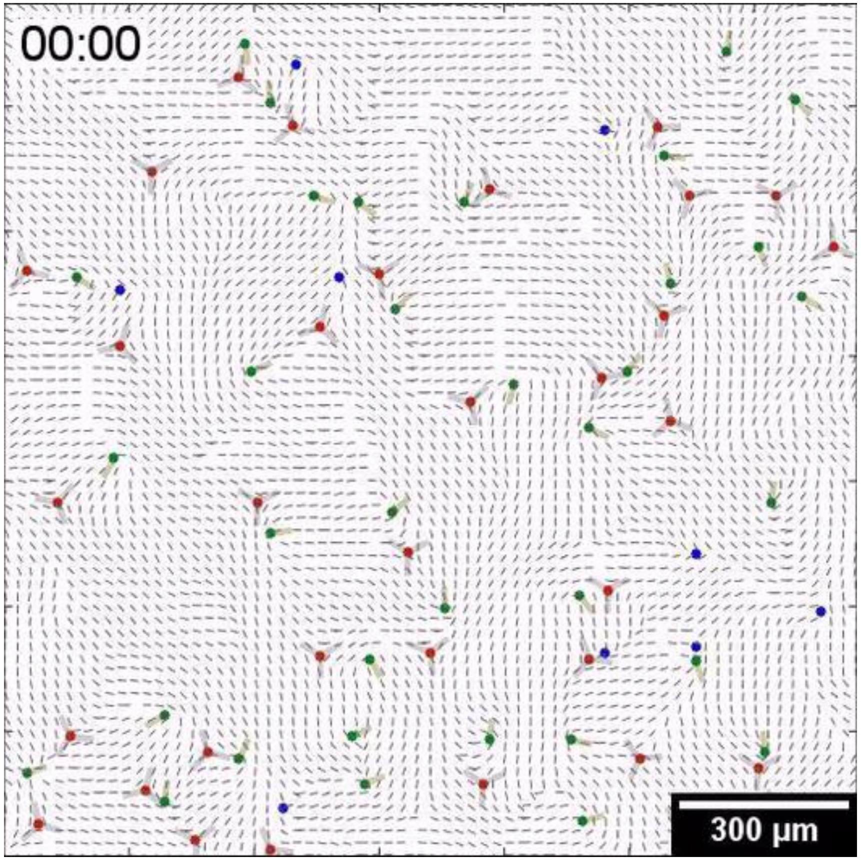

+1/2

-1/2

Defects

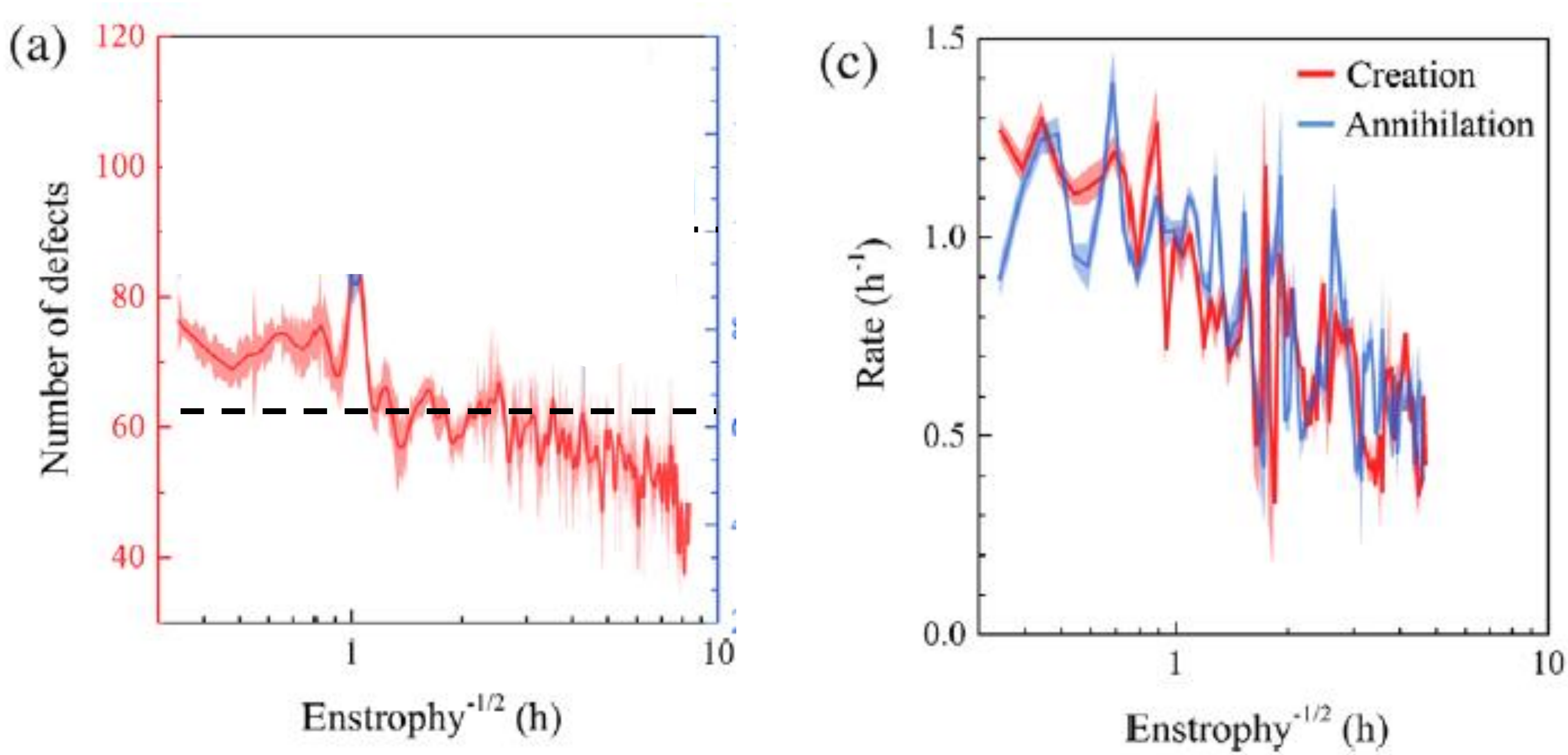

Dynamical balance creation-anihilation

Defects

MSD

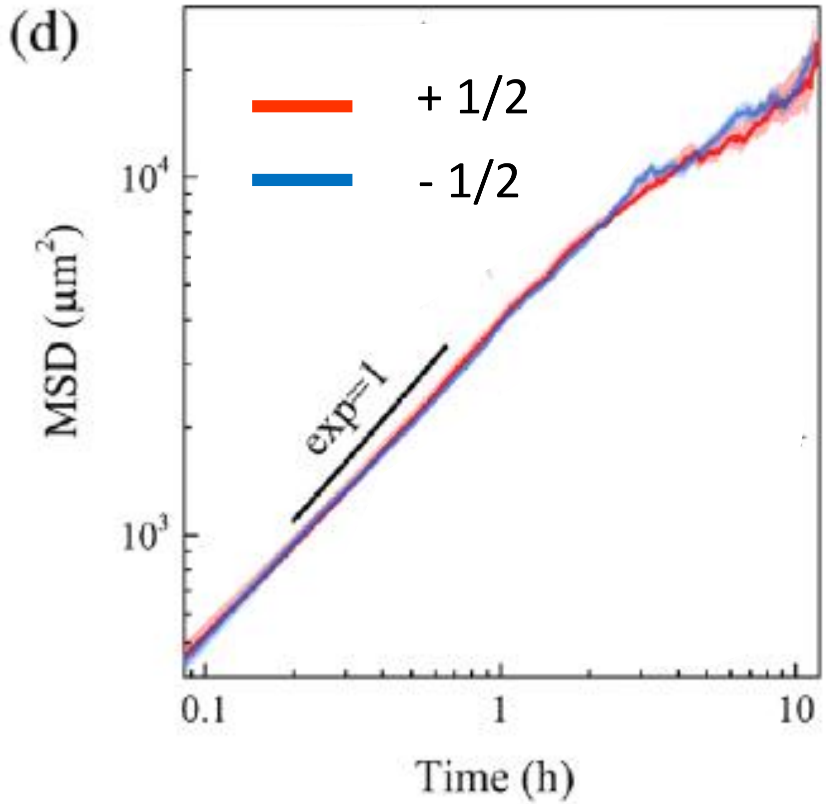

Diffusive

Direction of the flow field with respect to the defect axis

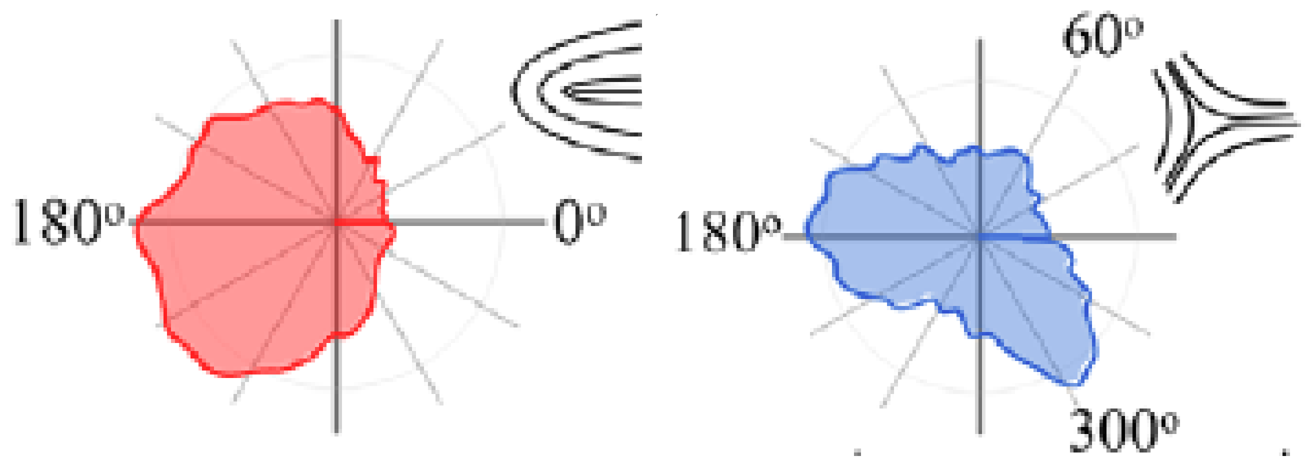

Flows and topological defects

Experiments
N > 10 000

Theory
(Giomi 2015)

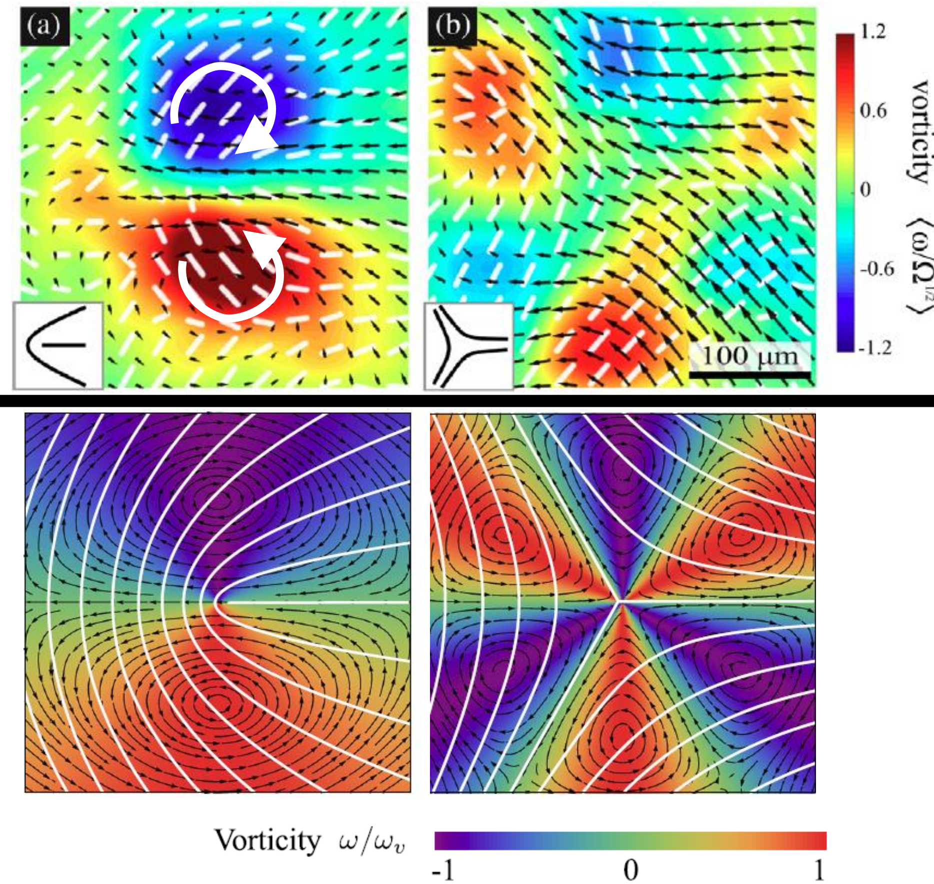

- Interplay between the defects and the vertices :

  Defects → vertices → transport of defects and chaotic mixing

Conclusions

- A cellular monolayer can undergo a transition from a low-density disordered state to a highly **ordered nematic state after confluence** / “**Meso-contact guidance**”

- In the final state, **activity is secondary to nematic elasticity** (jamming). Activity screened out by **friction**.

- Spontaneous **active Fréedericksz transition** {tilted/shear} to {untilted/immobile}. Very general physical principles / parameters’ values

- **Turbulent** collective flows, Chaotic dynamics. Coupling of defects with the vertices - Transition to jamming (increase of η). **Physiological** function?

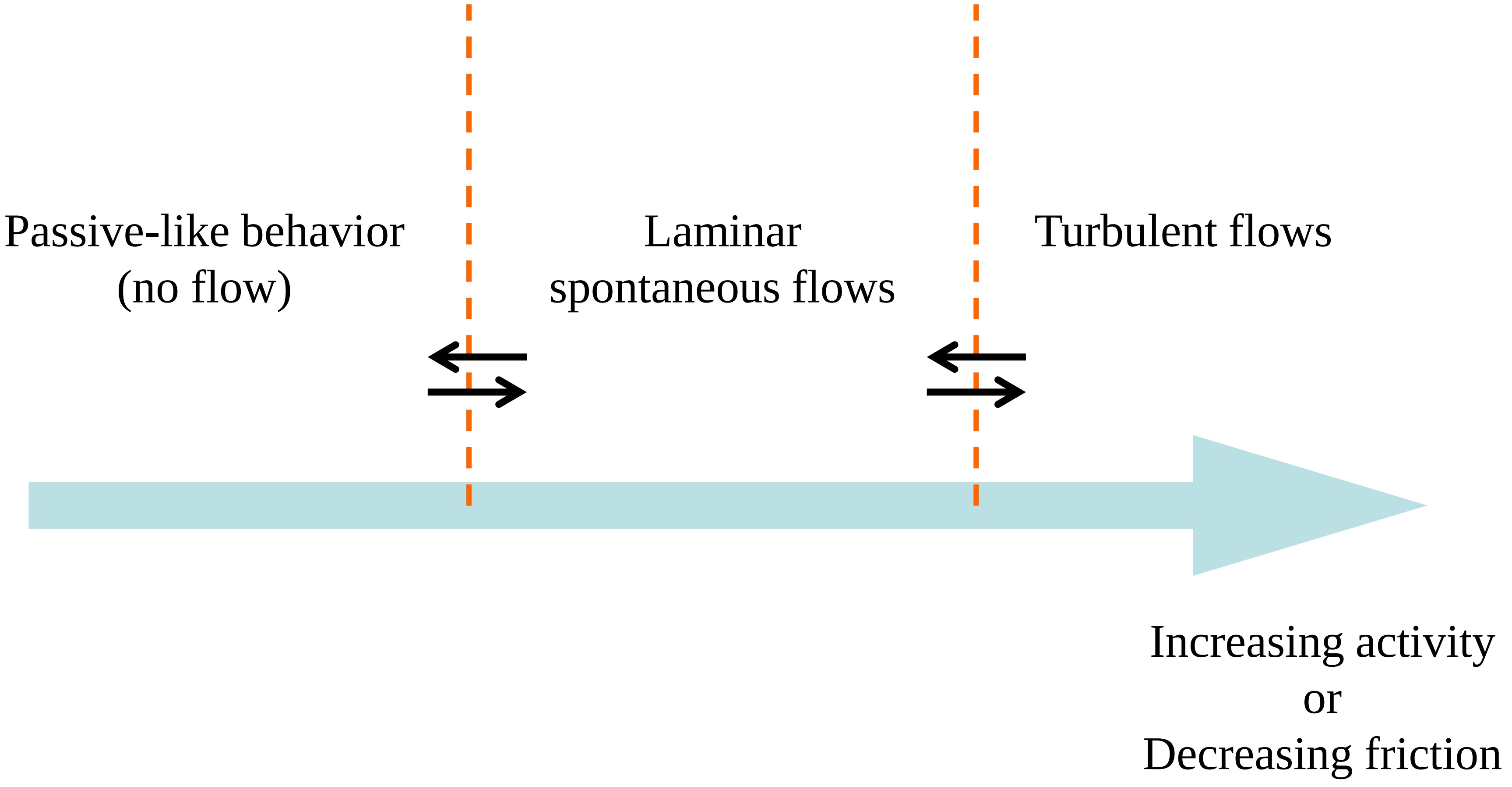
Passive-like behavior
(no flow)
Laminar
spontaneous flows
Turbulent flows
Increasing activity
or
Decreasing friction


- A. Buguin, I. Bonnet, S. Coscoy

- G. Duclos, T. Aryaksama, T. Sarkar, M. Lacroix
- V. Yashunsky, T. Vourc'h, F. Ascione, B. Smeets

- N. Sepulveda, V. Hakim (ENS, Paris)
- J. Camonis, M. C. Parrini (Curie)
- J.-F. Joanny, J. Prost, C. Blanch-Mercader, C. Erlenkaemper (Curie)
- L. Giomi (Leiden)


INSTITUT DU RADIUM
PAVILLON CURIE